

558479

Sandia National Laboratories
Waste Isolation Pilot Plant

**Determining the Hydrodynamic Shear Strength of Surrogate
Degraded TRU Waste Materials as an Estimate for the Lower
Limit of the Performance Assessment Parameter TAUFAIL**

Revision 0

This work has been carried out under Test Plan TP 09-01: Waste Erodibility with Vertical and Horizontal Erosion Flumes, WIPP Records Center package ERMS 556992.

WIPP:1.4.2.3:TD:QA-L:RECERT:556992

Information Only

APPROVALS PAGE

Author: Courtney G. Herrick (6211) Courtney G. Herrick 11/5/12
Print Signature Date

Author: Michael D. Schuhen (6212) Michael Schuhen 11-5-2012
Print Signature Date

Author: D. Michael Chapin (6212) DMC 11/5/2012
Print Signature Date

Author: Dwayne C. Kicker (6211) D. Kicker 11/5/2012
Print Signature Date

Technical Review: Daniel J. Clayton (6223) Shelly R. Nielsen for 11-5-12
Print Signature Date

QA Review: Shelly R. Nielsen (6210) Shelly R. Nielsen 11-5-12
Print Signature Date

Management Review: Sean Dunagan (6211) Sean Dunagan (For) 11-5-12
Print Signature Date

Executive Summary

The Waste Isolation Pilot Plant Performance Assessment (WIPP PA) scenarios include cases of human intrusion in which a future borehole intersects the repository. Drilling mud flowing up the borehole will apply a hydrodynamic shear stress to the borehole wall which, if high enough, could result in erosion of the wall material. This process may result in a release of radionuclides being carried up the borehole with the drilling mud.

The hydrodynamic shear strength of a material can only be measured in the laboratory by flume testing. Flume testing is typically performed in a channel in which the fluid is horizontal, mimicking a stream or ocean current. However, in a WIPP intrusion event, the drill bit would penetrate the degraded waste and the drilling mud would flow up the borehole in a predominantly vertical direction. In order to simulate this, a flume was designed and built so that the eroding fluid enters a vertical channel from the bottom and flows up past a specimen of surrogate waste material held in a cylindrical sample holder.

The surrogate materials used correspond to a conservative estimate of degraded TRU waste materials at the end of the regulatory period. The waste recipes were previously developed by SNL based on anticipated future states of the waste considering inventory, underground conditions and their evolution, and theoretical and experimental results. The recipes were conceived to represent the degraded waste in its weakest condition and can be divided into materials that simulate 50, 75, and 100% degraded waste by weight. The percent degradation indicates the anticipated amount of iron corrosion and decomposition of cellulose, plastics, and rubbers. Samples were die compacted to two pressures, 2.3 and 5.0 MPa. Testing has established that the less the degree of degradation the surrogate material represents and the higher the compaction stress it undergoes, the stronger the sample is.

The 50% degraded surrogate waste material compacted at 5.0 MPa was accepted for use in obtaining input parameters for another WIPP PA model by a conceptual model peer review panel and the EPA. The use of the 50% degraded surrogate waste material in vertical flume testing would provide an improved estimate of the waste shear strength and establish consistency between PA models in the approach used to obtain input parameters.

In WIPP PA, the waste shear strength parameter BOREHOLE : TAUFAIL is used in the computer program CUTTINGS_S. The current values and distribution of TAUFAIL, as given in the performance assessment parameter database, are:

Material	Property	Distribution	Range	Description
Borehole	TAUFAIL	Log-uniform	0.05 – 77.0 Pa	Effective shear strength for erosion of waste.

Based on experimental results that realistically simulate the effect of a drilling intrusion on an accepted surrogate waste material, we propose the following changes be made to TAUFAIL in the performance assessment parameter database:

Material	Property	Distribution	Range	Description
Borehole	TAUFAIL	Uniform	5.05 – 77.0 Pa	Effective shear strength for erosion of waste.

Acknowledgments

Sandia National Laboratories is a multi-program laboratory operated by Sandia Corporation, a wholly owned subsidiary of Lockheed Martin company, for the U.S. Department of Energy's National Nuclear Security Administration. This research is funded by WIPP programs administered by the Office of Environmental Management (EM) of the U.S Department of Energy.

CONTENTS

1	Introduction	1
2	Historical Development of the TAUFAIL Parameter	2
3	Development of Surrogate Wastes	4
4	Testing Apparatus Description	12
4.1	Vertical Flume Design and Operation	12
4.2	Determination of Applied Hydrodynamic Shear Stress.....	17
4.3	Data Acquisition and Control	18
4.3.1	Hardware	18
4.3.2	Instrumentation.....	19
4.3.3	Software.....	19
4.4	Sample Preparation	20
4.4.1	Specimen Assembly	21
5	Determination of Critical Shear Stress for Erosion.....	27
5.1	Bilinear Fit	27
5.2	SEDflume-based Methods for Determining Critical Shear Stress.....	28
5.2.1	Linear Interpolation.....	29
5.2.2	Power Law Relationship	29
5.3	Records Keeping.....	29
6	Vertical Flume Tests on Surrogate Degraded Waste Samples.....	31
6.1	The Test Matrix.....	31
6.2	100% Degraded Surrogate Waste Material Tests	34
6.3	75% Degraded Surrogate Waste Material Tests	37
6.3.1	75% Degraded Surrogate Waste Material Tests, Die Compacted to 2.3 MPa. 38	
6.3.1.1	Discussion of Results for 75% Degraded Surrogate Waste Material Tests, Die Compacted to 2.3 MPa	47
6.3.2	75% Degraded Surrogate Waste Material Tests, Die Compacted to 5.0 MPa. 51	
6.3.2.1	Discussion of Results for 75% Degraded Surrogate Waste Material Tests, Die Compacted to 5.0 MPa	59
6.3.3	Comparison of Results Using Socorro and Albuquerque Goethites	61
6.4	50% Degraded Surrogate Waste Material Tests	62
6.4.1	50% Degraded Surrogate Waste Material Tests, Die Compacted to 2.3 MPa. 63	
6.4.1.1	Discussion of results for 50% Degraded Surrogate Waste Material Tests, Die Compacted to 2.3 MPa	69
6.4.2	50% Degraded Surrogate Waste Material Tests, Die Compacted to 5.0 MPa. 71	
6.4.2.1	Discussion of results for 50% Degraded Surrogate Waste Material Tests, Die Compacted to 5.0 MPa	76
7	Testing Summary and Recommendation for the Lower Limit of TAUFAIL	78
8	References	82

FIGURES

Figure 1. Example of transuranic radioactive waste at WIPP.	10
Figure 2. Picture of the fully enclosed erosion channel and components of the vertical erosion flume. The eroding fluid is delivered to the channel by a supply line. The erosion channel is long enough to develop laminar flow at the lowest flow rates and fully turbulent flow at the highest anticipated flow rates. The vent is used to control the pressure on the face of the sample, which is monitored by the pressure gauge. The fluid is returned to the fluid supply tanks (Figure 3).	13
Figure 3. Picture of the fluid storage system. Fluid is recycled back from the erosion channel to the return tank, which acts as a baffle tank to drop out large or heavier pieces of eroded material. The fluid is then screened and transferred to the supply tank. The purpose of the screening is to capture large light material such as pieces of plastic that can foul the pump. The fluid is pumped back to the erosion channel. Both tanks are 300 gal (1135 L). 14	
Figure 4. Picture of fluid pump, diverter valve, and associated plumbing. Diverting the fluid back into the supply tank helps control the flow when slow flow rates required.	15
Figure 5. Picture of apparatuses used to advance the specimen into the flow of the channel. A step motor controlled by the DAS system is used to move the linear rail table with attached reaction plate. The push rod connects to a plunger in the sample holder, in front of which is the sample. In this picture the sample has been eroded away and the plunger is at the side of the channel.	16
Figure 6. Steel, alloys, iron oxide, and glass constituent materials.	23
Figure 7. Sawdust, cotton, paper, and peat constituent materials.	23
Figure 8. Poly sheet and poly bottle constituent materials.	23
Figure 9. O-rings, rubber bands, plastic bag, and rubber glove constituent materials.....	23
Figure 10. Soil, sheetrock, WIPP salt, and concrete constituent materials.....	23
Figure 11. Batch of 100% degraded surrogate material being readied to be introduced into a Lexan sample holder.	24
Figure 12. Aluminum and Lexan sample holders.	25
Figure 13. Aluminum jacket and associated hardware for sample assembly and load-cell introduction.	25
Figure 14. Sample assembly preparation.	25
Figure 15. The sample is loaded in the aluminum jacket with the associated hardware	25
Figure 16. Prior to loading, the aluminum or Lexan® jacket into the compression actuator, a compression sleeve is applied to support the sample.....	26
Figure 17. The final, load compressed product ready for erosion in the flume. The itemized sheet lists the weight of each constituent.	26

Figure 18. (a) Idealization of the bilinear method of analyzing erosion data. Extrapolation of the upper line, which represents the erosion behavior of the bulk of the material, back to an erosion rate of zero represents the critical shear stress τ_c . (b) Analysis of the experimental results of Jepsen et al. on surrogate waste specimen B2 using the bilinear approach. 28

Figure 19. Schematic depictions of the modes of deformation the samples and Lexan sample holders were found to have undergone upon being removed from the split shell after unloading: (a) barreling around the middle, (b) bulging at one of the ends, (c) bending, and (d) shearing. The dashed line represents the original axis of the specimen before deformation. 35

Figure 20. Analyses of the test results for Sample WF-100-203-04. (a) UF bilinear fit yielding $\tau_m = 0.17$ Pa and (b) the UCSB fits around a critical shear stress of 10^{-4} cm/sec giving for the linear interpolation $\tau_{cr} = 0.21$ Pa (two orange points) and for the power law fit $\tau_{cr} = 0.22$ Pa (three black points). 36

Figure 21. The Albuquerque goethite outcrop near the Geomechanics Laboratory at Sandia National Laboratories – Albuquerque..... 38

Figure 22. Analyses of the test results for Sample 75-080112. Uses Socorro goethite. (a) UF bilinear fit yielding $\tau_m = 1.60$ Pa and (b) the UCSB fits around a critical shear stress of 10^{-4} cm/sec giving for the linear interpolation $\tau_{cr} = 1.46$ Pa (two orange points) and for the power law fit $\tau_{cr} = 1.62$ Pa (three black points). 40

Figure 23. Analyses of the test results for Sample 75-082212. Uses Socorro goethite. (a) UF bilinear fit yielding $\tau_m = 1.22$ Pa and (b) the UCSB fits around a critical shear stress of 10^{-4} cm/sec giving for the linear interpolation $\tau_{cr} = 1.06$ Pa (two orange points) and for the power law fit $\tau_{cr} = 1.34$ Pa (three black points). 41

Figure 24. Analyses of the test results for Sample 75-082712. Uses Socorro goethite. (a) UF bilinear fit yielding $\tau_m = 1.79$ Pa and (b) the UCSB fits around a critical shear stress of 10^{-4} cm/sec giving for the linear interpolation $\tau_{cr} = 1.75$ Pa (two orange points) and for the power law fit $\tau_{cr} = 1.85$ Pa (three black points). 42

Figure 25. Analyses of the test results for Sample 75-082912. Uses Albuquerque goethite. (a) UF bilinear fit yielding $\tau_m = 2.00$ Pa and (b) the UCSB fits around a critical shear stress of 10^{-4} cm/sec giving for the linear interpolation $\tau_{cr} = 1.32$ Pa (two orange points) and for the power law fit $\tau_{cr} = 1.35$ Pa (three black points). 43

Figure 26. Analyses of the test results for Sample 75-091012. Uses Albuquerque goethite. (a) UF bilinear fit yielding $\tau_m = 1.06$ Pa and (b) the UCSB fits around a critical shear stress of 10^{-4} cm/sec giving for the linear interpolation $\tau_{cr} = 1.05$ Pa (two orange points) and for the power law fit $\tau_{cr} = 1.05$ Pa (three black points). 44

Figure 27. Analyses of the test results for Sample 75-091312. Uses Albuquerque goethite. (a) UF bilinear fit yielding $\tau_m = 1.84$ Pa and (b) the UCSB fits around a critical shear stress of 10^{-4} cm/sec giving for the linear interpolation $\tau_{cr} = 1.75$ Pa (two orange points) and for the power law fit $\tau_{cr} = 1.85$ Pa (three black points). 45

Figure 28. Analyses of the test results for Sample 75-091912. Uses Albuquerque goethite. (a) UF bilinear fit yielding $\tau_m = 1.19$ Pa and (b) the UCSB fits around a critical shear stress of

10 ⁻⁴ cm/sec giving for the linear interpolation $\tau_{cr} = 1.25$ Pa (two orange points) and for the power law fit $\tau_{cr} = 1.34$ Pa (three black points).	46
Figure 29. Analyses of the test results for Sample 75-080212. Socorro goethite. (a) UF bilinear fit yielding $\tau_m = 2.22$ Pa and (b) the UCSB fits around a critical shear stress of 10 ⁻⁴ cm/sec giving for the linear interpolation $\tau_{cr} = 1.61$ Pa (two orange points) and for the power law fit $\tau_{cr} = 1.90$ Pa (three black points).	52
Figure 30. Analyses of the test results for Sample 75-082312. Socorro goethite (a) UF bilinear fit yielding $\tau_m = 2.57$ Pa and (b) the UCSB fits around a critical shear stress of 10 ⁻⁴ cm/sec giving for the linear interpolation $\tau_{cr} = 2.37$ Pa (two orange points) and for the power law fit $\tau_{cr} = 2.65$ Pa (three black points).	53
Figure 31. Analyses of the test results for Sample 75-082812. Socorro goethite. (a) UF bilinear fit yielding $\tau_m = 1.60$ Pa and (b) the UCSB fits around a critical shear stress of 10 ⁻⁴ cm/sec giving for the linear interpolation $\tau_{cr} = 1.85$ Pa (two orange points) and for the power law fit $\tau_{cr} = 2.16$ Pa (three black points).	54
Figure 32. Analyses of the test results for Sample 75-083012. Albuquerque goethite. (a) UF bilinear fit yielding $\tau_m = 2.64$ Pa and (b) the UCSB fits around a critical shear stress of 10 ⁻⁴ cm/sec giving for the linear interpolation $\tau_{cr} = 2.08$ Pa (two orange points) and for the power law fit $\tau_{cr} = 2.01$ Pa (three black points).	55
Figure 33. Analyses of the test results for Sample 75-091212. Albuquerque goethite. (a) UF bilinear fit yielding $\tau_m = 1.46$ Pa and (b) the UCSB fits around a critical shear stress of 10 ⁻⁴ cm/sec giving for the linear interpolation $\tau_{cr} = 1.31$ Pa (two orange points) and for the power law fit $\tau_{cr} = 1.34$ Pa (three black points).	56
Figure 34. Analyses of the test results for Sample 75-091812. Albuquerque goethite. (a) UF bilinear fit yielding $\tau_m = 1.93$ Pa and (b) the UCSB fits around a critical shear stress of 10 ⁻⁴ cm/sec giving for the linear interpolation $\tau_{cr} = 1.83$ Pa (two orange points) and for the power law fit $\tau_{cr} = 1.86$ Pa (three black points).	57
Figure 35. Analyses of the test results for Sample 75-092012. Albuquerque goethite. (a) UF bilinear fit yielding $\tau_m = 2.80$ Pa and (b) the UCSB fits around a critical shear stress of 10 ⁻⁴ cm/sec giving for the linear interpolation $\tau_{cr} = 1.63$ Pa (two orange points) and for the power law fit $\tau_{cr} = 1.86$ Pa (three black points).	58
Figure 36. Analyses of the test results for Sample WF-50-02. (a) UF bilinear fit yielding $\tau_m = 2.54$ Pa and (b) the UCSB fits around a critical shear stress of 10 ⁻⁴ cm/sec giving for the linear interpolation $\tau_{cr} = 2.74$ Pa (three orange filled points) and for the power law fit $\tau_{cr} = 3.21$ Pa (four black points).	64
Figure 37. Analyses of the test results for Sample Flume 50-01. (a) UF bilinear fit yielding $\tau_m = 1.60$ Pa and (b) the UCSB fits around a critical shear stress of 10 ⁻⁴ cm/sec giving for the linear interpolation $\tau_{cr} = 2.14$ Pa and for the power law fit $\tau_{cr} = 2.30$ Pa (two orange filled points).	65
Figure 38. Analyses of the test results for Sample WF 50-203-01. (a) UF bilinear fit yielding $\tau_m = 3.09$ Pa and (b) the UCSB fits around a critical shear stress of 10 ⁻⁴ cm/sec giving for the linear interpolation $\tau_{cr} = 3.05$ Pa and for the power law fit $\tau_{cr} = 3.35$ Pa (three orange filled points).	66

Figure 39. Analyses of the test results for Sample WF-50-203-02. (a) UF bilinear fit yielding $\tau_m = 1.78$ Pa and (b) the UCSB fits around a critical shear stress of 10^{-4} cm/sec giving for the linear interpolation $\tau_{cr} = 2.07$ Pa and for the power law fit $\tau_{cr} = 2.08$ Pa (two orange filled points). 67

Figure 40. Analyses of the test results for Sample WF-50-203-03. (a) UF bilinear fit yielding $\tau_m = 2.10$ Pa and (b) the UCSB fits around a critical shear stress of 10^{-4} cm/sec giving for the linear interpolation $\tau_{cr} = 2.91$ Pa (two orange filled points) and for the power law fit $\tau_{cr} = 3.29$ Pa (three black points). 68

Figure 41. Flume results for Sample WF-50-5-01 plotted on a scale typically used for 50% degraded surrogate waste samples. The bulk erosion of the sample was not considered to have been started. In addition, the UCSB critical erosion rate was never reached. Beyond a shear stress of 3.5 Pa, erosion stopped. After 17½ hrs of testing, less than 7.5 mm ($\frac{1}{3}$ inch) of material was removed..... 72

Figure 42. Flume results for Sample WF-50-5-02B plotted on a scale typically used for 50% degraded surrogate waste samples. The bulk erosion of the sample was not considered to have been started. In addition, the UCSB critical erosion rate was never reached. Beyond a shear stress of 4.5 Pa, erosion stopped. After 12½ hrs of testing, less than 9 mm ($\frac{1}{3}$ inch) of material was removed..... 72

Figure 43. Analyses of the test results for Sample WF-50-5-03. (a) UF bilinear fit yielding $\tau_m = 3.79$ Pa and (b) the UCSB fits around a critical shear stress of 10^{-4} cm/sec giving for the linear interpolation $\tau_{cr} = 3.84$ Pa (two orange filled points) and for the power law fit $\tau_{cr} = 4.32$ Pa (three black points). 73

Figure 44. Analyses of the test results for Sample WF-50-5-04. (a) UF bilinear fit yielding $\tau_m = 5.13$ Pa and (b) the UCSB fits around a critical shear stress of 10^{-4} cm/sec giving for the linear interpolation $\tau_{cr} = 5.28$ Pa (two orange filled points) and for the power law fit $\tau_{cr} = 5.48$ Pa (four black points)...... 74

Figure 45. Analyses of the test results for Sample WF-50-5-05. (a) UF bilinear fit yielding $\tau_m = 4.96$ Pa and (b) the UCSB fits around a critical shear stress of 10^{-4} cm/sec giving for the linear interpolation $\tau_{cr} = 5.01$ Pa (two orange filled points) and for the power law fit $\tau_{cr} = 5.27$ Pa (three black points). 75

TABLES

Table 1. Simulated waste materials (Butcher et al., 1991, Table 2-1).....	5
Table 2. Test materials for drum collapse tests (Butcher et al., 1991, Table 2-9).....	6
Table 3. Anticipated initial waste characteristics and concentrations (Papenguth and Myers, Appendix A, Tables 1 and 2 in Hansen et al., 1997)	8
Table 4. Degraded surrogate waste materials. Cases 1 and 2 are from Hansen et al. 1997, Table 2-2, Table 2-3, and Appendix A, Table 8. Case 3 uses the same methodology as discussed in Hansen et al. (1997) and was developed for the present set of tests.....	11
Table 5. Measurement and test equipment in use on the vertical flume.....	19
Table 6. Material recipes for the dry ingredients for each sample type: 50%, 75%, and 100% degraded surrogate wastes. These are batch target weights in grams (g).	21
Table 7. Simulant material particle sizes for the surrogate waste materials.	22
Table 8. Test matrix for the flume tests performed to assess the lower limit of TAUFAIL. Three different materials were tested representing 100%, 75%, and 50% degradation of the WIPP wastes. Each material was tested at two levels of die compaction: 2.3 or 5.0 MPa. In the 75% degraded surrogate waste material tests, two different sources of goethite were used. One is from an outcrop on Kirkland Air Force Base, Albuquerque, NM (“Alb”) and the other is from a private mine outcrop outside Socorro, NM (“Socorro”).	32
Table 9. Compilation of critical shear stresses for the 75% degraded surrogate waste samples compacted at 2.3 MPa.....	49
Table 10. Compilation of critical shear stresses for the 75% degraded surrogate waste samples compacted at 5.0 MPa.....	61
Table 11. Critical shear stress results from UF analyses on the 75% degraded surrogate waste materials by goethite type.	62
Table 12. Compilation of critical shear stresses for the 50% degraded surrogate waste samples compacted at 2.3 MPa.....	70
Table 13. Compilation of critical shear stresses for the 50% degraded surrogate waste samples compacted at 5.0 MPa.....	77
Table 14. Average shear strengths, or critical shear stress, for each type of surrogate waste material and compaction pressure as determined by the three analysis methods.	79
Table 15. Statistics for BOREHOLE : TAUFAIL to be entered into the parameter database.	81

1 INTRODUCTION

The Waste Isolation Pilot Plant (WIPP) is a U.S. Department of Energy (DOE) mined underground repository, certified by the U.S. Environmental Protection Agency (EPA), and designed for the safe management, storage, and disposal of transuranic (TRU) radioactive waste resulting from defense related programs. The wastes are emplaced in panels excavated at a depth of 655 m in the Permian Salado Formation. Following the emplacement of waste and the MgO engineered barrier material, the panels will be isolated from the mine using an approved closure system.

The DOE demonstrates compliance with the containment requirements according to 40 CFR 194 by means of performance assessment (PA) calculations carried out by Sandia National Laboratories (SNL). WIPP PA calculations estimate the probability and consequences of radionuclide releases from the repository to the accessible environment for a regulatory period of 10,000 years. WIPP PA scenarios include cases of human intrusion in which a future borehole intersects the repository. Drilling mud flowing up the borehole will apply a hydrodynamic shear stress to the borehole wall which, if high enough, could result in erosion of the wall material. This process may result in a release of radionuclides being carried up the borehole with the drilling mud. WIPP PA uses the parameter TAUFAIL to represent the hydrodynamic waste shear strength in their computer codes.

To simulate the borehole conditions of a WIPP drilling intrusion event, a flume was designed and built so that the eroding fluid enters a vertical channel from the bottom and flows up past a specimen of surrogate waste material held in a cylindrical sample holder. The surrogate materials used in the flume experiments correspond to a conservative estimate of degraded TRU waste materials at the end of the regulatory period. The waste recipes were previously developed by SNL based on anticipated future states of the waste considering inventory, underground conditions including their evolution, and theoretical and experimental results. The recipes were conceived to represent the degraded waste in its weakest condition and can be divided into materials that simulate 50, 75, and 100% degraded waste by weight. The percent degradation indicates the anticipated amount of iron corrosion and decomposition of cellulose, plastics, and rubbers.

2 HISTORICAL DEVELOPMENT OF THE TAUFAIL PARAMETER

Berglund (1992) created the original models for cuttings, cavings, and spallings for WIPP purposes and performed the first analyses. Berglund assumed that, “In the absence of experimental data, the effective shear strength for erosion of the repository material is assumed to be similar to that of a montmorillonite clay, with an effective shear strength of 1 to 5 Pa.”

Butcher (1994) argued that, from a mechanical standpoint, the degraded waste would be similar to a clay-sand mixture. Based on literature values, he estimated that the strength of such a mixture would range between 0.1 and 1 Pa, with a median value of 0.5 Pa. Later, Butcher et al. (1995) changed the range to 0.1 to 10 Pa with a median of 1 Pa using a constructed distribution, again based on another literature review.

For the Compliance Certification Application (CCA) (DOE, 1996a), the DOE assumed a uniform distribution of the waste shear strength with a range of 0.05 to 10 Pa with a median of 5.0 Pa. This range was based on Berglund’s (1996) review of soil erosion tests. The lower limit of the range is based on erosion tests of a San Francisco Bay mud (Partheniades and Paaswell, 1970). The upper limit was arbitrarily chosen, based on the same literature review, as a value less than the highest threshold value reported.

The sensitivity of the Cavings model to changes in the waste shear strength was studied by the EPA as part of their evaluation for the Performance Assessment Validation Test (PAVT) (Trovato, 1997a). They found that the cavings model is sensitive to the values chosen for TAUFAIL, in particular the lower limit since weaker material would result in greater cavings release. As a result, the EPA required that the DOE to change its method for estimating the waste shear strength and use an estimation based on particle size distributions instead of analog experimental data as was done for the CCA (Trovato, 1997b).

For the PAVT, the waste shear strength was estimated based on particle size distributions determined by an expert elicitation panel (CTAC, 1997). The estimates used the Shields parameter, which relies on a measure of the central point of a population of particles of different sizes, to determine the critical shear stress for a sediment bed. With this approach, the calculated critical shear strength ranged from 0.64 to 77 Pa (Wang, 1997; Wang and Larsen, 1997). For conservatism, the EPA required that the low value from the CCA be retained, while the high value from the Shields parameter method be used for the upper value (EPA, 1998). A log-uniform distribution for the waste was selected for the PAVT to provide equal weighting over the three orders of magnitude in the range (Tierney, 1996). The range of values and distribution for TAUFAIL became:

Material	Property	Distribution	Range	Description
Borehole	TAUFAIL	Log-uniform	0.05 – 77.0 Pa	Effective shear strength for erosion of waste.

These remain the current values and distribution for TAUFAIL, as given in the performance assessment parameter database.

The reason mud or clay was chosen as an analog for the shear strength of the waste was a lack of experimental results on either real degraded waste or an adequate surrogate material. Jepsen et al. (1998) performed erosional shear testing on highly degraded surrogate waste samples developed by Hansen et al. (1997). The surrogate materials were developed in a systematic and logical manner based on consideration of the anticipated future state of the waste and the estimated inventory of standard waste drums (Hansen et al., 1997; Hansen, 2005). Hansen et al. (1997) asserted that the surrogate degraded waste material properties represented the lowest plausible realm of the future waste state because degradation of each constituent was considered, no strengthening processes were included such as compaction, cementation, mineral precipitation, and more durable packaging. The surrogate materials were believed to represent an unobtainable degraded state, far weaker than any possible future state of the waste (Hansen, 2005, Hansen et al., 2003). The 50% degraded surrogate waste material compacted at 5.0 MPa was used by Hansen et al. (2003) to establish the parameters for the spallings model, which was accepted by the Spallings Conceptual Model Peer Review Panel (Yew et al., 2003) and incorporated into the CRA-2004 PABC (EPA, 2006). Hansen (2005) advocated using the experimental results of Jepsen et al. (1998) to establish the lower limit of the TAUFAIL range.

Herrick et al. (2007a, 2007b) re-analyzed Jepsen et al.'s (1998) results and also endorsed their use. Herrick et al. (2007b) used a method proposed by Parchure and Mehta (1985), and advanced in Teeter (1987), to assess the shear strength using a piecewise linear fit of the erosion rate versus the shear stress data. In addition, Herrick et al. (2007a, 2007b) conducted another thorough review of erosion of cohesive materials and methods of analysis, including the addition of other San Francisco Bay mud data since it is the currently accepted model for the erosion behavior of WIPP waste. Herrick et al. (2007a) also performed numerical modeling to assess the effect of compaction due to creeping salt and consolidation due to gravity on the degraded waste.

Despite numerous approaches to define a realistic value of TAUFAIL, in particular the lower limit of its possible range of strengths, none have been adopted. Its value remains based on flume erosion experiments performed on a bay mud. The approach that received the most support was the use of flume tests to directly measure the erosion resistance of surrogate degraded waste material (Jepsen et al., 1998). The primary criticism of this approach was that waste strength values were derived from horizontal flume testing (Coons et al., 2007), as are all the results in literature. The concern is that tests conducted in a horizontal configuration may overestimate the shear strength due to the effect of gravity holding the material in place. Another concern that Coons et al. (2007) had was that the samples were compacted in a die to 5 MPa. The numerical modeling performed by Herrick et al (2007a) suggested that the minimum stress the degraded waste would be subjected to, which corresponds to the highest gas generation rate, is 2.3 MPa. On the other hand, Hansen et al. (1997, 2003) demonstrated that the 5.0 MPa compaction stress is a conservative estimate for the lower bound of pressure that the waste will undergo in the underground.

In order to address the need of having flow running vertically up a flume channel to more realistically simulate field conditions where a drilling fluid is flowing up a borehole, a vertical flume was designed and built. The tests samples were made of an accepted surrogate waste material. Variations from that waste material, such as degree of degradation of the waste the surrogate material represents and compactions pressure applied to the samples, were also tested.

3 DEVELOPMENT OF SURROGATE WASTES

Surrogate materials are used to represent a conservative estimate of degraded TRU waste materials throughout the WIPP regulatory period. Suitable surrogate materials have been selected based on anticipated future states of the waste considering inventory, underground conditions, evolution of the underground environment, and the physical and chemical processes that occur. Butcher et al. (1991) investigated the mechanical compaction of simulated wastes. They identified five dominant waste components contained within contact handled TRU waste drums:

- Plastics
- Fibers (cellulosics: paper, cloth, wood, etc.)
- Sorbents
- Metals and metal components
- Sludge

Based on these waste components, a range of simulation materials were selected as described in Table 1. The simulation materials were classified into three major components (summarized in Table 2):

- Combustible Waste: Fiber and plastic, with smaller quantities of metals and sorbents
- Metallic Waste: Metals, with smaller quantities of fiber, plastics and sorbents
- Sludge Waste: Inorganic or organic sludge with smaller quantities of plastics and sorbents.

Wawersik (2001) conducted one-quarter scale laboratory experiments to evaluate the response of waste packages and crushed salt backfill to quasi-static loading. Wawersik evaluated a combustible waste mixture based on Butcher et al. (1991) (see Tables 1 and 2) consisting of the following materials:

- | | |
|--|-----|
| • Metal parts (2-in long pieces of 1/2-in steel conduit and 3/8-in copper tubing) | 9% |
| • Wood waste (1-in wood cubes); rags | 37% |
| • Plastics (2-in long pieces of 5/8-in diameter polyethylene pipe and 1/2-in diameter schedule 40 PVC pipe; thin-wall bottles with a wall thickness of 0.035 in) | 45% |
| • Sorbents (50:50 mixture of Portland cement and Oil-Dri®) | 9% |

Table 1. Simulated waste materials (Butcher et al., 1991, Table 2-1)

Mixture Number	Description
1	Pine sawdust
2	Pine wood cubes, approximately 1" in dimension
3	A mixture of 60% by weight pine wood cubes; 40% by weight cut-up rags
4	A mixture of intact (small) and cut-up (large) polyethylene bottles
5	Polyethylene pellets (Phillips Petroleum Marlex bottle blowing grade or equivalent)
6	A mixture of 40% by weight intact (small) and cut-up (large) polyethylene bottles with caps; 40% by weight polyvinyl chloride (PVC) conduit of various diameters with fittings (loose); 20% by weight surgical gloves
7	A mixture of 50% by weight polyethylene pellets and 50% by weight PVC conduit of various diameters with fittings (loose)
8	Oil-Dri®
9	Vermiculite
10	Portland cement
11	1" dimension cut-up steel, copper, lead, and aluminum scrap (thin-walled conduit, curtain rods, light hardware, small pipe fittings, other metal junk)
12	Up to 3" dimension cut-up steel, copper, lead, and aluminum scrap (thin-walled conduit, curtain rods, light hardware, small pipe fittings, other metal junk)
13	A layered mixture of moist sand and dry cement. Several layers of each in a sample with the thickness of the sand layers at least equal to or as much as 2 times the thickness of the cement layers (simulated inorganic sludge)
14	The bottom of the sample was a layer of crushed salt with the rest of the sample metal waste

Table 2. Test materials for drum collapse tests (Butcher et al., 1991, Table 2-9)

Material Number	Material Type	Material Description	
1	Combustible Wastes	Metal	9%
		Fiber	37%
		Plastics	45%
		Sorbents	9%
2	Metallic Wastes	Metal	83%
		Fiber	2%
		Plastics	10%
		Sorbents	5%
3	Sludge Wastes	Sludge	91%
		Plastics	1%
		Sorbents	8%

Notes:

Individual materials were as follows:

Metal: Up to 12" dimension cut-up steel, copper, lead, and aluminum scrap (conduit, fittings, junk). Approximately 60% of the metal for each drum was steel.

Fiber: A mixture of 60% by weight pine wood cubes or pieces (maximum dimension 12" long x 3" wide x 1" thick: 50% of the pieces full size, the remainder equal to or less than 6" long): 40% by weight rags.

Plastics: A mixture of 50% by weight polyethylene bottles with caps and other pieces of polyethylene: 40% by weight PVC conduit and fittings: 10% by weight surgical gloves.

Sorbents: 50% by weight Oil-Dri® (baked clay pellets): 50% Portland cement. The materials were not mixed.

Sludge: A layered mixture of moist sand and dry cement, with the thickness of the sand layers equal to, up to twice, the thickness of the cement layers.

All commercial grade materials were obtained from local retailers or standard manufacturing or laboratory suppliers. Materials were tested "as purchased" (e.g., surface paint was not removed). Both new and used metals were tested.

Hansen et al. (1997) identified the initial characteristics of the waste anticipated for the WIPP based on the TRU waste baseline inventory report (DOE, 1996b), including waste categories, descriptions, and the relative proportions of the waste constituents as provided in Table 3. Example TRU waste at WIPP is shown in Figure 1. Degraded waste properties using surrogate materials were determined by Hansen et al. (1997) for use as input parameters for modeling the release of waste material to the surface during an inadvertent borehole intrusion.

Surrogate mixtures were defined by Hansen et al. (1997) for four waste degradation and MgO backfill emplacement scenarios:

1. A 50% case where half of the iron is corroded and half of the cellulose, plastics, and rubber are degraded.
2. A 100% case where all of the iron is corroded and all cellulose, plastics, and rubber are degraded.
3. A 50% case with MgO, which is identical to Number 1 above with an appropriate amount of MgO added.
4. A 100% case with MgO, which is identical to Number 2 above with an appropriate amount of MgO added.

For the tests conducted herein, a 75% degraded surrogate material was developed based on the methodology developed Papenguth and Myers (Appendix A, Hansen et. al., 1997).

Representative surrogate materials for degraded waste and their relative proportions for each level of degradation used in the tests reported herein are listed in Table 4. No MgO was included in any of the surrogate waste materials.

Table 3. Anticipated initial waste characteristics and concentrations (Papenguth and Myers, Appendix A, Tables 1 and 2 in Hansen et al., 1997)

Waste Category	Description	Inventory		
		Average (kg/m ³)	w/out MgO (weight %)	w/ MgO (weight %)
Iron-base metal/alloys	This designation is meant to include iron and steel alloys in the waste and does not include the waste container materials. This also includes an iron-base metallic phase associated with any vitrification process, if applicable.	170	22%	14%
Steel container material	The weight of the steel part of the packaging from container information provided by the TRU generator/storage sites. Any necessary overpacking is included in the weight.	139	18%	12%
Aluminum-base metals/alloys	Aluminum or aluminum-base alloys in the waste materials.	18	2%	1%
Other metals/alloys	All other metals found in the waste materials (e.g., copper, lead, zirconium, tantalum, etc.). The lead portion of lead rubber gloves/aprons is also included in this category.	67	9%	6%
Other inorganic materials	Includes inorganic non-metal waste materials such as concrete, glass, firebrick, ceramics, graphite, sand, and inorganic sorbents.	31	4%	3%
Vitrified	This refers to waste that has been melted or fused at high temperatures with glass forming additives such as soil or silica in appropriate proportions to result in a homogeneous glass-like matrix. (Note that any unoxidized metallic phases, if present, are included in the "iron-base metal/alloys" waste material parameter).	55	7%	5%
Cellulosics	Includes those materials, generally derived from high polymer plant carbohydrates. Examples are paper, cardboard, Kimwipes, wood, cellophane, cloth, etc.	54	7%	4%
Rubber	Includes natural or manmade elastic latex materials. Examples are Hypalon®, Neoprene, surgeons' gloves, leaded-rubber gloves (rubber part only), etc.	10	1%	1%

Table 3. (continued).

Waste Category	Description	Inventory		
		Average (kg/m ³)	w/out MgO (weight %)	w/ MgO (weight %)
Plastics	Includes generally manmade materials, often derived from petroleum feedstock. Examples are polyethylene, PVC, Lucite®, Teflon, etc.	34	4%	3%
Plastic container/liner material	The weight of any plastic packaging submitted by the TRU site. When weight of a rigid liner is not given a 90-mil HDPE (high-density polyethylene) liner is assumed.	26	3%	2%
Solidified inorganic material (including the cement)	Includes any homogeneous materials consisting of sludge or aqueous-base liquids that are solidified with cement, Envirostone®, or other solidification agents. Examples are wastewater treatment sludge, cemented aqueous liquids, and inorganic particulate, etc. If a TRU waste site has not reported cement used as part of the solidification process in the “cement (solidified)” waste material parameter, the density of the cement is included in this field.	54	7%	4%
Solidified organic material not (including the cement)	Includes cemented organic resins, solidified organic liquids, and sludges.	5.6	1%	0%
Solidification cement	Includes the cement used in solidifying liquids, particulate, and sludges. If for a solidified final waste form this field is left blank, it means that either cement is not the solidifying agent or that the cement is included in the “solidified inorganic material” WMP.	50	7%	4%
Soils	Generally consists of naturally occurring soils that have been contaminated with inorganic radioactive waste materials.	44	6%	4%
MgO backfill	Serves as an engineered barrier by decreasing the solubilities of the actinide elements in TRU waste in any brine present in the repository after closure.	451	0%	37%



Figure 1. Example of transuranic radioactive waste at WIPP.

Table 4. Degraded surrogate waste materials. Cases 1 and 2 are from Hansen et al. 1997, Table 2-2, Table 2-3, and Appendix A, Table 8. Case 3 uses the same methodology as discussed in Hansen et al. (1997) and was developed for the present set of tests.

Waste Category	Example Waste Simulants	Relative Weight Proportions of Surrogate Waste Constituents		
		Case 1	Case 2	Case 3
Iron-base metal, alloys; steel container material	Strips of steel sheet metal, small nails (cut up), scraps of steel or iron material	1.9	0.0	0.9
Corroded iron-base metal, alloys; steel container material; corroded nonferrous metal and alloys	Scrapings from rusted steel or iron; supplement with Fe(III)O.OH (goethite or limonite rock samples) crushed sand- to silt-sized particles	4.6	7.3	6.0
Other inorganic materials: vitrified	Broken labware, broken glassware	1.0	1.0	1.0
Cellulosics; rubber; plastics; plastic container/liner material	Equal masses of finely shredded paper, snipped cotton balls, sawdust, shredded plastic grocery bags, o-rings, rubber gloves, rubber bands, polyethylene sheet and bottles, and peat (no vermiculite)	0.7	0.0	0.4
Solidification cement	Broken hydrated concrete and mortar, crumbled sheet-rock	1.2	1.2	1.2
Soils	Natural soil	0.5	0.5	0.5
Salt precipitate. corrosion induced		0.5	0.9	0.7
Total Batch Size		10.4	10.9	10.7

Notes:

- Case 1 – A 50% degraded surrogate waste material representing the case where half of the iron is corroded and half of the cellulosics, plastics, and rubber are degraded.
- Case 2 – A 100% degraded surrogate waste material representing the case where all of the iron is corroded and all cellulosics, plastics, and rubber are degraded.
- Case 3 – A 75% degraded surrogate waste material representing the case where three quarters of the iron is corroded and three quarters of the cellulosics, plastics, and rubber are degraded.

4 TESTING APPARATUS DESCRIPTION

4.1 Vertical Flume Design and Operation

The vertical erosion flume is based on a horizontal sediment flume first built and routinely used in the Department of Mechanical and Environmental Engineering, University of California, Santa Barbara (UCSB) (Taylor and Lick, 1996; McNeil et al., 1996; Jepsen et al., 1997). The UCSB flume was named the Sediment Erosion at Depth flume, or SEDflume for short. The original purpose of SEDflume was to directly measure the erosion rate and critical shear stress of relatively undisturbed or laboratory developed sediments over a wide range of unidirectional flow induced shear stresses and their variation with depth below the sediment-water interface. The SEDflume's capabilities were a tremendous step forward in the science of sediment dynamics. Today SEDflume is considered the industry standard for measuring sediment erosion and is being widely used by the US EPA, the US Army Corps of Engineers (USACE), and consulting companies (Lick, 2009).

Pictures of the vertical erosion flume are shown in Figure 2 through Figure 5. It is an enclosed straight flume, containing a test section with an open side through which a polycarbonate tube having a circular cross-section containing surrogate waste sample is inserted. The flume can be rotated and operated in either a vertical or horizontal position for standard erosion testing. The main components of the flume are the erosion channel including erosion test section (Figure 2); a flow inlet section for uniform, fully developed, laminar and turbulent flow; a flow exit section; fluid storage tanks (Figure 3); a pump to force fluid through the system (Figure 4); a diverter valve; the sample container; and a step motor in combination with a linear rail table used to advance the sample into the flume channel (Figure 5). A data acquisition system (DAS) is used to control all mechanical components and record sample movement distance, fluid flow rate, fluid pressure in the erosion channel, and fluid temperature and conductivity.

The test section, inlet section, and exit section are made of clear polycarbonate (Lexan[®]) and stainless steel so that the sample-fluid interactions can be observed visually. The fluid in the flume is contained in two storage tanks that act as a baffle tank to help prevent fouling of the pump. The heavier eroded surrogate waste debris settles out of suspension in the return tank prior to the fluid passing over into the supply tank for recirculation in the system. To prevent lighter material from recirculation, screens are placed on the outlet hoses of the return tank going into the supply tank. Fluid from the supply tank is pumped through the system through a 5 cm (2 in) diameter pipe, and then into the rectangular erosion channel. The outlet of flume channel is routed through a 7.6 cm (3 in) return line comprised of flexible hosing and PVC piping. The increase diameter of the return line is intended to minimize the head pressure of the fluid inside the channel. The fluid used in these tests was tap water. Of importance is that the density and viscosity of the fluid are determined through water quality measurements (temperature and conductivity) so that the flow can be regulated to subject the samples to a known hydrodynamic shear stress. The method for determining the applied shear stress is a function of fluid properties.

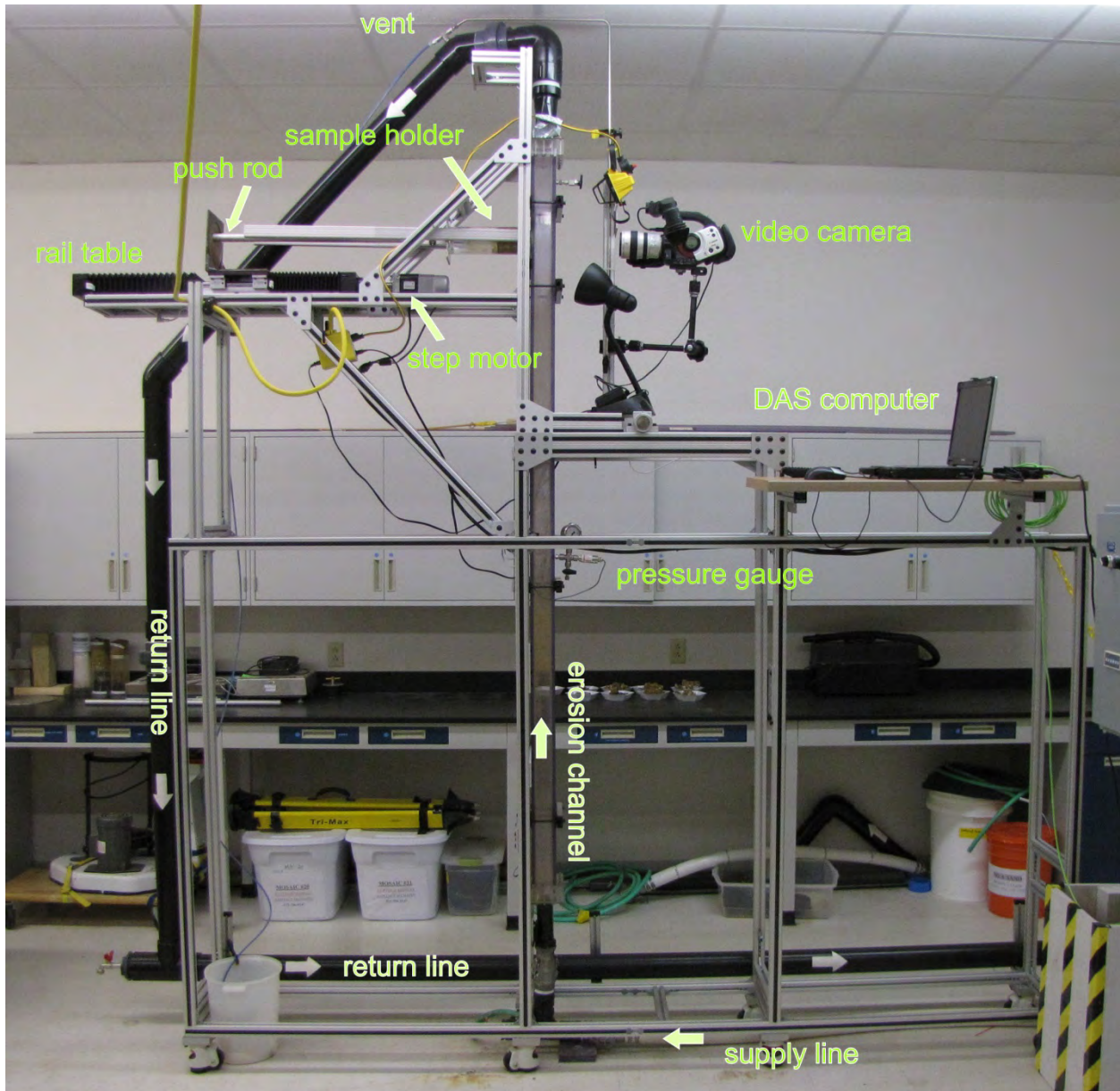


Figure 2. Picture of the fully enclosed erosion channel and components of the vertical erosion flume. The eroding fluid is delivered to the channel by a supply line. The erosion channel is long enough to develop laminar flow at the lowest flow rates and fully turbulent flow at the highest anticipated flow rates. The vent is used to control the pressure on the face of the sample, which is monitored by the pressure gauge. The fluid is returned to the fluid supply tanks (Figure 3).

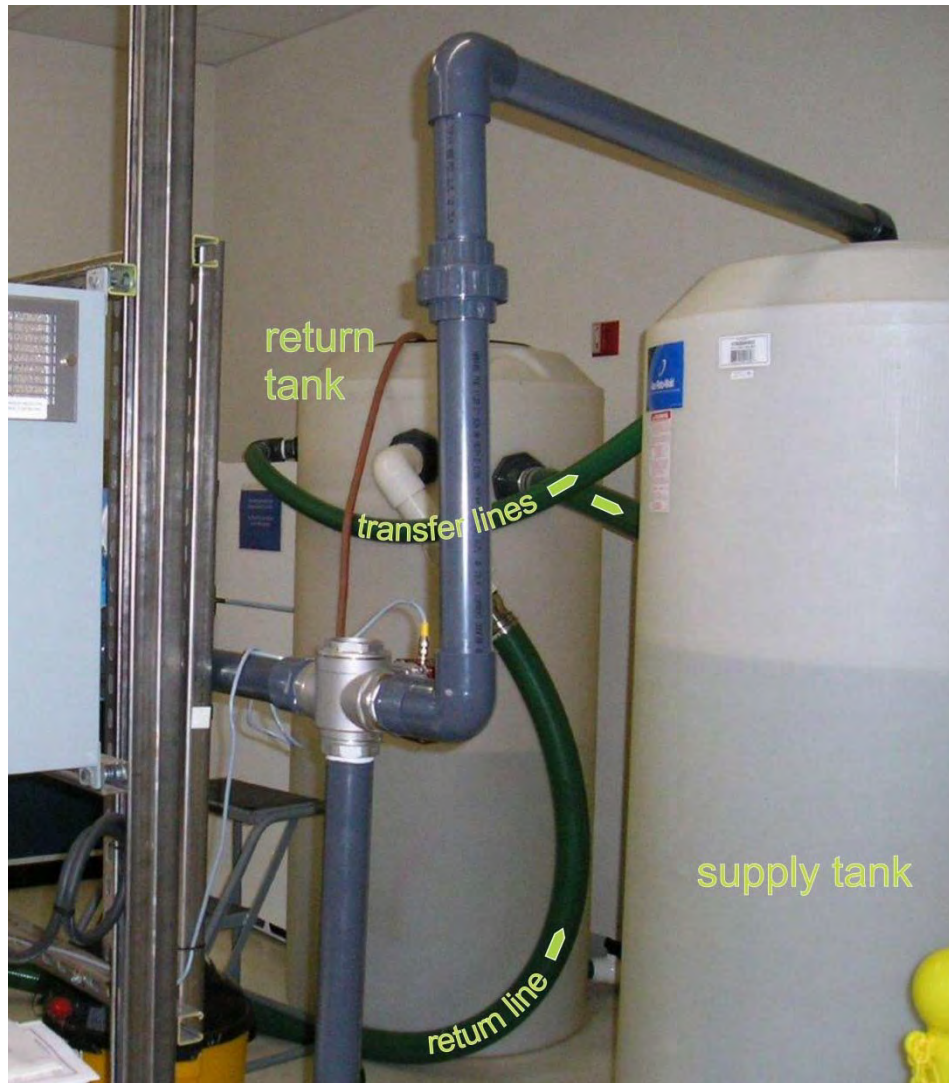


Figure 3. Picture of the fluid storage system. Fluid is recycled back from the erosion channel to the return tank, which acts as a baffle tank to drop out large or heavier pieces of eroded material. The fluid is then screened and transferred to the supply tank. The purpose of the screening is to capture large light material such as pieces of plastic that can foul the pump. The fluid is pumped back to the erosion channel. Both tanks are 300 gal (1135 L).

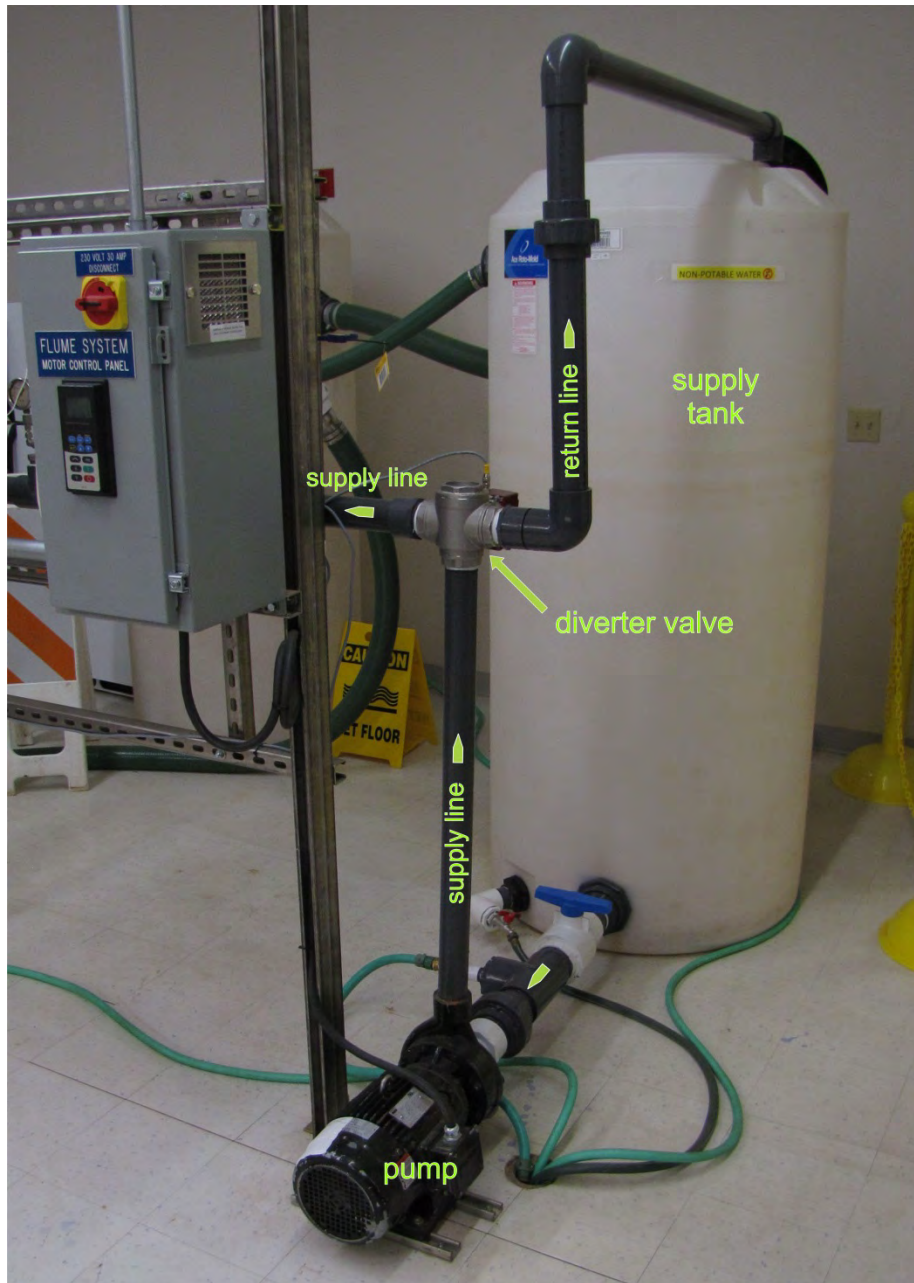


Figure 4. Picture of fluid pump, diverter valve, and associated plumbing. Diverting the fluid back into the supply tank helps control the flow when slow flow rates required.

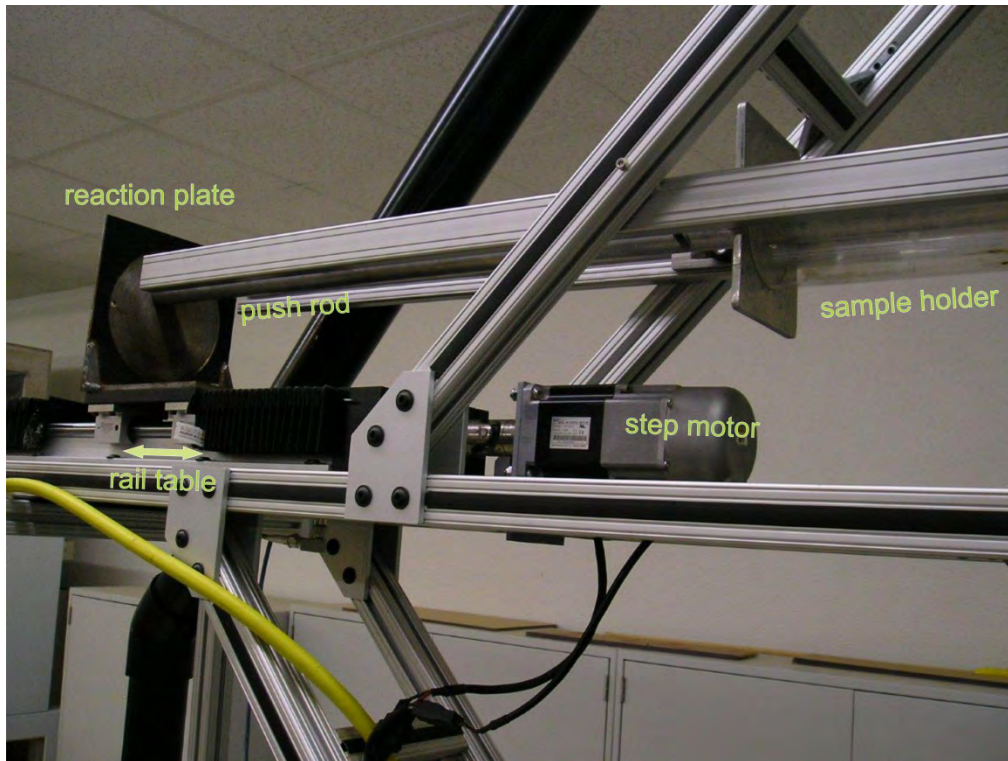


Figure 5. Picture of apparatuses used to advance the specimen into the flow of the channel. A step motor controlled by the DAS system is used to move the linear rail table with attached reaction plate. The push rod connects to a plunger in the sample holder, in front of which is the sample. In this picture the sample has been eroded away and the plunger is at the side of the channel.

The erosion flume is modular in design such that the erosion channel and pump can be swapped out to generate a variety of flow conditions. The erosion channel can be rotated on an axle that allows the flume to operate in either the vertical or horizontal position. For the tests discussed in this document the flume was operated in the vertical position. The flume's enclosed (internal flow) erosion channel has a height of $5.4 \text{ cm} \pm 0.1 \text{ cm}$, a width of $10.345 \text{ cm} \pm 0.1 \text{ cm}$, and a length of $240 \text{ cm} \pm 1 \text{ cm}$ (Figure 2). In this way, the height of the channel, that is the distance between the channel's far edge and the surrogate waste sample surface, matches the typical distance between the borehole wall and the drill stem (5.4 cm). The erosion channel houses the erosion test section, presently fitting an 8.25 cm (3.25 in) diameter test specimen. The erosion test section is preceded by approximately 212 cm of enclosed rectangular channel needed to create fully developed flow over the surrogate waste sample. Note that the sample diameter at 8.25 cm is narrower than the erosion channel (10.345 cm). This is to reduce the effect of the walls.

A variable speed pump and three-way diverter valve regulates the flow so that part of the flow goes into the erosion channel while the remainder returns to the supply tank for the low shear stress regimes (Figure 4). As the shear stress setpoint increases a greater portion of fluid is routed into the flume channel. Both the pump and the valve are controlled by the data acquisition system (DAS). The flow rate of the circulating fluid can exceed 550 L/min (145 gal/min) and is monitored by an Endress-Hausser flow meter. There is a small vent valve in the erosion channel

immediately downstream from the test section, which is operated to maintain a consistent pressure gradient at the surrogate waste material insertion point.

At the start of each test, the sample holder and the surrogate waste sample are attached to the test section on the side of the channel. An operator moves the sample laterally using a piston inside the sample holder (Figure 5). The piston is connected to the linear rail table which is driven by the step motor, the combination of which can extrude samples with lengths up to 70 cm. For this testing activity the samples were nominally 20 cm. The rail table step motor is controlled by the DAS. The extrusion speed of the surrogate waste sample can be controlled at a variable rate of 1-200 rpm, where one revolution is equal to 5.14 mm. When advancing a sample a step increment as small as 0.25 mm is measurable and controllable with this system.

As a general test procedure, the fluid is forced upward through the enclosed channel and across the surface of the sample. The shear produced by this flow may cause the sample to erode. If at a particular flow rate and shear stress no erosion is observed, the flow is incrementally increased until erosion is observed or the limit of the pump is reached. If the surrogate waste sample in the tube erodes, additional material is advanced laterally by the operator so that the sample-fluid interface remains flush with the side of the test sections. The erosion rate is recorded as the lateral movement of the sample in the coring tube over time. The time of erosion and the sample extrusion distance, for each shear stress level are recorded by both the DAS and the operator in a scientific notebook. Additionally, the surrogate waste sample erosion activity is documented using a digital video camera.

4.2 Determination of Applied Hydrodynamic Shear Stress

Turbulent flow through pipes has been studied extensively, and empirical functions have been developed which relate the mean flow rate to the wall shear stress. In general, flow in circular cross-section pipes has been investigated. However, the relations developed for flow through circular pipes can be extended to non-circular cross-sections by means of a shape factor. An implicit formula relating the wall shear stress to the mean flow in a pipe of arbitrary cross-section can be obtained from Prandtl's Universal Law of Friction (Schlichting, 1979). For a pipe with a smooth surface, this formula is

$$\frac{1}{\sqrt{\lambda}} = 2.0 \log \left[\frac{UD\sqrt{\lambda}}{\nu} \right] - 0.8 \quad (1)$$

where U is the mean flow speed, ν is the kinematic viscosity, λ is the friction factor, and D is the hydraulic diameter defined as the ratio of four times the cross-sectional area to the wetted perimeter. For a pipe with a rectangular cross-section, or duct, the hydraulic diameter is

$$D = 2hw / (h + w) \quad (2)$$

where w is the duct width and h is the duct height. The friction factor is defined by

$$\lambda = \frac{8\tau}{\rho U^2} \quad (3)$$

where ρ is the density of water and τ is the wall shear stress. Inserting Eqs. (2) and (3) into Eq. (1) gives the wall shear stress τ as an implicit function of the mean flow speed U .

For all shear stresses in the range of 0.05 to an anticipated 10 Pa created with the use of tap water, the Reynolds numbers, UD/ν , are on the order of 10^4 to 10^5 . These values are sufficient for turbulent flow to exist for the shear stresses of interest in this study. For flow in a circular pipe, turbulent flow theory suggests that the transition to fully developed turbulent flow occurs within 25 to 40 diameters from the entrance to the pipe. Since the hydraulic diameters of the ducts ranges from 6.8-8.7 cm, this suggests an entry length as short as approximately 170-220 cm and as long as 270-350 cm. The length of the erosion channel leading to the test section is 212 cm and is preceded by a 20 cm flow converter and several meters of inlet pipe. These arguments, along with direct observations, insure fully developed turbulent flow in the test section.

4.3 Data Acquisition and Control

The incorporation of a data acquisition system (DAS) on the vertical flume has greatly enhanced the accuracy and reliability of this experimental program. The DAS consists of three subsystem components that control processes and collect the data. The three components are: hardware, instrumentation, and the operator interface computer and software.

4.3.1 Hardware

The DAS hardware was designed and built utilizing a modular approach that incorporates components directly available from SIXNET, Inc. The SIXNET hardware includes the SixTRAK remote terminal unit (RTU), discrete input/output (I/O) modules, and analog I/O modules. The SixTRAK RTU processor is equipped with: 512 KB static RAM, 16 MB dynamic RAM, and 16 MB flash RAM; uses the LINUX operating system; and features both Ethernet and serial communication ports. The I/O modules can measure various types of analog signals to a 16-bit resolution and can be expanded from 8 to 512 channels with additional modules. All modules have an operating temperature range of -30° to 70°C . The DAS components are mounted within a rack mounted enclosure, which also incorporates the power supplies, circuit breakers, fuses, and relays to protect and control the system.

The hardware includes a 3-way valve to proportionally divide the direction of the fluid flow and a variable frequency drive (VFD) to control the pump motor speed. This control includes the starting/stopping of the pump motor and control of the motor speed. A closed loop control process is established by monitoring the flow rate (as the control variable) and automatically adjusting the 3-way valve position and the motor speed (as the process variable) to maintain a constant flow through the system. The target flow rate are selected by the operator, and the system will maintain flows at better than $\pm 2\%$ of the target flow rate.

4.3.2 Instrumentation

Flow through the flume system is measured by an in-line flow meter located in the upstream end of the flume supply line. The flow meter is capable of measuring the flow to an accuracy of $\pm 1\%$ of the full scale range of the instrument (Table 5). The flow into the primary flume line is controlled using the 3-way directional valve and pump motor speed controller (a VFD to power the pump). The pump and associated controls are capable of developing water flow rates of 0-550 L/min in the flume channel. The pump performance will vary if other than water is used as the erosion fluid. The flow meter is used as the control variable for the 3-way valve position and the pump motor speed.

Water quality (temperature and specific conductance), used for the determination of fluid density and viscosity, is also measured in the flume supply line. The temperature is measured with a resistive temperature device (RTD) having an accuracy of $\pm 1.0^\circ\text{C}$. The conductance of the fluid used in the flume is measured using a GLI 3725E2T probe with an accuracy of $\pm 5.0\%$ of selected range of measurement (Table 5).

The sample feed rate and control systems for advancing the sample into the flow stream are based on a linear rail table that advances the sample by using an encoder to count the revolutions of the screw-type step motor. The number of revolutions correlates with the distance that the table advances. Using this method the travel of the sample can be tracked within ± 0.1 mm.

Table 5. Measurement and test equipment in use on the vertical flume.

Type	Function	Accuracy
Endress-Hauser ProMag 53 magnetic flow meter	Measures flow rates between 0 and 950 L/min (water)	1% of full scale
GLI 3725E2T specific conductance probe & Pro-E3 transmitter	Measures specific conductance of produced water; data logged by DAS	5% of full scale
Omega 3-Wire RTD 806 Series temperature probe	Measures fluid and laboratory temperatures	1.0°C
Omegadyne PX209 pressure transducer	Used to measure pressure in the erosion channel	0.50% of full scale

4.3.3 Software

Using the Human Machine Interface (HMI) software the operator is able to select and configure system set points that are utilized to operate the test. This includes setting flow rates for the test, sample advancement, and data storage times, etc. The operator interface visually displays real-time feedback on the test parameters being monitored. These parameters can be presented both graphically and in tabular form. The system automatically calculates certain test values such as the shear stress based on the measured parameters, eliminating the need to process the data off-line after the test completion.

4.4 Sample Preparation

Conceptualization of the underground suggested that the most likely future state of the waste materials includes crushing, compaction, cementation by MgO and degradation byproducts, and entombment by the surrounding salt. The waste inventory is comprised of large steel components including standard 55-gallon drums, standard waste boxes, thick steel pipe overpacks, and supercompacted waste “pucks” stored in overpacks. The bulky nature of the inventory suggests that freeing and transporting of radionuclides extremely difficult. In the most extreme cases, however, the expected processes of iron corrosion and microbial activity result in predictions of extensive degradation especially of waste from standard drums, which make up the majority of the WIPP inventory. This end state represents a bounding condition for the waste, providing a means to quantify the lowest strength conditions of the future state of the degraded waste. Other, denser, waste forms such as pipe overpacks and supercompacted waste packages are expected to degrade and corrode to a lesser extent, and therefore will have material characteristics which are much less conservative than those assumed for standard drum wastes.

Hansen et al. (1997) developed their model material from the estimated inventory of standard waste drums, the anticipated future state of the waste, evolution of the underground environment, and relevant experimental results. The surrogate waste comprised a mixture of raw materials including iron, glass, cellulose, rubber, plastic, degradation byproducts, solidified cements, soil, and WIPP salt. Hansen et al. (1997) considered degradation of each waste constituent. Subsurface processes leading to extreme degradation are based on several contributing conditions including ample brine availability, extensive microbial activity, corrosion, and the absence of cementation, and salt encapsulation effects. Hansen et al. (1997) assert that the degraded waste material properties represented the lowest plausible realm of the future waste state because no strengthening processes were included such as compaction, cementation, mineral precipitation, more durable packaging, compressed waste, and less corrosion. It is believed that the samples used by Jepsen et al. (1998) and the tests reported herein represent an unobtainable degraded state of the waste, are thus far weaker than any possible future state, and will pertain to any changes that may occur in the waste inventory (Hansen et al., 2003; Hansen, 2005).

The surrogate waste material developed for the tests performed by Jepsen et al. (1998) and the procedure followed to form the specimens were re-created as part of this test program with a few changes. Three surrogate waste types were used, 50%, 75%, and 100% degraded surrogate waste, saturated in brine similar to the WIPP brine, as discussed in Section 3. The surrogate waste samples for the Jepsen et al. tests were subjected to 5 MPa compaction pressures for a minimum of 15 hours during fabrication. Numerical modeling performed by Herrick et al. (2007a) suggests that a compacting pressure of 2.3 MPa is the minimum level the waste in the underground will be subject to. This is the second compacting pressure used.

The flume test samples were fabricated in the SNL Geomechanics Laboratory in Albuquerque under WIPP Quality Assurance guidelines according to the procedure outlined below. The samples were picked up and hand delivered to SNL-Carlsbad in an automobile by Sandia staff members. The samples remained sealed in the sample holders until testing.

4.4.1 Specimen Assembly

The dry constituents are assembled first. The sample mixture recipes for a sample are listed in Table 6 for the three levels of waste degradation simulated. The amount of each constituent added to a sample is recorded on a sample preparation form.

Table 6. Material recipes for the dry ingredients for each sample type: 50%, 75%, and 100% degraded surrogate wastes. These are batch target weights in grams (g).

Simulant Material	50% Degraded	75% Degraded	100% Degraded
Steel	196.96	100.01	0.00
Alloys	196.96	100.01	0.00
Iron Oxide	953.72	1312.18	1707.79
Glass	207.32	227.67	233.94
Paper	14.51	8.03	0.00
Cotton	14.51	8.03	0.00
Sawdust	14.51	8.03	0.00
Peat	14.51	8.03	0.00
Poly-Sheet	14.51	8.03	0.00
Poly-Bottle	14.51	8.03	0.00
Plastic Bags	14.51	8.03	0.00
Gloves	14.51	8.03	0.00
Rubber Bands	14.51	8.03	0.00
O-Rings	14.51	8.03	0.00
Sheetrock	124.40	134.64	140.36
Concrete	124.40	134.64	140.36
Soil	103.67	113.92	116.97
Salt	97.44	151.69	210.55
Total	2150	2350	2550

The particle sizes of each material constituent are listed in Table 7. Photographs of the materials used in the surrogate waste samples are shown in Figure 6 through Figure 10.

Table 7. Simulant material particle sizes for the surrogate waste materials.

Simulant Material	Details and Particle Size
Iron, not corroded:	Steel (1 to 2 mm thick), ~ 5 to 10 mm squares, (3/8" sieve material).
	Alloys are (1 to 2 mm thick), ~ 5 to 10 mm squares. Hardware includes bolts, nuts, washers, and nails.
Corroded iron and other metals:	Iron oxide (goethite) to pass no. 18 (1 mm or 0.0394") sieve.
Glass:	2 to 3 mm thick and pass a 3/8" (9.5mm) sieve.
Cellulosics:	Paper (6 to 8 mm squares).
	Cotton (thin strands ~ 0.5 to 1" long).
	Sawdust (as received).
	Peat (as received).
Plastics:	Poly-sheet (6 to 8 mm max. dimension).
	Poly-bottle (6 to 8 mm max. dimension).
	Shredded plastic grocery bags.
Rubber:	Rubber gloves (6 to 8 mm maximum size).
	Rubber bands (6 to 8 mm maximum size).
	O-rings (6 to 8 mm maximum size).
Solidification cements:	Sheetrock and Concrete: all pass 3/8" (9.5mm) sieve.
Soil:	Typical soil (collected outside machine shop door of the Geomechanics Lab - passes the 3/8" (9.5mm) sieve.
Salt:	WIPP Salt: to pass the 3/8" (9.5mm) sieve.



Figure 6. Steel, alloys, iron oxide, and glass constituent materials.

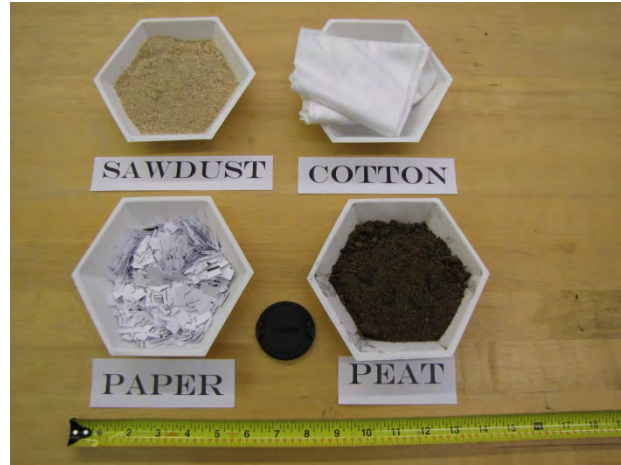


Figure 7. Sawdust, cotton, paper, and peat constituent materials.



Figure 8. Poly sheet and poly bottle constituent materials.



Figure 9. O-rings, rubber bands, plastic bag, and rubber glove constituent materials.



Figure 10. Soil, sheetrock, WIPP salt, and concrete constituent materials.

Brine derived from WIPP salt is then introduced to saturate the material recipes. The amount of brine required for each different degraded material sample is as follows:

- a.) 50% degraded material sample; 887.95 (g) WIPP salt derived brine,
- b.) 75% degraded material sample; 737.20 (g) WIPP salt derived brine,
- c.) 100% degraded material sample; 586.50 (g) WIPP salt derived brine.

After the dry material constituents are thoroughly mixed in a steel bowl, the brine is then introduced, and complete assimilation is then accomplished (Figure 11).



Figure 11. Batch of 100% degraded surrogate material being readied to be introduced into a Lexan sample holder.

In the most timely fashion possible, each brine saturated recipe is then introduced into either an aluminum jacket (75% degraded surrogate material), or a Lexan® jacket (50% or 100% degraded surrogate materials (Figure 12). Aluminum jackets (12" H, 3.125" I.D.) and Lexan® jackets (10" H, 3.125" I.D.) are assembled with: (1) a bottom aluminum platen, filtered topped, fitted with an 'O'-ring on the top, (2) a bottom support base with a steel spacer, (3) two square bottom spacers to keep the aluminum or Lexan® jacket from sliding to the support base, (4) a top, Lexan® platen, fitted with an 'O'-ring around it's center (Figure 13 through Figure 15). The sample recipe material introduced into each jacket should not exceed 7 inches in fill height.

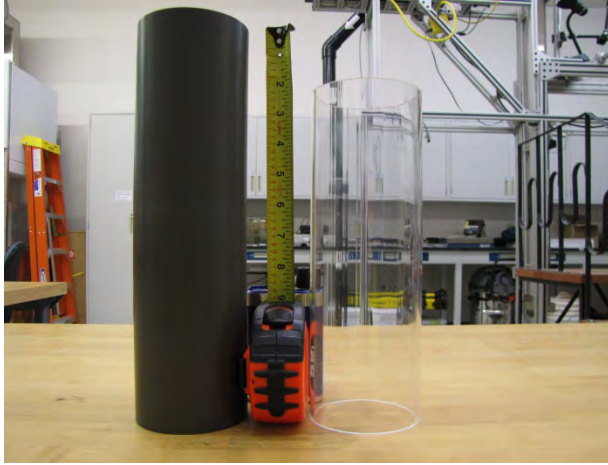


Figure 12. Aluminum and Lexan sample holders.



Figure 13. Aluminum jacket and associated hardware for sample assembly and load-cell introduction.



Figure 14. Sample assembly preparation.

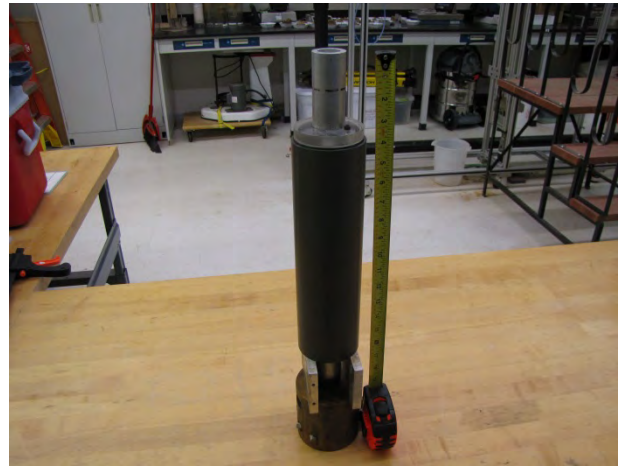


Figure 15. The sample is loaded in the aluminum jacket with the associated hardware

The jacketed samples are then fitted with a center split, compression sleeve. This protects the sample during the compressional load test (Figure 16). After compaction at stresses of 2.3 MPa or 5.0 MPa, and a load time of approximately 13 – 17 hours, the final product is measured for sample length and weight. The compression load and load time are also recorded on the sample preparation form. The sample is now ready to undergo flume erosional testing (Figure 17).

5 DETERMINATION OF CRITICAL SHEAR STRESS FOR EROSION

To determine the critical shear stress for the initiation of erosion, it is necessary to subject the sample to a range of shear stresses such that at the lowest applied shear stresses no erosion will occur. Progressively higher levels are applied, leading to the beginning of erosion and multiple erosion rates thereafter. The manner in which the shear stresses are raised is noted in the laboratory notebook. Each shear stress level is typically run for one hour depending on whether or not the sample is eroding and how fast it is occurring. The DAS records the time, extrusion distance, and all test parameters automatically when the sample is moved. After the predetermined duration is reached at a particular stress level, the flow is increased to the next shear stress. This procedure continues until the highest shear stress is reached or the sample is completely eroded away.

The samples are fabricated as described above, attached to the testing apparatus, and then moved laterally into the test section until the sample surface is even with the channel surface. The flume is then run at a specific flow rate corresponding to a particular shear stress. In its present configuration the flume is capable of creating shear stresses exceeding just over 5.5 Pa on the surface of the sample. As the fluid speed is increased, the shear stress across the face of the sample increases until erosion of the material begins. Erosion rates are obtained by measuring the amount of sample movement over a time interval at a particular shear stress level.

Due to a gradual increase in erosion as the shear stress increases, it is difficult to precisely define a critical velocity or shear stress at which erosion first takes place. This complexity is compounded as the nature of the erosion often occurs in isolated spots over a larger surface. Critical shear stress is calculated from the measurement of erosion rates in a number of ways. The most widely accepted methods are described in briefly test plan TP 09-01. The three methods are:

1. Bilinear fit
2. SEDflume based linear interpolation
3. SEDflume based power law relationship

5.1 Bilinear Fit

The bilinear method was originally proposed by Parchure and Mehta (1985). They showed that a plot of the erosion rate versus shear stress of their flume testing results could typically be divided into two distinct linear regions. The lower line corresponds to the behavior of the surface layer and the upper line to the mass or bulk of the material which represents the behavior of the sample away from end effects of the sample. Teeter (1987) suggested that the most conservative estimate of the mass shear strength of the material is given by an extension of the upper line to where the erosion rate is zero. The two lines were determined based on the highest R^2 value according to the precedence: (1) overall, then (2) the upper line. Herrick et al. (2007b) used this value as an estimate of the minimum shear strength of the surrogate waste material tested by Jepsen et al (1998) (Figure 18). Herrick et al. (2007b) used the symbol τ_m to describe this shear strength value, where m indicates that it represents the interior mass of the sample. This method is referred to in the following analysis as the University of Florida (UF) or Mehta method.

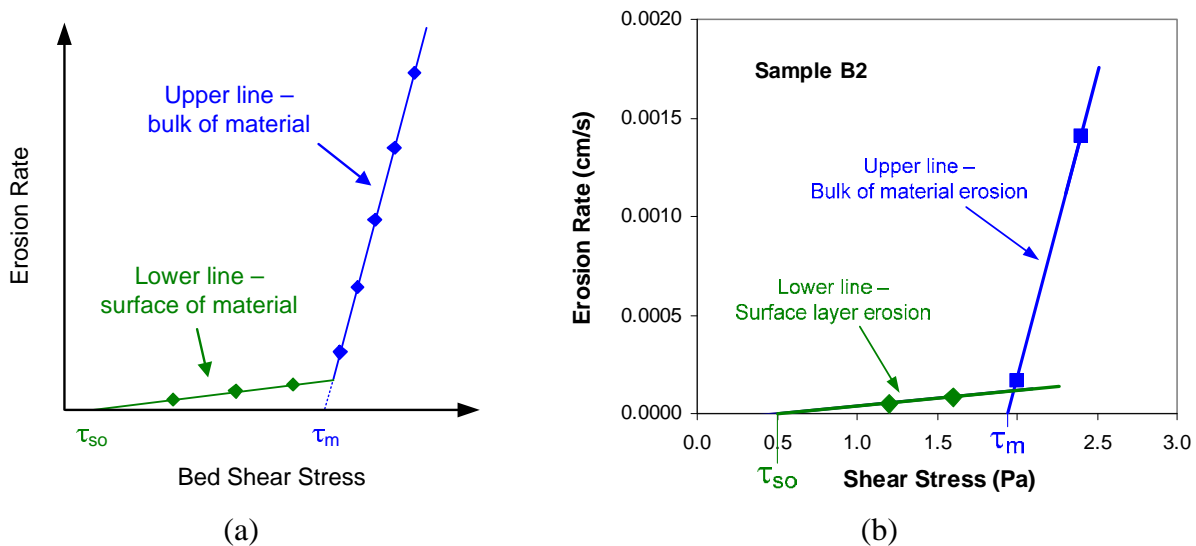


Figure 18. (a) Idealization of the bilinear method of analyzing erosion data. Extrapolation of the upper line, which represents the erosion behavior of the bulk of the material, back to an erosion rate of zero represents the critical shear stress τ_c . (b) Analysis of the experimental results of Jepsen et al. on surrogate waste specimen B2 using the bilinear approach.

5.2 SEDflume-based Methods for Determining Critical Shear Stress

SEDflume is the name of the state-of-the-art erosion testing system originally developed at the University of California – Santa Barbara (UCSB). The system was developed to overcome a major drawback of previous flume designs: obtaining the shear strength of a material away from the unconsolidated surface layer. By using critical shear stress values based on the erosion of the surface layer, practitioners often overestimated the amount of expected erosion. SEDflume allowed practitioners to obtain and test long cores of sediment, eroding past the surface sediments and into the bulk material. Because long cores of material could be tested, the system was named “SEDflume,” which stands for “sediment erosion at depth” flume.

At UCSB, the critical shear stress of a sediment bed, τ_{cr} , is defined quantitatively as the shear stress at which a very small, but accurately measurable, rate of erosion occurs. This rate of erosion has been practically defined as 10^{-4} cm/s (= 0.06 mm/min). This represents about 1 mm of erosion in 15 minutes.

Since it is difficult to measure τ_{cr} exactly at 10^{-4} cm/s, erosion rates are typically measured above and below 10^{-4} cm/s. The τ_{cr} is then determined by linear and power law regression (McNeil et al., 1996; Roberts et al., 1998). This is done at different depths within the sample to account for surface effects.

This method is referred to in the following analysis as the University of California – Santa Barbara (UCSB). It is further distinguished by “linear” and “power law” as described below.

5.2.1 Linear Interpolation

The linear interpolation method is simply a linear regression between the shear stresses where the critical erosion rate 10^{-4} cm/s is not achieved and where it is exceeded.

5.2.2 Power Law Relationship

A power law relationship that describes the erosion behavior of well mixed sediments is (Jepsen et al., 1997):

$$E = A\tau^n\rho^m \quad (4)$$

where E is the erosion rate (cm/s), τ is the shear stress exerted by the moving fluid on the sediment surface (Pa), and ρ is the material bulk density (g/cm^3) and A , n , and m are constants that depend on the material characteristics. The equation used in this analysis is an abbreviated variation of Eq. 4:

$$E = A\tau^n \quad (5)$$

Due to the compacting of the surrogate waste samples to represent the evolution of waste over time, density variations will be minimal and any effect will be absorbed by the constant A .

Three erosion measurements at different shear stresses below and beyond the critical erosion rate 10^{-4} cm/s are required to determine the constants A and n in the power law relationship.

5.3 Records Keeping

Raw test records were recorded in the scientific notebooks (FLM-1 and FLM-2) and by the DAS. The DAS files were exported to a CSV formatted file. Printouts of the raw data files are in the supplement to the scientific notebooks. It should be noted that there is often a several minute difference between the notebook entries and the DAS file. This is because of several reasons. The first is that a wall clock was often used to record in the notebook, and the wall clock was off from the computer clock. Secondly, the DAS would only record when the “Force data store” button was pushed or the sample was moved. The operator would select a new flow rate and write that in the notebook. The new flow rate would then be entered into the DAS. The flume would require a short period of time to stabilize. Then the operator would press the “Force data store.” These actions could only be accomplished sequentially, not simultaneously, creating the difference between the digital and laboratory entries. Lastly, the flow rate could not be changed when the sample is being moved. This could also create a lag in the digital and notebook entries, compounded by the fact the operator is writing information in the notebook. When obvious and justified, the DAS computer record was given precedence. There were times when the DAS record was skipped, usually because the sample was not moved and the operator forgot to push the store data button. In these cases the scientific notebook entries were used. It should be kept in mind that the most important variable to obtain is the erosion rate, which is erosion over a time interval. It is the required parameter in the data analyses. Therefore, the exact time is not as

important as the time interval over which erosion took place, or did not, at a shear stress level. This concept drives how the data was analyzed.

In the analysis of the data, an adjustment was made to the calculated shear stress. The shear stress on DAS computer is calculated from the flow rate. The flow rate is the control variable for the flume operation. The operator decides on a shear stress level and enters that in the DAS computer. The computer calculates the flow rate. The DAS computer was programmed before the channel was constructed. The final channel dimensions after construction are slightly different than the design. In addition, the eroding fluid, especially up until the time that erosion starts, is assumed to have properties of fresh water at room temperature. More precise water property values were used in calculating the adjusted shear stress in the analysis of each test's data. These values are considered conservative because inclusion of any suspended load or dissolved materials would only increase the density and viscosity of the fluid and therefore the shear stress it applies.

Analysis of the raw data was performed in Excel for each test. The Excel files are on a CD in the records package associated with test plan TP 09-01 in the WIPP Records Center. In addition, the two scientific notebooks (FLM-1 and FLM-2) and notebook supplement are also in the WIPP Records Center. The records package number is ERMS 556992.

6 VERTICAL FLUME TESTS ON SURROGATE DEGRADED WASTE SAMPLES

6.1 The Test Matrix

The test matrix for the flume experiments conducted in support of evaluation of the waste shear strength lower limit is given in Table 8. The flume experimental matrix was based on the same materials used in the previous flume experiments conducted by UCSB (Jepsen et al, 1998) since it was desired to make comparisons between the two sets of tests. In the UCSB experiments, two types of materials were used: 50% and 100% degraded surrogate waste materials. Those materials were compacted at 5.0 MPa overnight. The 5.0 MPa compaction level was determined to be conservative by Hansen et al. (1997). The number of surrogate waste materials was expanded in the present set of experiments to represent not only 50% and 100% degradation of the waste materials, but also to add a 75% degraded surrogate waste material. Following the procedure outlined by Papenguth and Myers in Appendix A of Hansen et al. (1997) the 75% degraded surrogate waste material was developed and determined to be an average mixture of the 50% and 100% degraded materials.

In addition, even though 5.0 MPa compaction pressure was considered conservative when the material parameter tests were performed for the Spallings model and presented to the model's peer review panel, Herrick et al. (2007b) found that the minimum compaction pressure the waste was expected to undergo was 2.3 MPa. Therefore, the 50%, 75%, and 100% degraded surrogate waste samples were subject to a compaction pressure of 2.3 MPa as well as the 5.0 MPa used previously. The calculations used to determine the compaction pressure on the waste were based on gas generation rates dating back to 1995 (Brush, 1995). Since then, Roselle (2012) has experimentally shown that the steel corrosion rate is approximately one half the rate assumed when the 1995 gas generation rates were calculated. The new gas generation rates are being determined, but they will be slower than the rates used by Herrick et al (2007a) in their assessment. Therefore, since gas pressure is the resistive force slowing down salt creep and the required gas pressure will take longer to develop, the waste will undoubtedly undergo a compaction pressure higher than 2.3 MPa.

The surrogate waste materials are described in an earlier section (Section 3) along with how the samples are built (Section 4.4).

In Table 8, the six different materials and compaction pressures are distinguished by different background colors. The following sections describe each set of tests in terms of the percent degradation of the waste the surrogate material represents. The initial intention of the experimental program was to test five samples at each representing each degree of degradation and at each compaction level to assess the reproducibility of the results (Roberts and Herrick, 2009). As seen in Table 8, that was generally accomplished.

Table 8. Test matrix for the flume tests performed to assess the lower limit of TAUFAIL. Three different materials were tested representing 100%, 75%, and 50% degradation of the WIPP wastes. Each material was tested at two levels of die compaction: 2.3 or 5.0 MPa. In the 75% degraded surrogate waste material tests, two different sources of goethite were used. One is from an outcrop on Kirkland Air Force Base, Albuquerque, NM (“Alb”) and the other is from a private mine outcrop outside Socorro, NM (“Socorro”).

Sample No.	Degradation %	Goethite	Compaction Pressure (MPa)	Compaction Hold Time (hrs)	Test Date Start	DAS Data File Name	Starting Shear Stress (Pa)	Ending Shear Stress (Pa)
100% degraded, 2.3 MPa compaction								
WF-100-01	100	Alb	2.6	1.5	9/1/2011	20110901	0.15	1.04
WF-100-203-01	100	Alb	2.3	18	10/17/2011	20111017	0.10	1.04
WF-100-203-02B	100	Alb	2.3	17	11/1/2011	20111101	0.05	1.04
WF-100-203-03	100	Alb	2.3	17	11/9/2011	20111109	0.05	0.78
WF-100-203-04	100	Alb	2.3	18.5	6/7/2012	20120607	0.02	0.52
100% degraded, 5.0 MPa compaction								
WF-100-5-1	100	Alb	5.0	17	9/22/2011	20110922	0.15	1.04
WF-100-5-02	100	Alb	5.0	overnight *	11/3/2011	20111103	0.05	1.04
WF-100-5-03	100	Alb	5.0	16	11/22/2011	20111122	0.05	0.65
75% degraded, 2.3 MPa compaction								
75-080112	75	Socorro	2.3	17.5	8/7/2012	20120807	0.05	2.08
75-082212	75	Socorro	2.3	17	8/28/2012	----	0.52	2.08
75-082712	75	Socorro	2.3	18	10/2/2012	100212	0.52	2.47
75-082912	75	Alb	2.3	16.5	9/5/2012	----	0.52	3.12
75-091012	75	Alb	2.3	15.4	9/17/2012	9172012	0.52	1.82
75-091312	75	Alb	2.3	18.25	9/19/2012	91912	0.52	2.34
75-091912	75	Alb	2.3	15	9/25/2012	92512	0.52	1.95

* “overnight” can be estimated to be at least 15 hours based on a loading time of 4:30 pm, assumed to be a half hour before the scheduled departure time, and an unload time of 7:30 am, assumed the same as the scheduled arrival time.

Table 8. continued.

Sample No.	Degradation %	Goethite	Compaction Pressure (MPa)	Compaction Hold Time (hrs)	Test Date Start	DAS Data File Name	Starting Shear Stress (Pa)	Ending Shear Stress (Pa)
75% degraded, 5.0 MPa compaction								
75-080212	75	Socorro	5.0	17	8/16/2012	20120816	0.39	3.12
75-082312	75	Socorro	5.0	18	8/30/2012	----	0.52	3.25
75-082812	75	Socorro	5.0	17	9/28/2012	92812	0.52	3.12
75-083012	75	Alb	5.0	21	9/10/2012	20120910	0.52	3.50
75-091212	75	Alb	5.0	17	9/18/2012	9182012	0.52	2.08
75-091812	75	Alb	5.0	17.5	9/24/2012	9242012	0.52	3.12
75-092012	75	Alb	5.0	17	9/26/2012	9262012	0.52	3.63
50% degraded, 2.3 MPa compaction								
WF-50-02	50	Alb	2.3	1.0	9/7/2011	20110907	0.15	5.17
Flume 50-01	50	Alb	2.3	13	9/28/2011	20110928	0.52	5.66
WF-50-203-02	50	Alb	2.3	17	11/30/2011	20111130	0.52	5.64
WF-50-203-01	50	Alb	2.3	16	12/6/2011	20111206	1.04	5.36
WF-50-203-03	50	Alb	2.3	16	1/12/2012	20120112	1.04	4.66
50% degraded, 5.0 MPa compaction								
WF-50-5-01	50	Alb	5.0	15	10/3/2011	20111003	0.52	5.69
WF-50-5-02B	50	Alb	5.0	16	10/12/2011	20111012	1.04	5.68
WF-50-5-03	50	Alb	5.0	17	10/25/2011	20111025	0.52	5.36
WF-50-5-04	50	Alb	5.0	15.5	12/19/2011	20111219	0.52	5.61
WF-50-5-05	50	Alb	5.0	16	1/10/2012	20120110	1.04	5.68

6.2 100% Degraded Surrogate Waste Material Tests

The 100% degraded surrogate waste material tests were some of the first performed. The tests unfortunately exposed a number of issues in the procedures conceived in Roberts and Herrick (2009). The original testing procedures were an extension of the methods used when collecting field samples for flume erosion experiments. When collecting samples in the field, a polycarbonate resin thermoplastic (Lexan[®]) tube is pushed into the sediment to collect a core of material. The material collected in this manner is generally from areas of low stress so no expansion of the material in the tube takes place.

For the present experiments, the samples were made in the sample holders (Section 4.4). For the 100% degraded surrogate material tests, Lexan sample tubes were used exclusively. The Lexan tubes were confined within a split die. The split die was used to keep the material in the plastic tube and the tube itself from bulging, bending, or otherwise deforming as the load was applied and as the excess brine from the samples was squeezed out. Throughout the course of testing, however, it was found out that this was not the case.

Initially, the first samples could not be moved by the servo motor/rail table system. The material had become fixed to the sides of the sample holders. There was some evidence of pieces of surrogate waste material (typically glass) becoming impregnated into the polycarbonate, but mostly it appeared to be caused by friction along the inside surface of the tube and/or deformation of the tube. To reduce friction, a thin coat of light oil was applied to the insides of the sample holders. This was quickly replaced with vacuum grease which is a better lubricant and less reactive.

Even with vacuum grease applied to the inside of the sample holder, the samples advanced in a stick-slip fashion. The samples would initially resist movement as the rail table was loaded, then it would jump forward quickly. The quick jump forward, followed by a quick stop, would cause material to break off of the sample's face. Material breaking off the face only occurred as the samples were advanced, whether there was fluid in the channel or not or whether the fluid was flowing or not. Material did not slough off the face by its own without movement of the specimens. Inspection of subsequent samples revealed that the sample holders had deformed in a number of ways (Figure 19). The first was by barreling around the middle of the sample's length. The second is bulging at one of the sample's ends. The third was bending of the sample so that it had a slight, roughly circular arc shape. The fourth mode of deformation was a shearing of the entire sample so that its specimen axis was no longer at right angles to the ends of the sample holders. The deformation of the samples in the Lexan sample holders prompted the move to aluminum sample holders which were hard anodized and impregnated with Teflon.

Another possible cause of the stick-slip motion was that the push rod from the rail table platform to the platen in the sample holder did not push straight down the axis of the specimen. This is almost equivalent to the effect of shearing the sample holder in that it produces an eccentricity in the loading of the specimens. This problem was solved by accurately measuring the location of axis of the specimen and translating it to the rail table platform, machining a reaction plate that holds the sample holder against the channel, and ensuring that all loading surfaces were squared to each other.

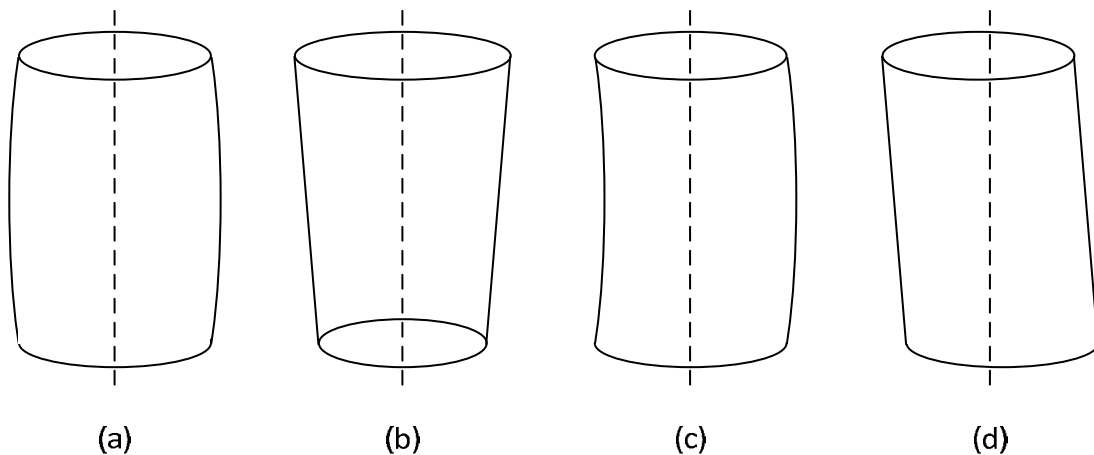
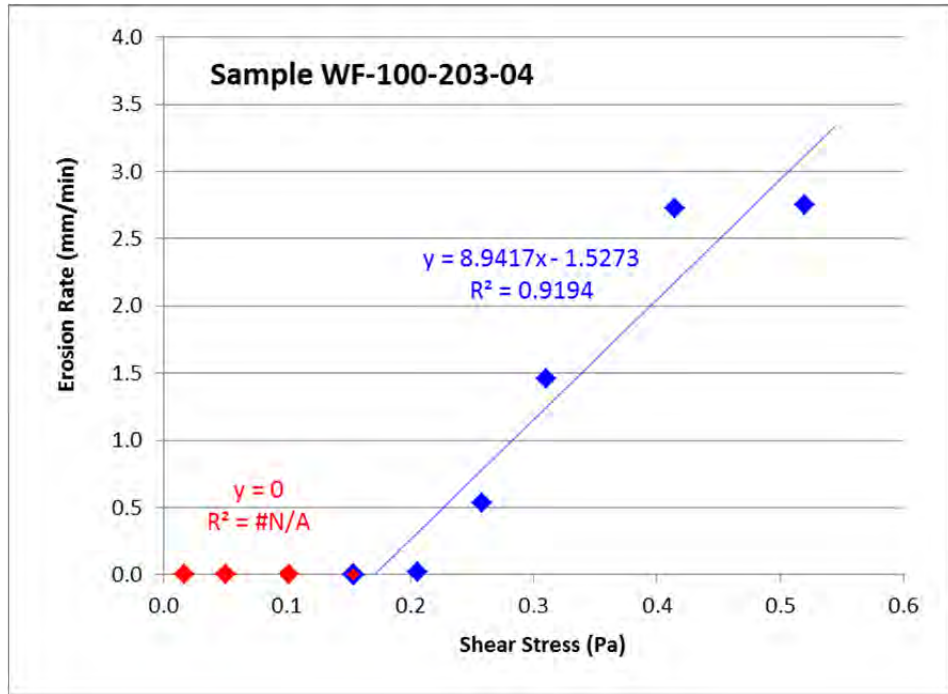


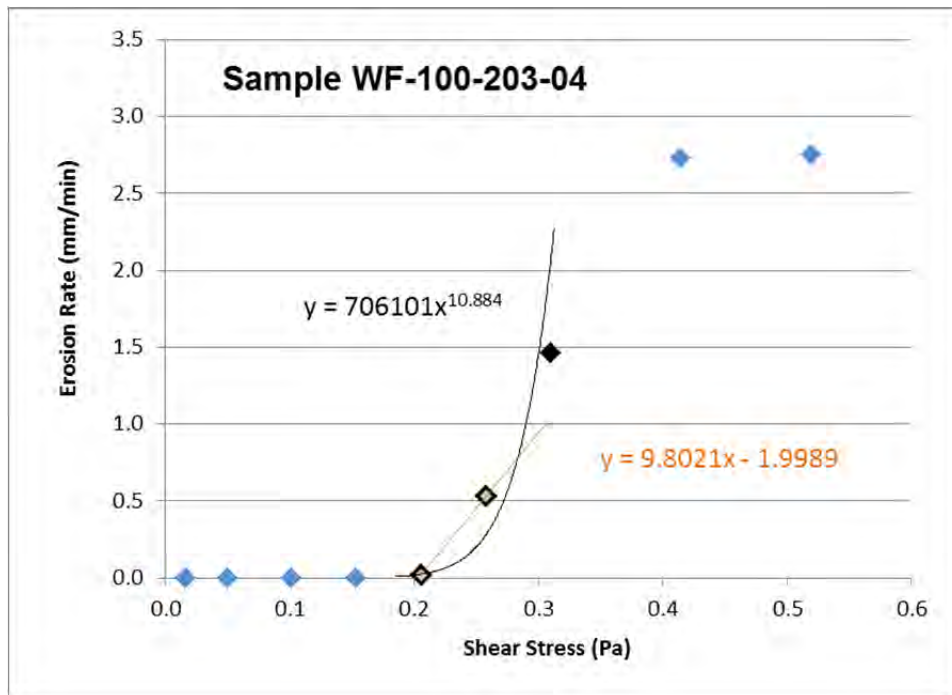
Figure 19. Schematic depictions of the modes of deformation the samples and Lexan sample holders were found to have undergone upon being removed from the split shell after unloading: (a) barreling around the middle, (b) bulging at one of the ends, (c) bending, and (d) shearing. The dashed line represents the original axis of the specimen before deformation.

During the first tests, up until Sample WF-100-5-03, a gasket was used between the sample holder and the channel to keep the system from leaking water. It was noticed that as the samples were pushed into the current they would sometimes scrape along the gasket. The 50% degraded surrogate waste samples, which were being tested at the same time as the 100% degraded surrogate waste samples, would shear the gasket off. However, the 100% degraded surrogate waste samples would not. It was felt that this scraping also affected the test results for the more highly degraded surrogate waste samples so a new system was designed. Starting with Sample WF-100-5-03, a new channel reaction plate was fabricated and the seal was changed to an O-ring. The samples then had a clear path into the current.

Because of the stick-slip motion and the obvious damage it produced on the faces of the samples as they were moved, it is felt that none of the results from the 100% degraded surrogate waste samples that had this motion are reliable. By the time the testing issues were identified and resolved, all the 100% degraded surrogate waste samples had been tested with the exception of Sample WF-100-203-04. Sample WF-100-203-04 did not undergo stick-slip motion during testing because virtually all the countermeasures to avoid detrimental behavior had been enacted. The final countermeasure was ensuring that the ends of the sample holder were square with the axis of the specimen. To do this, the sample holder was put in a lathe after releasing the load from the specimen and turned, machining the face. It is unclear what effect turning the specimen had on the cohesion of the sample, but the sample did move smoothly and no material fell off the face of the sample's face as it was moved. Only the test results for WF-100-203-04 are given below. The results are given in graphical form (Figure 20).



(a)



(b)

Figure 20. Analyses of the test results for Sample WF-100-203-04. (a) UF bilinear fit yielding $\tau_m = 0.17$ Pa and (b) the UCSB fits around a critical shear stress of 10^{-4} cm/sec giving for the linear interpolation $\tau_{cr} = 0.21$ Pa (two orange points) and for the power law fit $\tau_{cr} = 0.22$ Pa (three black points).

For the bilinear fit suggested by the University of Florida (UF), all the data points were considered. Different points were considered to belong to the upper and lower lines. The points were included or excluded until the best fit lines to the model were obtained. This fit was indicated by the highest R^2 values. The order of precedence in evaluating the best fit was first to the overall fit of both lines, then to the best fit of the upper line. Sometimes a data point was considered to belong to both lines. This is the case for the point at a shear stress of 0.15 Pa in Figure 20a. Inclusion of this point in both lines gives a slightly higher R^2 for the upper line and slightly lower τ_m ($= 0.17$ Pa) than excluding it and using points greater than 0.2 Pa ($\tau_m = 0.18$ Pa). It could be argued that using data points greater than 0.2 Pa makes more sense physically since it is obvious from the plot that the erosion rate increases steadily with increasing shear stress after that shear stress, however using the higher R^2 value was deemed to be less subjective and more consistent.

The UCSB/SEDflume fits are shown in Figure 20b. For the linear fit, two points were used, one below the critical erosion rate 10^{-4} cm/s ($= 0.06$ mm/min) and one beyond it. This suggests a $\tau_{cr} = 0.21$ Pa. For the power law fit, three points are required, one below the critical erosion rate and two above it. This method is usually slightly higher than the linear interpolation method and gives a $\tau_{cr} = 0.22$ Pa for Sample WF-100-203-04.

Because the sample was placed in a lathe and turned to square the ends of the sample holder, it is questionable whether the experimental results are truly representative of the behavior of a 100% degraded surrogate waste material compacted under 2.3 MPa. However, the experiment ran well compared to the other 100% degraded surrogate waste material tests which were not considered reliable or representative of the material behavior due testing procedure problems mentioned above, specifically the stick-slip motion. In addition, no redundant tests were performed to confirm this single result. Therefore, the reader should take a skeptical view of the results from this test and is warned about trying to draw any conclusions from it. What can be taken away from this test is that with the modifications to the vertical flume, new sample holders, more care in the test set-up with better alignment, and improved testing procedures samples of 100% degraded surrogate waste materials can be successfully eroded.

6.3 75% Degraded Surrogate Waste Material Tests

The 75% degraded surrogate waste material samples were the last to be tested. All of the samples were made in the hard anodized aluminum sample holders in which the anodized surface was impregnated with Teflon. In addition, all other improvements to the testing system and procedures mentioned in the vertical flume design and operation section (Section 4) and the previous section about the 100% degraded surrogate waste material tests (Section 6.2) were in use at the time these samples were tested.

The surrogate material descriptions were given previously in Section 3. The materials used make up the 75% degraded surrogate waste samples are the same as the materials used in the 100% and 50% degraded surrogate waste samples except that two different sources for iron oxide in the form of goethite were used. The primary source of goethite is from Kirkland Air Force Base, Albuquerque, NM, which is in close proximity to the Geomechanics Laboratory at Sandia National Laboratories where the samples were made. It is labeled “Alb” or “Albuquerque”

goethite. This goethite was used in all samples except the six 75% degraded surrogate waste material samples listed in Table 8. Albuquerque goethite outcrop is located at UTM coordinates: 13S 363409E 387186N. Figure 21 shows a picture of the outcrop where the goethite was sorted and collected by hand. The second iron oxide source is called “Socorro” goethite since it was mined in an outcrop just south of Socorro, NM. Due to vandalism of the mine, believed to be due to the museum quality of the goethite found there, the owner has asked that the mine’s location not be revealed. Socorro goethite is an extremely pure, botryoidal (globular, like bunches of grapes) accumulation. The goethite was purchased through Rio Grande Rock and Gems in Socorro, NM.



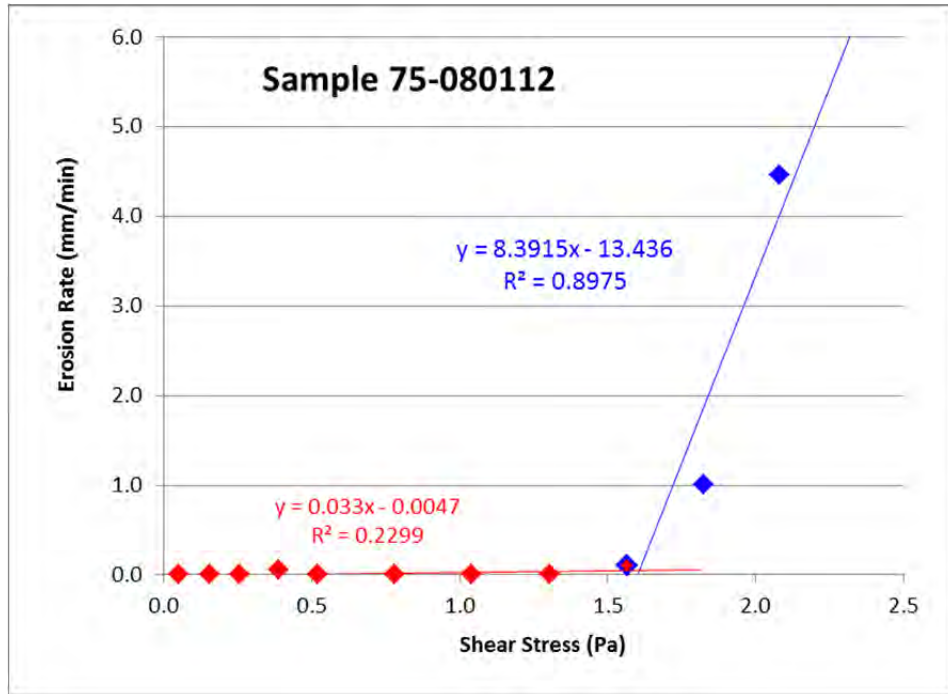
Figure 21. The Albuquerque goethite outcrop near the Geomechanics Laboratory at Sandia National Laboratories – Albuquerque.

The following two sections will consider the 75% degraded surrogate waste material tests as those die compacted to 2.3 MPa and those die compacted to 5.0 MPa separately.

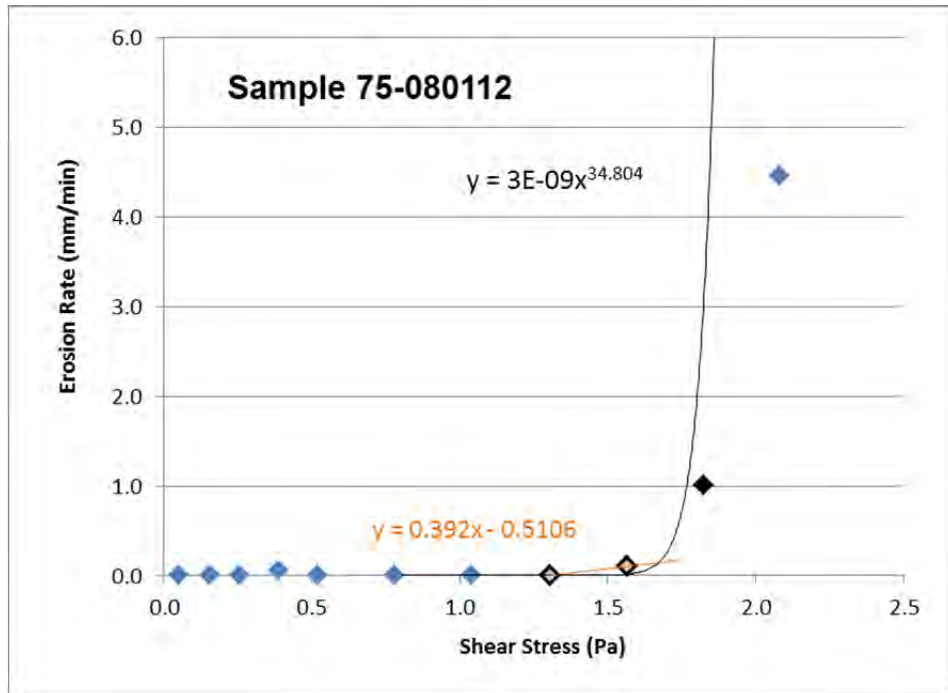
6.3.1 75% Degraded Surrogate Waste Material Tests, Die Compacted to 2.3 MPa

The results for the seven 75% degraded surrogate waste material tests die compacted to 2.3 MPa are given graphically in Figure 22 through Figure 28, on the next seven pages. The first three figures are for those samples made with Socorro goethite (Samples 75-080112, 75-082212, and

75-082712) and the final four figures are for those samples made with Albuquerque goethite (Samples 75-082912, 75-091012, 75-091312, and 75-091912).

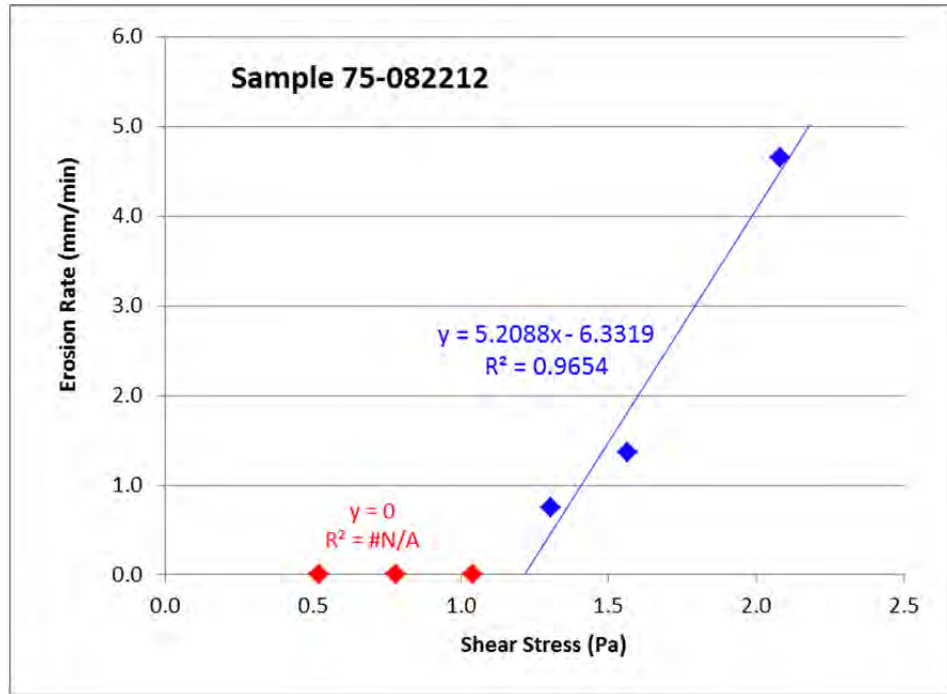


(a)

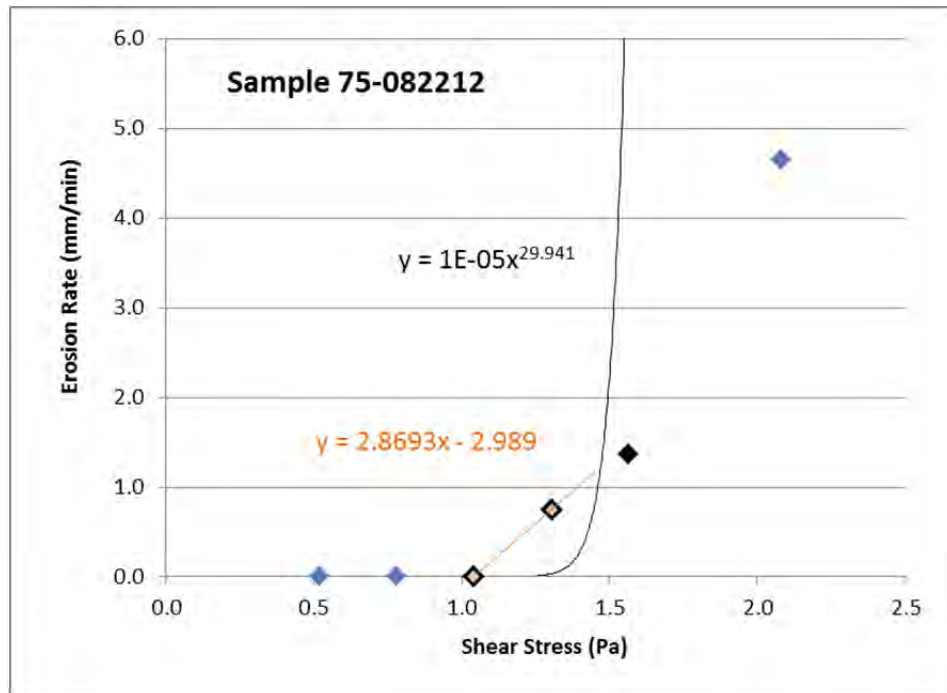


(b)

Figure 22. Analyses of the test results for Sample 75-080112. Uses Socorro goethite. (a) UF bilinear fit yielding $\tau_m = 1.60$ Pa and (b) the UCSB fits around a critical shear stress of 10^{-4} cm/sec giving for the linear interpolation $\tau_{cr} = 1.46$ Pa (two orange points) and for the power law fit $\tau_{cr} = 1.62$ Pa (three black points).

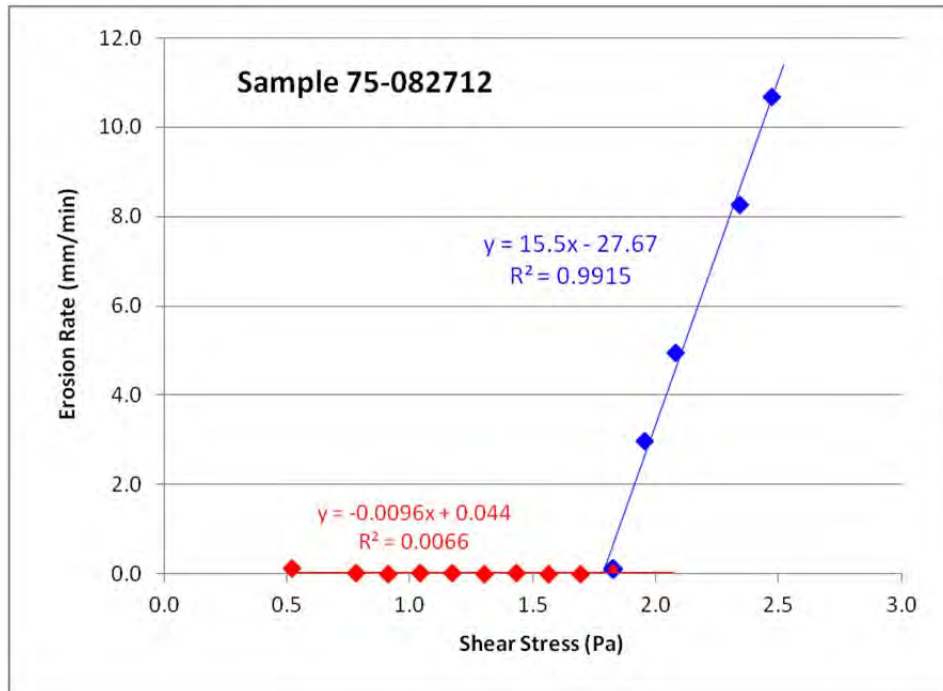


(a)

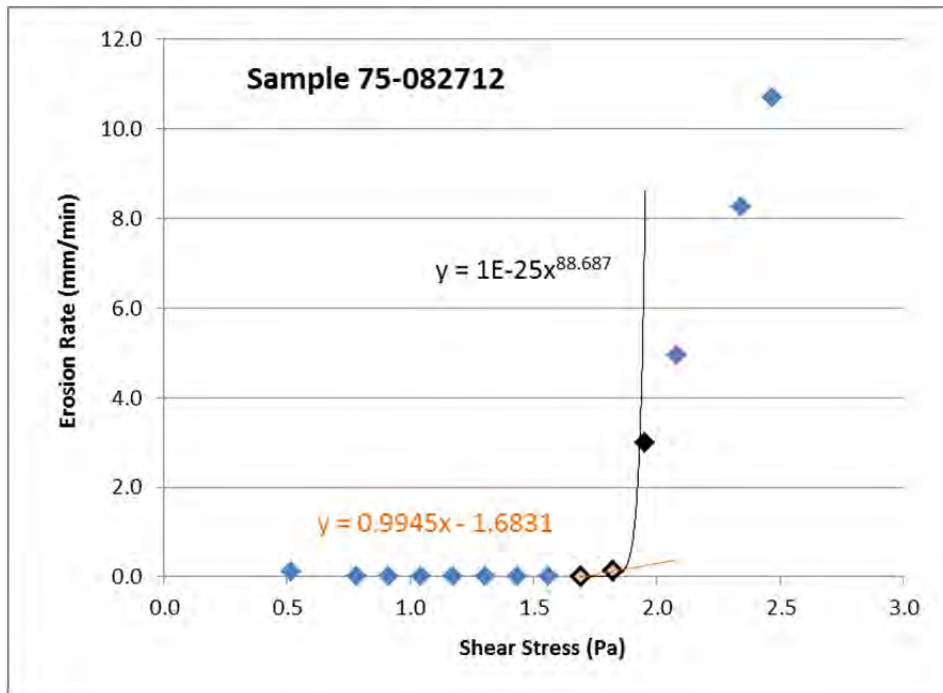


(b)

Figure 23. Analyses of the test results for Sample 75-082212. Uses Socorro goethite. (a) UF bilinear fit yielding $\tau_m = 1.22$ Pa and (b) the UCSB fits around a critical shear stress of 10^{-4} cm/sec giving for the linear interpolation $\tau_{cr} = 1.06$ Pa (two orange points) and for the power law fit $\tau_{cr} = 1.34$ Pa (three black points).

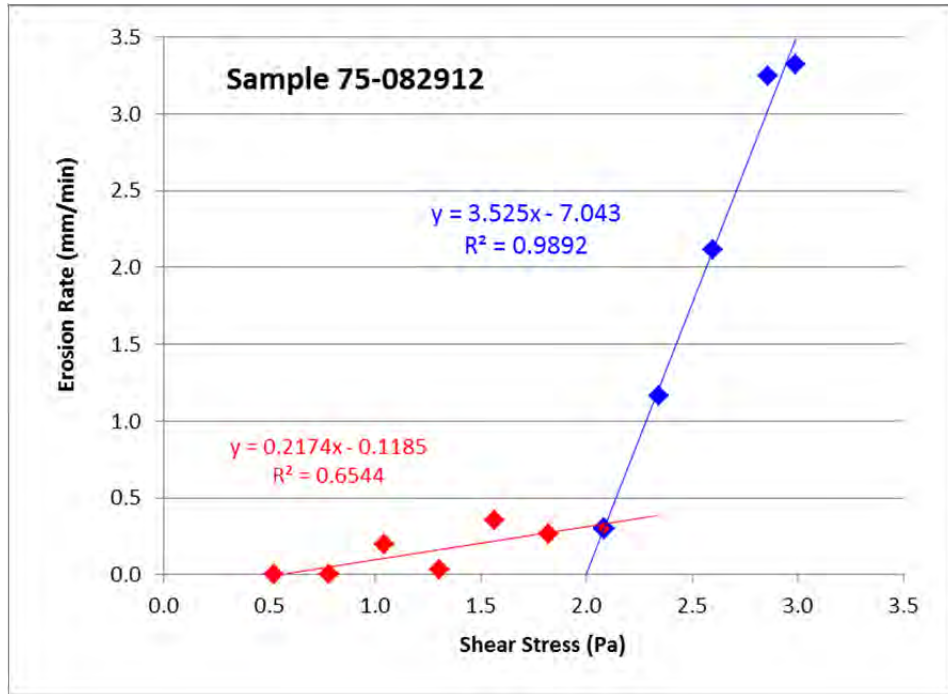


(a)

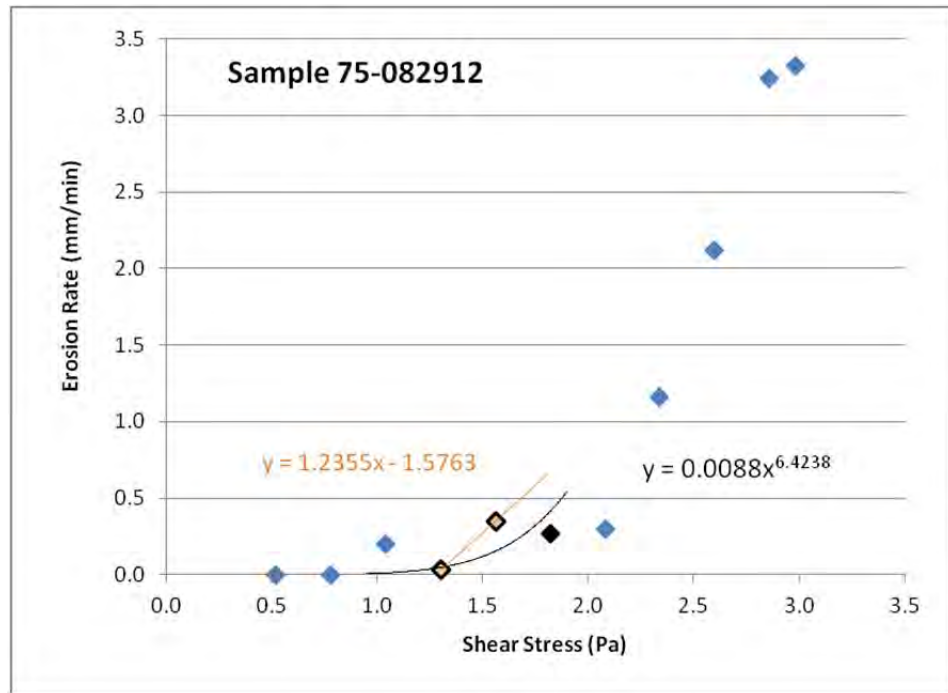


(b)

Figure 24. Analyses of the test results for Sample 75-082712. Uses Socorro goethite. (a) UF bilinear fit yielding $\tau_m = 1.79$ Pa and (b) the UCSB fits around a critical shear stress of 10^{-4} cm/sec giving for the linear interpolation $\tau_{cr} = 1.75$ Pa (two orange points) and for the power law fit $\tau_{cr} = 1.85$ Pa (three black points).

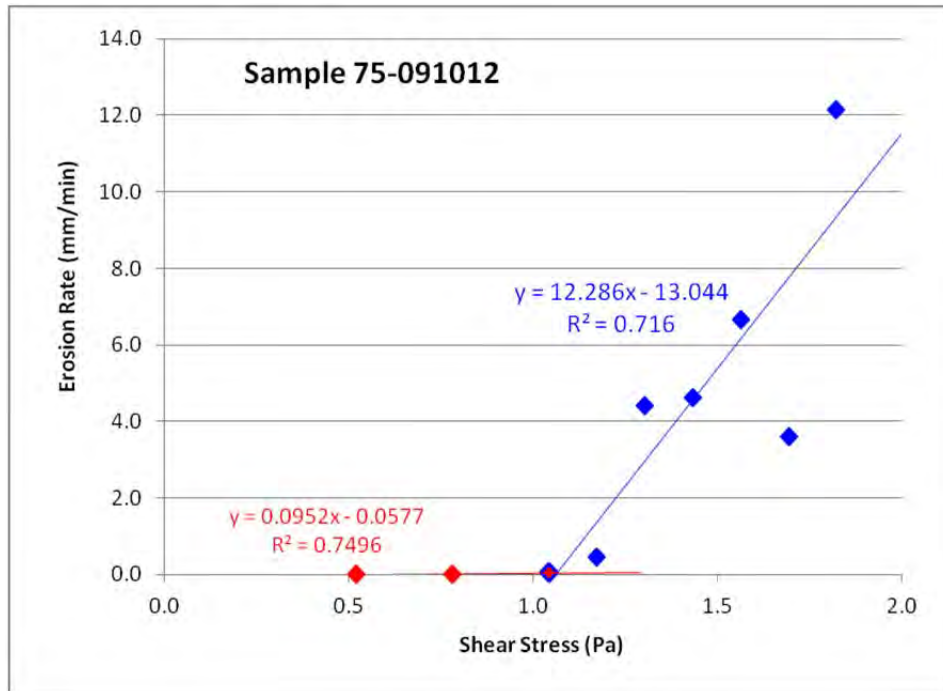


(a)

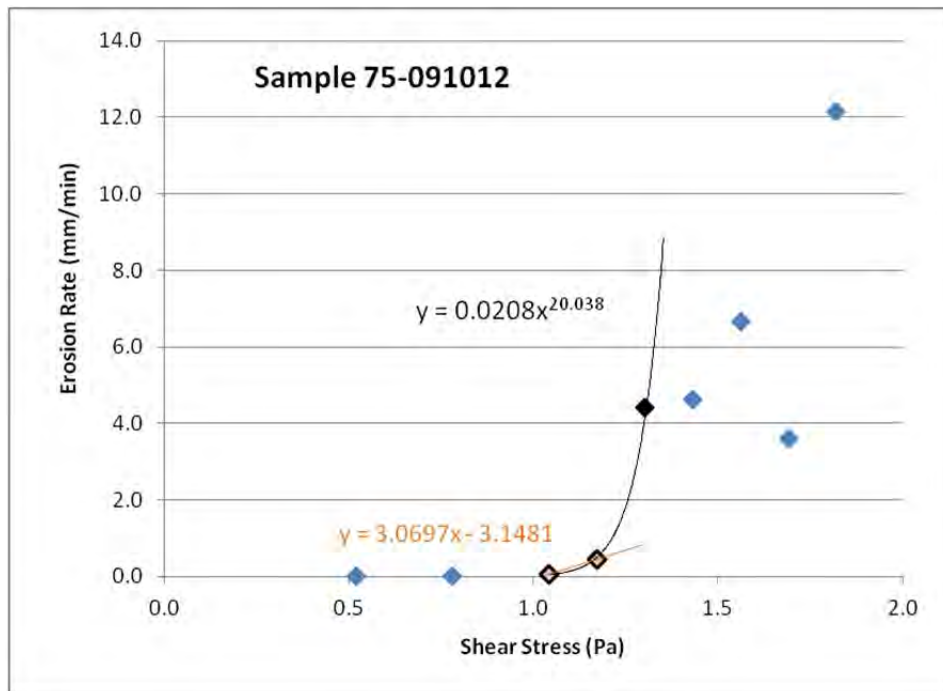


(b)

Figure 25. Analyses of the test results for Sample 75-082912. Uses Albuquerque goethite. (a) UF bilinear fit yielding $\tau_m = 2.00$ Pa and (b) the UCSB fits around a critical shear stress of 10^{-4} cm/sec giving for the linear interpolation $\tau_{cr} = 1.32$ Pa (two orange points) and for the power law fit $\tau_{cr} = 1.35$ Pa (three black points).

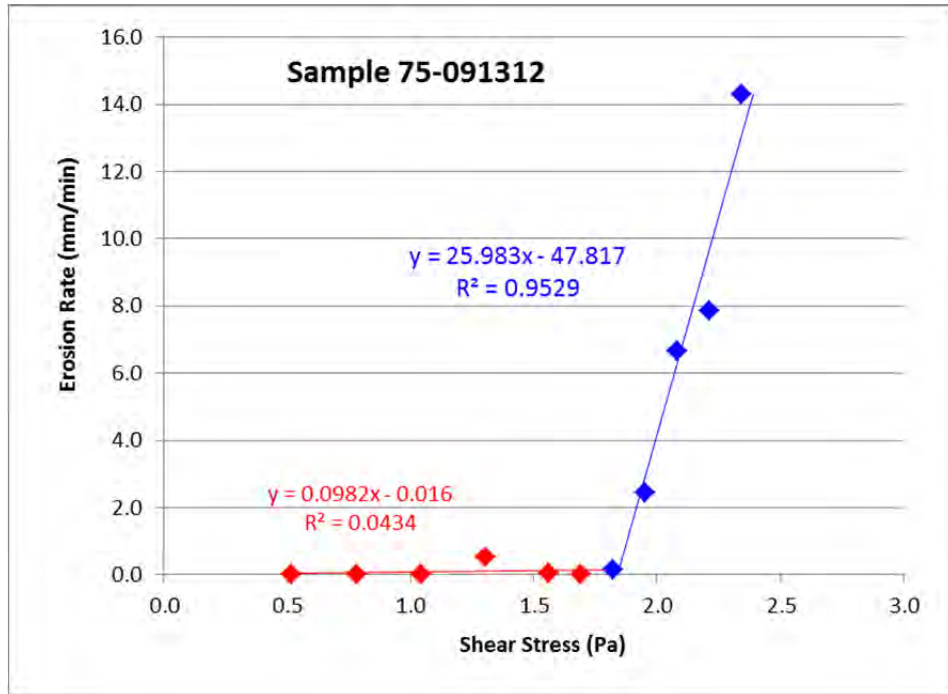


(a)

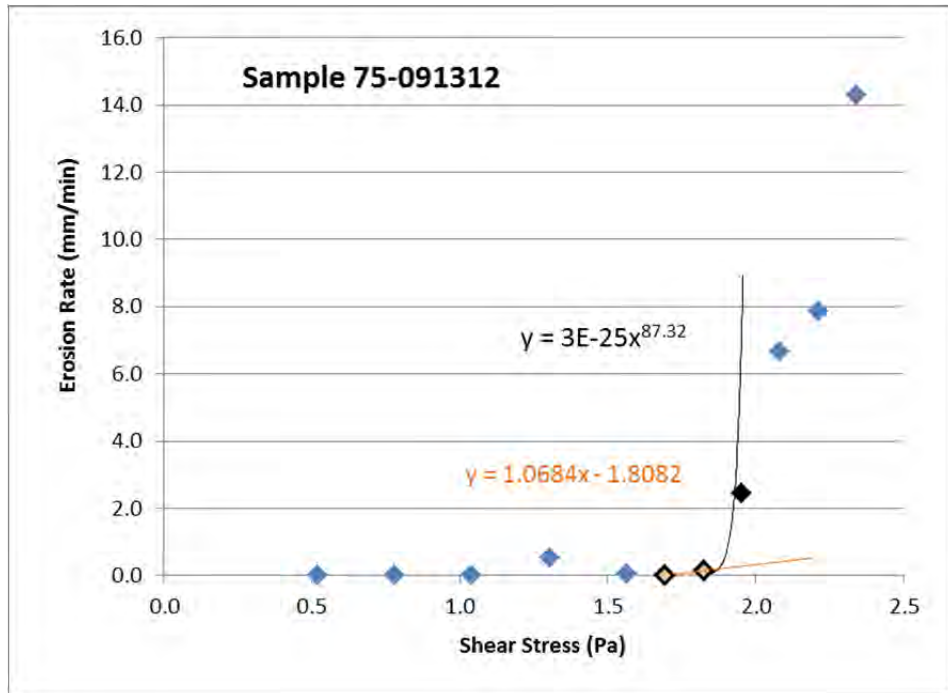


(b)

Figure 26. Analyses of the test results for Sample 75-091012. Uses Albuquerque goethite. (a) UF bilinear fit yielding $\tau_m = 1.06$ Pa and (b) the UCSB fits around a critical shear stress of 10^{-4} cm/sec giving for the linear interpolation $\tau_{cr} = 1.05$ Pa (two orange points) and for the power law fit $\tau_{cr} = 1.05$ Pa (three black points).

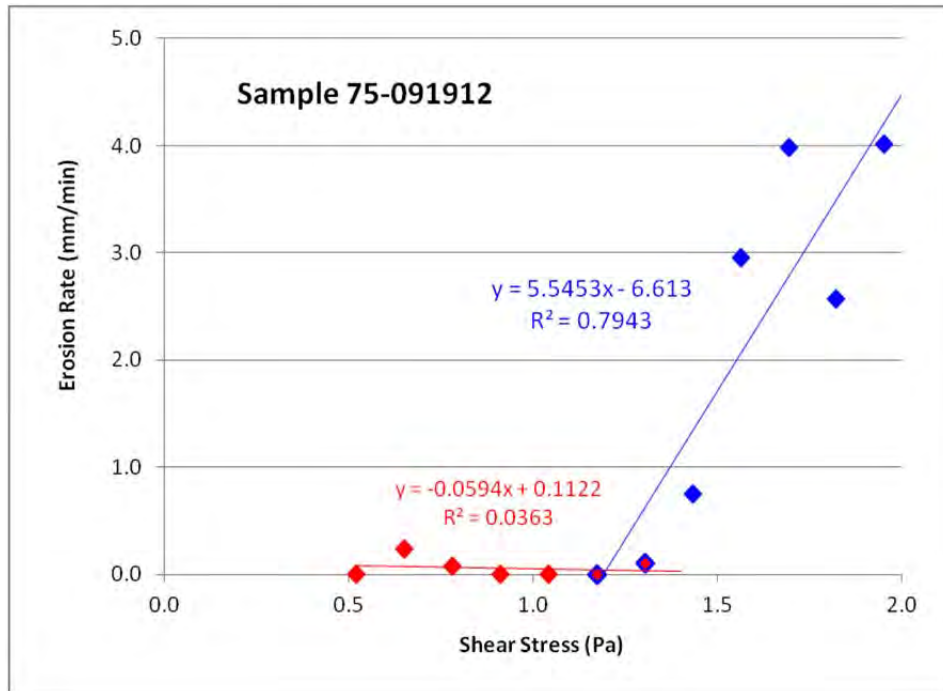


(a)

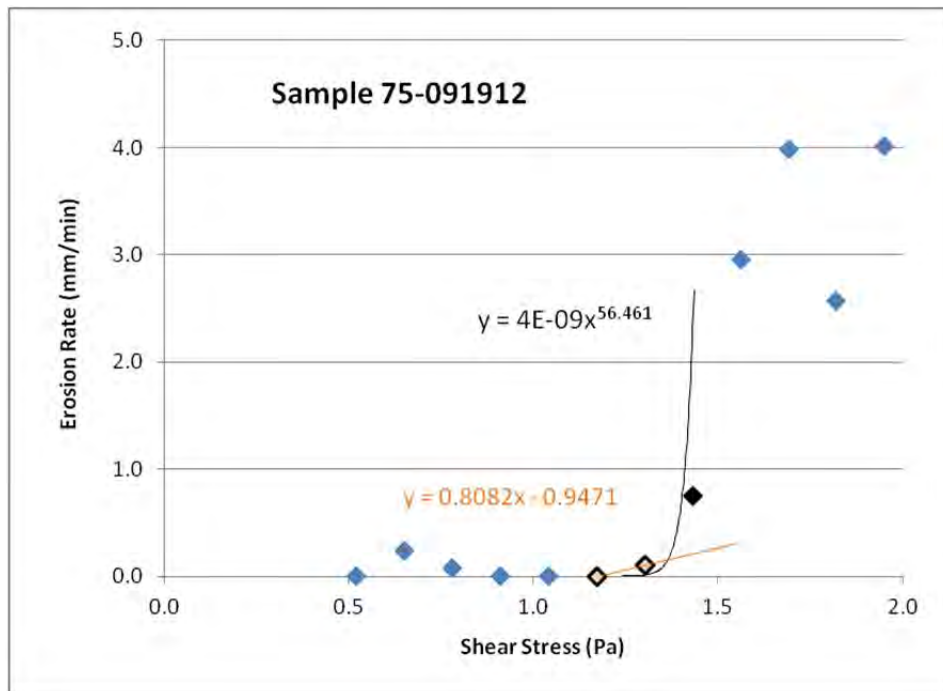


(b)

Figure 27. Analyses of the test results for Sample 75-091312. Uses Albuquerque goethite. (a) UF bilinear fit yielding $\tau_m = 1.84$ Pa and (b) the UCSB fits around a critical shear stress of 10^{-4} cm/sec giving for the linear interpolation $\tau_{cr} = 1.75$ Pa (two orange points) and for the power law fit $\tau_{cr} = 1.85$ Pa (three black points).



(a)



(b)

Figure 28. Analyses of the test results for Sample 75-091912. Uses Albuquerque goethite. (a) UF bilinear fit yielding $\tau_m = 1.19$ Pa and (b) the UCSB fits around a critical shear stress of 10^{-4} cm/sec giving for the linear interpolation $\tau_{cr} = 1.25$ Pa (two orange points) and for the power law fit $\tau_{cr} = 1.34$ Pa (three black points).

6.3.1.1 Discussion of Results for 75% Degraded Surrogate Waste Material Tests, Die Compacted to 2.3 MPa

Sample 75-080112 was made using Socorro goethite and was made in the anodized aluminum sample holders, as were all of the 75% degraded surrogate waste samples. It was tested over two days. There was no erosion during the first day which involved shear stresses 0.05 to 0.78 Pa. During the second day of testing, no erosion was noticed at stress levels 1.04 to 1.30 Pa. When testing was stopped for lunch, the water in the channel was drained. Until this time the valve at the end of the channel that controls the pressure of the fluid was kept closed during drainage of the channel so that the water level fell slowly and did not affect the material on the sample's face. With the aluminum sample holders, being much slicker than the Lexan sample holders, the slight vacuum formed with the valve closed caused the sample to get sucked into the channel by about 3-4 cm. This movement caused the material at the end of the specimen to get damaged. Upon restarting the pump, the pressure caused the specimen to be pushed back into the sample holder. Approximately 5 cm had to be sheared off the end of the sample to get to where the sample was behaving as it was before the extrusion. This suggested that the damaged material had been removed. The test was continued from that point.

Erosion of Sample 75-080112 indicates that the bilinear model predicts the material's behavior quite well (Figure 22). There was very little surface erosion. The number of points obtained while the material was undergoing bulk erosion was reduced compared to the majority of other tests due to the removal of damaged material. The two SEDflume methods are consistent with the interpretation of the bilinear method, however both methods predict slightly higher shear strength values. Based on the bilinear method the critical shear stress is $\tau_m = 1.60$ Pa. The critical shear strength according to the UCSB SEDflume methods are $\tau_{cr} = 1.46$ Pa for linear interpolation and $\tau_{cr} = 1.62$ Pa for the power law fit.

Sample 75-082212 was also made using Socorro goethite. Analysis of this test relied solely on the laboratory notebook entries. Unfortunately the DAS data buffer had filled up so no data was recorded. The full data buffer also affect tests on Samples 75-082312, 75-082912, and 75-0830121 which were conducted sequentially after 75-082212. Once this problem was discovered, the size of the data buffer was increased fivefold and the raw data files were downloaded after each test to keep the buffer from filling up again. In general, the laboratory notebook had entries at the beginning and end of each time interval at which a specific shear stress was run, except for this test. Between shear stresses of 1.56 and 2.08 Pa, the travel distances were not recorded (Figure 23). The points from running the test at shear stresses of 1.82 and 1.95 Pa could not be included. This mistake only affects the bilinear fit to the data as it might affect the slope of the bulk erosion line. The mistake does not affect the UCSB analyses because a sufficient number of points immediately below and above the critical erosion rate of 10^{-4} cm/s are available. The data from Sample 75-082212 suggest that the UF bilinear model and the UCSB linear model best describe the material's behavior. Based on the bilinear method the critical shear stress is $\tau_m = 1.22$ Pa and there was no surface layer erosion. The critical shear strength according to the UCSB SEDflume methods are $\tau_{cr} = 1.06$ Pa for linear interpolation and $\tau_{cr} = 1.34$ Pa for the power law fit. Results from the UCSB method surround the UF bilinear method for this sample.

Sample 75-082712 was the last 75% degraded surrogate waste sample compacted at 2.3 MPa made using Socorro goethite. There are no notebook entries or other testing peculiarities worth noting. As seen in Figure 24, the UF bilinear model fits the data very well and all three methods yield consistent results for the critical shear stress of the material. Based on the bilinear method the critical shear stress is $\tau_m = 1.79$ Pa. The critical shear strength according to the UCSB SEDflume methods are $\tau_{cr} = 1.75$ Pa for linear interpolation and $\tau_{cr} = 1.85$ Pa for the power law fit.

Sample 75-082912 is the first of four 75% degraded surrogate waste samples compacted at 2.3 MPa made using Albuquerque goethite. The analyses of this sample's erosion behavior are shown in Figure 25. The sharp dogleg in the data suggests that the UF bilinear model can be used to adequately describe the data. This is borne out in the good fit of the model in Figure 25a. The lower line suggests that the first 25 mm (1 inch) of material has end effects caused by the sample building and/or loading process. As discussed in Herrick et al. (2007a), the surface layer may extend several inches down in natural sediments suggesting that the behavior of this sample is not uncommon. The critical shear stress is $\tau_m = 2.00$ Pa based on the UF bilinear model. The bimodal nature of how this sample eroded is not captured well using either SEDflume analysis method. The critical erosion rate criterion of 10^{-4} cm/s = 0.06 mm/min was exceeded at 1.04 Pa (Figure 25b). However, the erosion rate dropped down to 0.03 mm/min at 1.30 Pa. Due to that drop in the erosion rate, it was not felt that bulk erosion had begun. After 1.30 Pa, the erosion rate started to increase steadily. Therefore, UCSB methods were applied to shear stresses greater than 1.30 Pa. Even with this adjustment, the UCSB methods yield a critical shear stress much lower than the UF bilinear analysis. The critical shear strength according to the UCSB SEDflume methods are $\tau_{cr} = 1.32$ Pa for linear interpolation and $\tau_{cr} = 1.35$ Pa for the power law fit.

Sample 75-091012 is another 75% degraded surrogate waste samples compacted at 2.3 MPa made using Albuquerque goethite. Even though the testing on this sample was completed in one day, a testing break occurred for lunch. Because of possible sample extrusion noted with the use of aluminum sample holders, the pressure valve at the end of the channel was fully open when the flow was stopped. This allows the water in the channel to drain rapidly, disturbing the end of the sample. Upon restarting the pump, a small amount of material was sheared off to ensure the material is at a condition similar to what it was at before the pump was stopped. For this test, it was accomplished by shearing off enough of the face so that no erosion was occurring at 1.04 Pa, the stress level prior to the lunch break.

The erosion behavior of Sample 75-091012 is equally well described by all three models (Figure 26). Again there is a strong dogleg in the erosion rate data. There was effectively no erosion until the stress was increased to 1.17 Pa, after that point the erosion rate increased steadily with shear stress. Based on the bilinear method the critical shear stress is $\tau_m = 1.06$ Pa. The critical shear strength according to the UCSB SEDflume methods are $\tau_{cr} = 1.05$ Pa for linear interpolation and $\tau_{cr} = 1.05$ Pa for the power law fit.

Sample 75-091312 is the third 75% degraded surrogate waste sample compacted at 2.3 MPa made using Albuquerque goethite. Like Sample 75-091012, there was a testing break which occurred during testing, however this time it was for overnight. Upon resumption of testing, the possibly damaged face was sheared off until a condition similar to the previous day was

achieved; that is, no erosion at a shear stress of 1.82 Pa. After that, testing was continued. The erosion behavior of Sample 75-091312 is strongly bilinear, indicating that bulk erosion begins at about $\tau_m = 1.84$ Pa according to the UF method (Figure 27). The UCSB methods yield critical shear stress values that envelope this value: $\tau_{cr} = 1.75$ Pa for linear interpolation and $\tau_{cr} = 1.85$ Pa for the power law fit.

The final 75% degraded surrogate waste sample compacted at 2.3 MPa made using Albuquerque goethite is Sample 75-091912. The data indicate that the erosion behavior is bilinear with little erosion of the surface material, followed a behavior in which the erosion rate increases steadily with shear stress indicative of bulk material erosion. There are no testing procedures of note for this sample. Based on the UF bilinear method, the critical shear stress is $\tau_m = 1.19$ Pa (Figure 28a). The critical shear strength according to the UCSB SEDflume methods are $\tau_{cr} = 1.25$ Pa for linear interpolation and $\tau_{cr} = 1.34$ Pa for the power law fit (Figure 28b).

A compilation of the critical shear stress at which bulk erosion initiates according to the three methods of analysis for all the 75% degraded surrogate waste samples compacted at 2.3 MPa is given in Table 9. Also given is the average from each method. In general, the three methods of evaluation yield similar results. It should be noted that the two most commonly accepted methods of analysis for flume data are the UF bilinear fit and the UCSB power law fit, and the averages from these two are remarkably close.

Table 9. Compilation of critical shear stresses for the 75% degraded surrogate waste samples compacted at 2.3 MPa.

Sample No.	Critical Shear Stress (Pa)		
	UF bilinear τ_m	UCSB, linear interpolation τ_{cr}	UCSB, power law τ_{cr}
75-080112	1.60	1.46	1.62
75-082212	1.22	1.06	1.34
75-082712	1.79	1.75	1.85
75-082912	2.00	1.32	1.35
75-091012	1.06	1.05	1.05
75-091312	1.84	1.75	1.85
75-091912	1.19	1.25	1.34
Average	1.53	1.38	1.49

Based on visual inspection of the data as plotted in Figure 22 through Figure 28 it is seen that the method that is most appropriate for this material is the method suggested by Parchure and Mehta (1985) – the UF bilinear fit. In every case except Sample 75-082912 (Figure 25) the lower line, indicative of the erosive behavior of the surface layer, has an erosion rate that is negligible compared the erosion behavior once the bulk of the material starts to erode. In addition, there is a sharp dogleg in the material behavior substantiating the idea that another mode of behavior is in

action. Also, a couple of the samples (75-082712 and 75-091912) display a behavior in which the line pertaining to the surface layer has a negative slope. This suggests that erosion of the bulk of the material has not actually begun even though at some shear stress levels a piece or two of material broke off.

The UCSB methods produce inconsistent results for this material. As mentioned, all plots indicate a shear stress at which the erosion rate continually increases with increasing shear stress. It is intuitive that for a uniform material, such as these samples, should erode more and more as the force that is causing erosion either stays the same or increases. The erosion rate should either stay the same or increase, depending on what happens with the shear stress. If the erosion rate decreases or stops under higher shear loads, it suggests that the critical stress level to initiate true erosion of the bulk of the material has not been reached. This is the underlying physics behind the UF method. Looking at the plots for the 75% degraded surrogate waste samples compacted at 2.3 MPa, at those stress levels in which bulk erosion is not taking place the trend of the erosion rate line with increasing shear stress is roughly flat or negative. However, there are stress levels at which the erosion rate has risen above the critical rate defined by UCSB. This happens for Sample 75-091312 (Figure 27) and Sample 75-091912 (Figure 28) as well as Sample 75-082912 (Figure 25). This suggests that the 10^{-4} cm/s threshold may not be representative of or applicable to this material. The threshold was chosen so that it gives results consistent with other practitioners using a pristine, quartz sand having a standard grain size (Roberts, pers. comm.). This sand was used during the checkout of the flume to ensure the system produced results of a known standard (Schuhen, 2011).

Concerning the fit of the UCSB/SEDflume methods, a line fit between two points will always have an $R^2 = 1.0$ unless the line is horizontal. For a horizontal line, R^2 cannot be defined. However, because of the choice to use the critical erosion rate of 10^{-4} cm/s, the two points surrounding this threshold at which the initiation of erosion is calculated are often less than the elbow in the dogleg where bulk erosion takes off. It is therefore not surprising that the predicted critical shear stresses by these methods are less than those predicted by the UF bilinear method. In practice, the power law fit is used since it is derived from a more comprehensive power law relationship that describes the erosion behavior of well mixed sediments is (Jepsen et al., 1997):

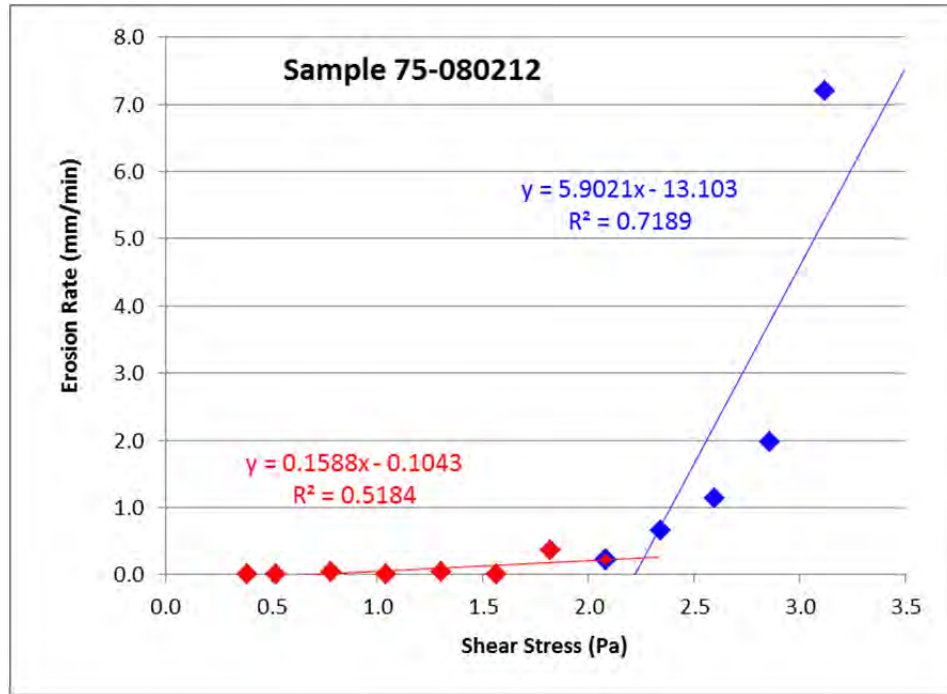
$$E = A\tau^n\rho^m \quad (6)$$

It is obvious from the plots that even though the relationship may fit the three points above and below the critical erosion rate needed to define it fairly well, the fit relationship does not describe the behavior of the material beyond that level well at all. Inclusion of more data points typically leads to a worse fit. In addition, the initial arc of the fit curve, looking from low shear stress to high shear stress, is almost horizontal. This pushes the estimate of the critical shear stress to higher values than the linear interpolation method. Based on visual inspection of plots for the 75% degraded surrogate waste samples compacted at 2.3 MPa in Figure 22 through Figure 28, it is obvious that this model is not representative of the material's behavior.

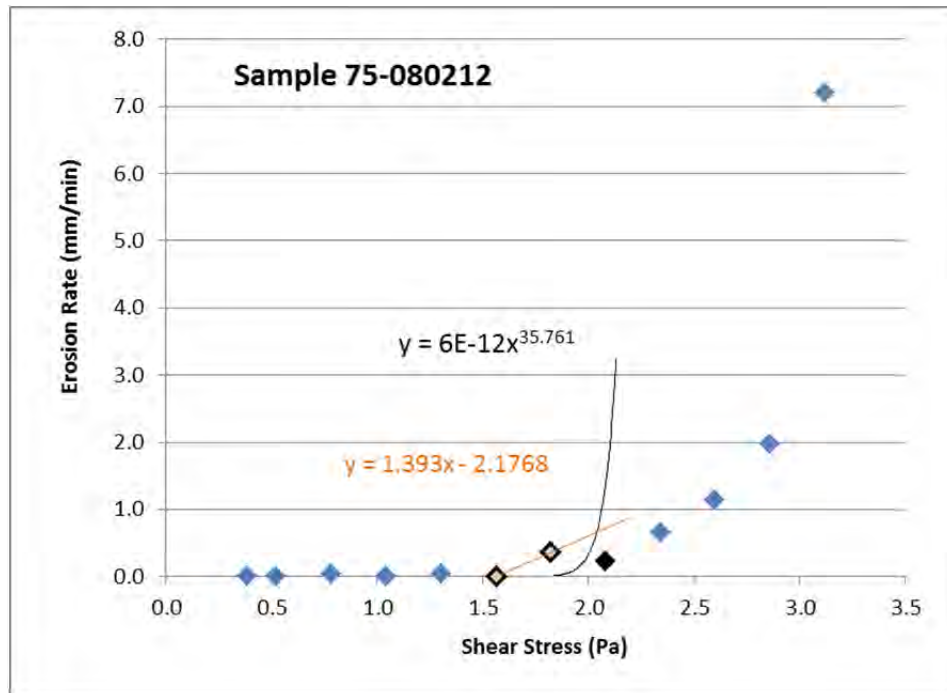
For these reasons, it is felt that the UF bilinear result yields the most reliable measure for the shear stress at the beginning of erosion for this material.

6.3.2 75% Degraded Surrogate Waste Material Tests, Die Compacted to 5.0 MPa

The results for the seven 75% degraded surrogate waste material tests die compacted to 5.0 MPa are given graphically in Figure 29 through Figure 35, on the next seven pages. The first three figures are for those samples made with Socorro goethite (Samples 75-080212, 75-082312, and 75-082812) and the final four figures are for those samples made with Albuquerque goethite (Samples 75-083012, 75-091212, 75-091812, and 75-092012).

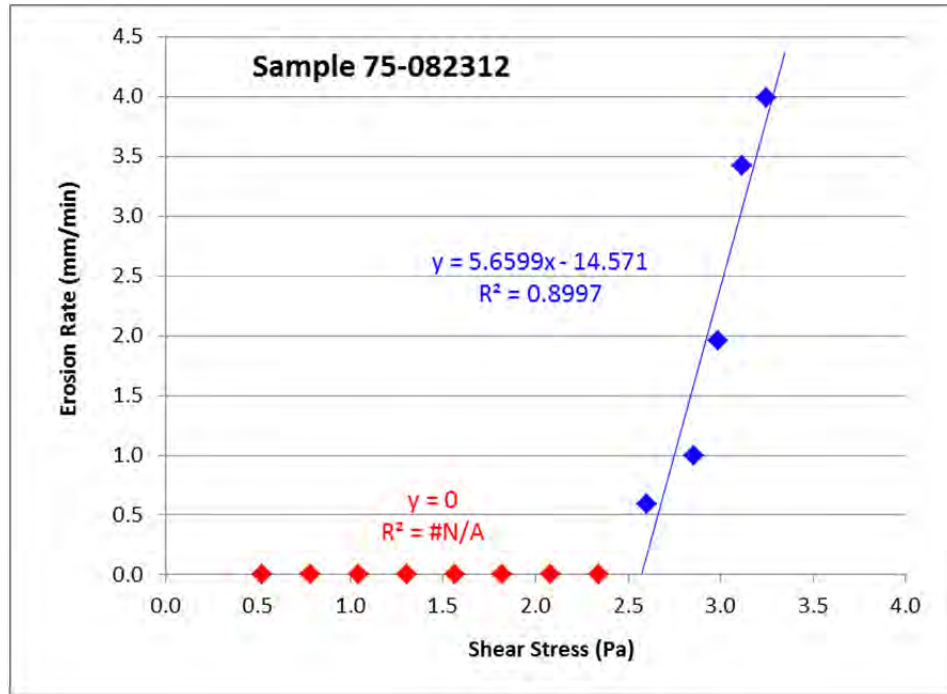


(a)

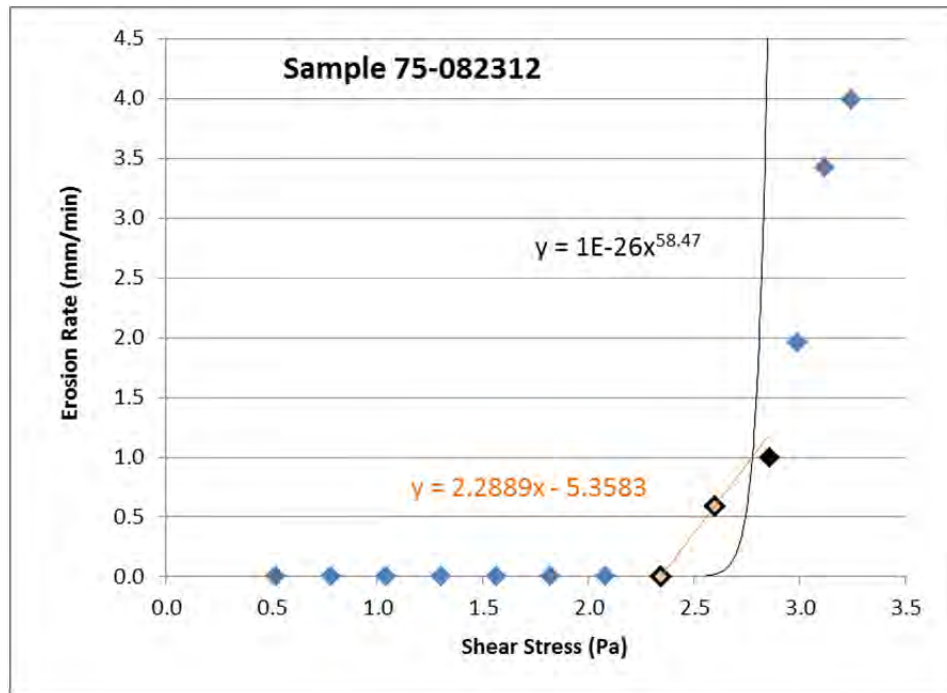


(b)

Figure 29. Analyses of the test results for Sample 75-080212, Socorro goethite. (a) UF bilinear fit yielding $\tau_m = 2.22$ Pa and (b) the UCSB fits around a critical shear stress of 10^{-4} cm/sec giving for the linear interpolation $\tau_{cr} = 1.61$ Pa (two orange points) and for the power law fit $\tau_{cr} = 1.90$ Pa (three black points).

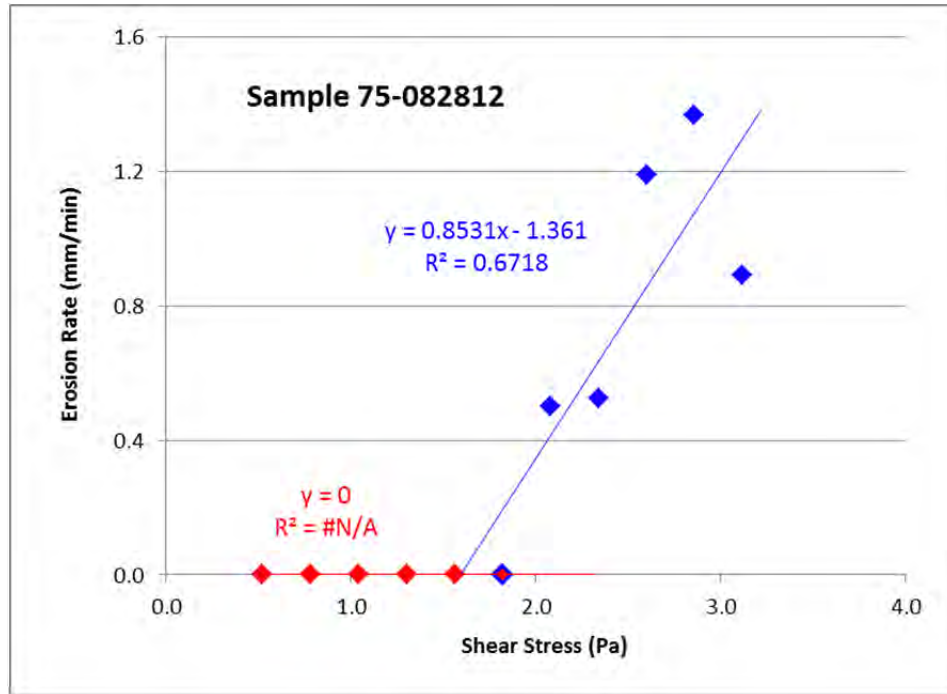


(a)

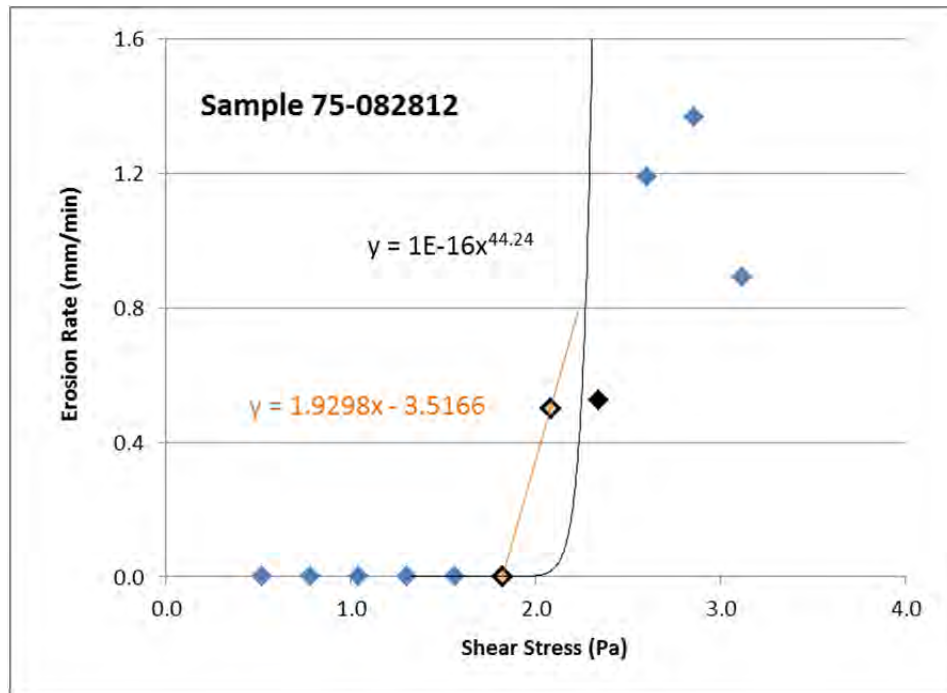


(b)

Figure 30. Analyses of the test results for Sample 75-082312. Socorro goethite (a) UF bilinear fit yielding $\tau_m = 2.57$ Pa and (b) the UCSB fits around a critical shear stress of 10^{-4} cm/sec giving for the linear interpolation $\tau_{cr} = 2.37$ Pa (two orange points) and for the power law fit $\tau_{cr} = 2.65$ Pa (three black points).

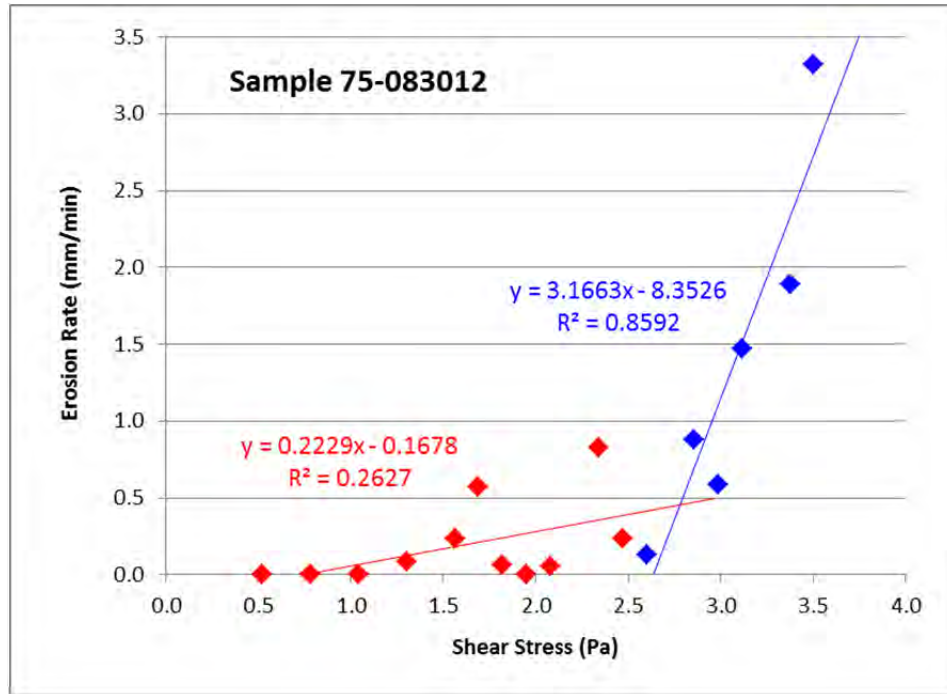


(a)

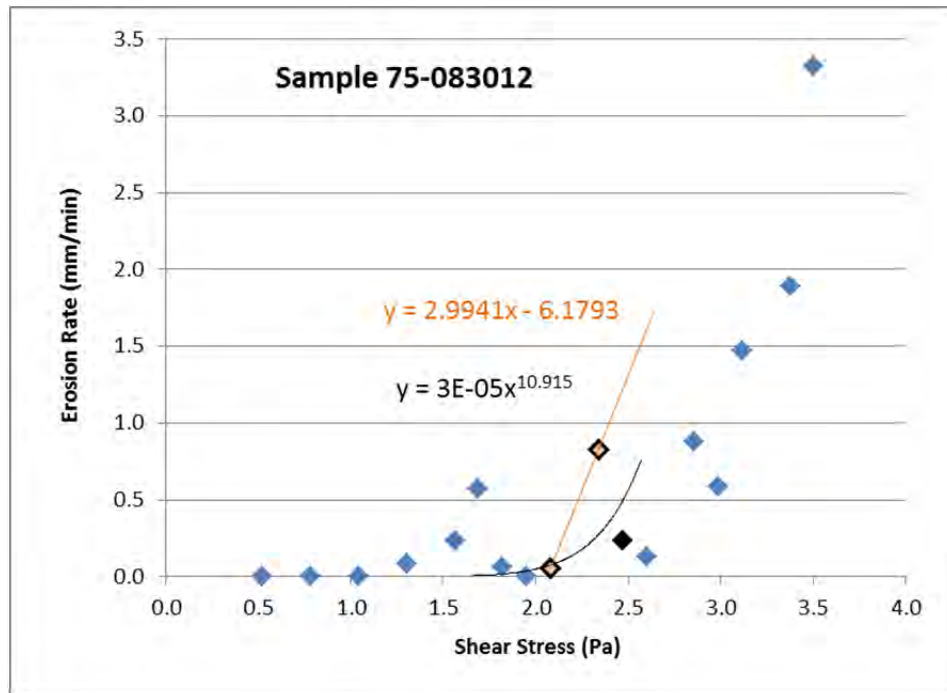


(b)

Figure 31. Analyses of the test results for Sample 75-082812, Socorro goethite. (a) UF bilinear fit yielding $\tau_m = 1.60$ Pa and (b) the UCSB fits around a critical shear stress of 10^{-4} cm/sec giving for the linear interpolation $\tau_{cr} = 1.85$ Pa (two orange points) and for the power law fit $\tau_{cr} = 2.16$ Pa (three black points).

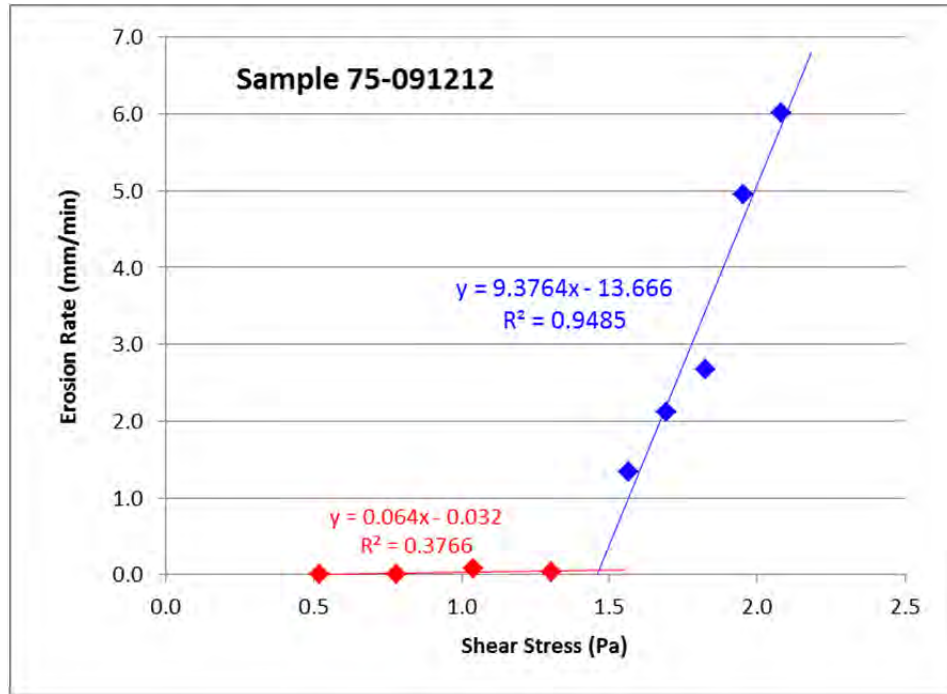


(a)

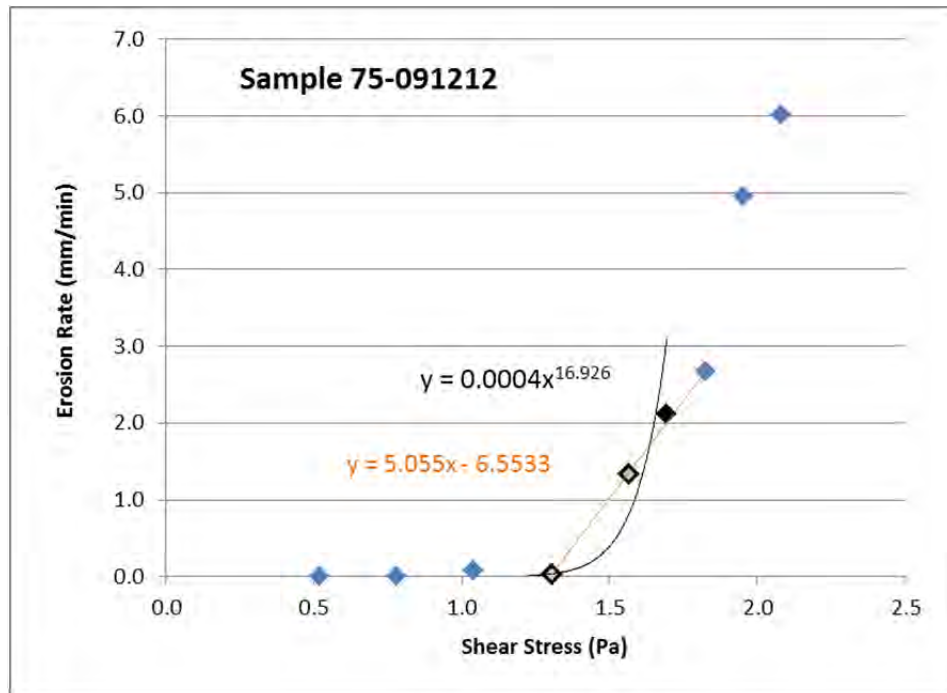


(b)

Figure 32. Analyses of the test results for Sample 75-083012. Albuquerque goethite. (a) UF bilinear fit yielding $\tau_m = 2.64$ Pa and (b) the UCSB fits around a critical shear stress of 10^{-4} cm/sec giving for the linear interpolation $\tau_{cr} = 2.08$ Pa (two orange points) and for the power law fit $\tau_{cr} = 2.01$ Pa (three black points).

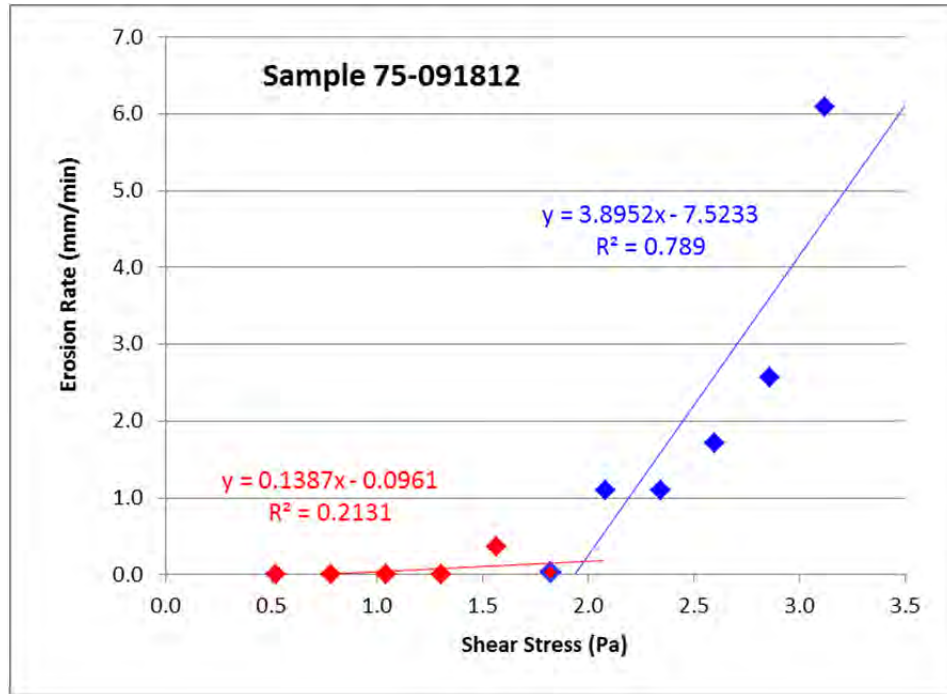


(a)

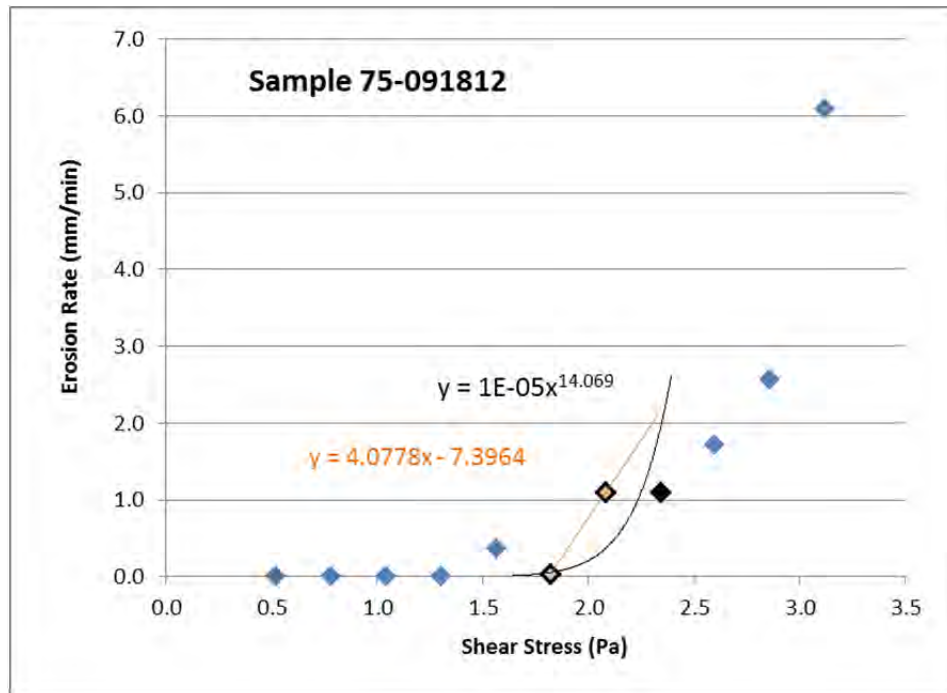


(b)

Figure 33. Analyses of the test results for Sample 75-091212, Albuquerque goethite. (a) UF bilinear fit yielding $\tau_m = 1.46$ Pa and (b) the UCSB fits around a critical shear stress of 10^{-4} cm/sec giving for the linear interpolation $\tau_{cr} = 1.31$ Pa (two orange points) and for the power law fit $\tau_{cr} = 1.34$ Pa (three black points).

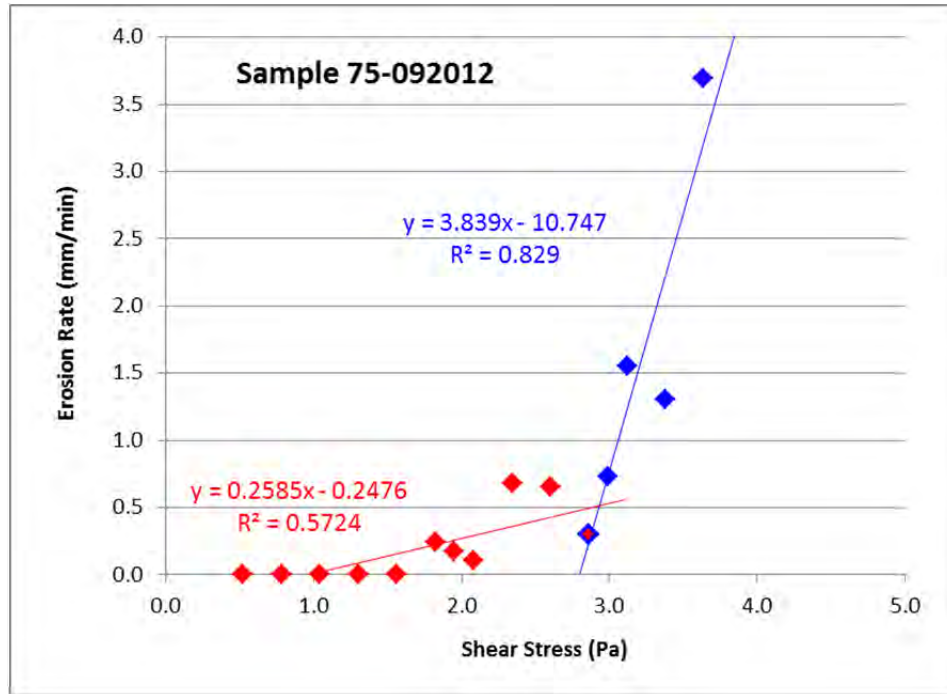


(a)

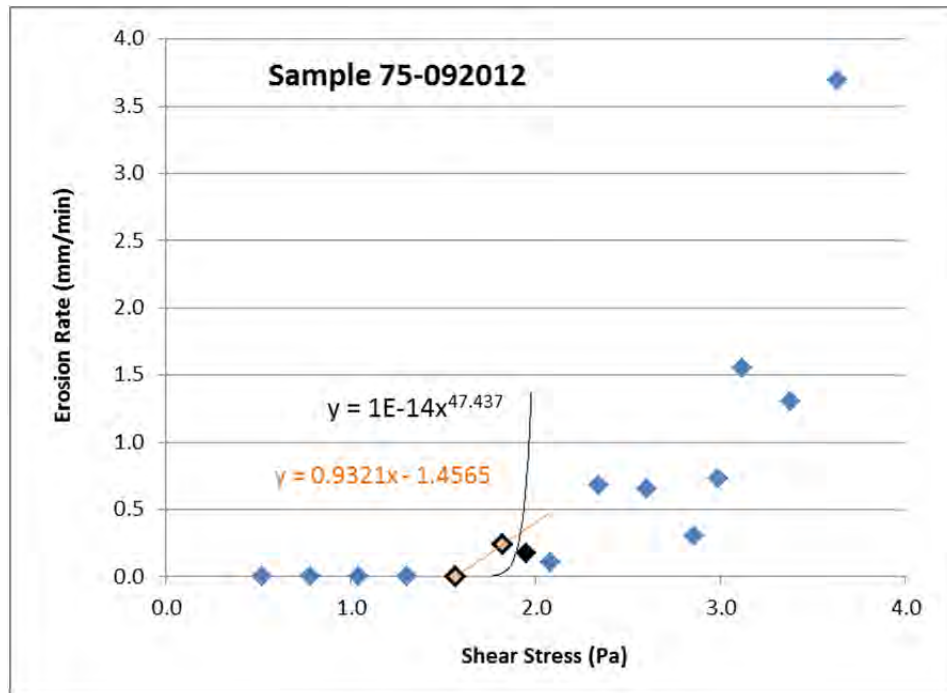


(b)

Figure 34. Analyses of the test results for Sample 75-091812, Albuquerque goethite. (a) UF bilinear fit yielding $\tau_m = 1.93$ Pa and (b) the UCSB fits around a critical shear stress of 10^{-4} cm/sec giving for the linear interpolation $\tau_{cr} = 1.83$ Pa (two orange points) and for the power law fit $\tau_{cr} = 1.86$ Pa (three black points).



(a)



(b)

Figure 35. Analyses of the test results for Sample 75-092012. Albuquerque goethite. (a) UF bilinear fit yielding $\tau_m = 2.80$ Pa and (b) the UCSB fits around a critical shear stress of 10^{-4} cm/sec giving for the linear interpolation $\tau_{cr} = 1.63$ Pa (two orange points) and for the power law fit $\tau_{cr} = 1.86$ Pa (three black points).

6.3.2.1 Discussion of Results for 75% Degraded Surrogate Waste Material Tests, Die Compacted to 5.0 MPa

Sample 75-080212 was made using Socorro goethite and was made in the anodized aluminum sample holders, as were all of the 75% degraded surrogate waste samples. It was tested over two days. There was little erosion during the first day which involved shear stresses 0.39 to 1.30 Pa (Figure 29). Most erosion occurred at 0.78 Pa, returning to no erosion as the stress was increased. Testing was interrupted the first day by a power outage, which abruptly stopped the pump. At the start of the second day, the face of the sample was sheared off to remove damaged material and allowed to stabilize at 1.30 Pa for ½ hour with no erosion occurring. This state was considered identical to the condition the sample was in before the power outage. During the second day of testing, no erosion was noticed at stress levels 1.30 and 1.56 Pa, followed by times of slow erosion at 1.82 and 2.08 Pa. After 2.08 Pa the erosion rate began to increase rapidly with increasing shear stress. The UF bilinear upper line fit to this data is fair ($R^2 = 0.72$), giving $\tau_m = 2.22$ Pa. The progression in the increase in erosion rate with shear stress from no erosion until obvious bulk erosion is gradual starting at 1.82 Pa. In other words, there is no distinct elbow in this data set. Application of the UCSB methods pick up this gradual increase in the erosion rate, yielding a smaller estimate of the critical shear stress for this sample: $\tau_{cr} = 1.61$ Pa for the linear interpolation model and $\tau_{cr} = 1.90$ Pa for the power law fit.

Sample 75-082312 was also made with Socorro goethite. For the analysis of this sample's erosion characteristics, only the laboratory notebook entries were used since the DAS buffer was full. Testing on this specimen was finished in one day. The erosion behavior of this sample indicates no erosion until about 2.60 Pa (Figure 30). After that stress level, the erosion rate increased linearly with increasing shear stress ($R^2 = 0.90$). The data fit the UF model quite well, yielding a critical shear stress of $\tau_m = 2.57$ Pa. The UCSB methods give critical shear stress values that are consistent with the UF method. The linear interpolation method predicts a slightly lower critical shear stress of $\tau_{cr} = 2.37$ Pa, while the power law model gives $\tau_{cr} = 2.65$ Pa.

The last sample of 75% degraded surrogate waste material made using Socorro goethite and compacted at 5.0 MPa is Sample 75-082812. No erosion of this sample occurred until about 2.0 Pa (Figure 31). After that shear stress, the erosion rate generally increased with increasing shear stress. The exception to this trend was for the erosion rate at 3.12 Pa dropped off slightly compared to the previous two stress levels. Even though the data suggest that the UF model is appropriate to describe the behavior of this sample, the line fit to the erosion of the material is fair ($R^2 = 0.67$). The critical shear stress predicted by the UF method is $\tau_m = 1.60$ Pa. Because of the sharp dogleg in the data, the UCSB methods give critical shear stress values that are fairly consistent with the UF method. The linear interpolation method predicts a critical shear stress of $\tau_{cr} = 1.85$ Pa, while the power law model gives $\tau_{cr} = 2.16$ Pa.

The 75% degraded surrogate waste material samples made using Albuquerque goethite and compacted at 5.0 MPa start with Sample 75-083012. The sample was tested over two days. For the first day, the DAS buffer was still full so no digital data was recorded. The DAS buffer was cleared the second day. Plots of the erosion rate versus shear stress are shown in Figure 32. Even though there is a gradual increase in the erosion rate with shear stress starting at 1.30 Pa, the data still suggest that the UF model is appropriate for this sample due to the rapid increase occurring

at about 2.75 Pa. The fit of the data to the upper line after that stress is good ($R^2 = 0.86$). Using the fit lines in Figure 32a, the UF model gives $\tau_m = 2.64$ Pa. It is difficult to interpret the data for the UCSB methods since the erosion rate jumped up at 1.69 and 2.34 Pa. For the former stress level, the erosion rates dropped down to zero again so that the analyses were deemed not applied to stress levels lower than 2.0. For the later stress, the erosion rates also dropped back down, but not below the critical threshold. For that reason the points between 2.0 and 2.5 Pa were used in the UCSB analyses. The linear interpolation method predicts a critical shear stress of $\tau_{cr} = 2.08$ Pa, while the power law model gives $\tau_{cr} = 2.01$ Pa. None of these were included in those points used to calculate the upper line in the UF model, so the UCSB analyses will undoubtedly yield critical shear stresses less than $\tau_m = 2.64$ Pa.

Sample 75-091212 is a sample made with Albuquerque goethite that displays an obvious bimodal character. There was effectively no erosion until about 1.5 Pa (Figure 33). After that, the increase of erosion rate with shear stress is quite linear, having an $R^2 = 0.95$. The UF model is a very good fit for this sample. The critical shear stress for erosion of the mass of the material is $\tau_m = 1.46$ Pa. Due to the sharp elbow in the erosion behavior it is expected that the UCSB analyses will give results consistent with the UF results. The UCSB/SEDflume results are $\tau_{cr} = 1.31$ Pa for the linear interpolation model and $\tau_{cr} = 1.34$ Pa for the power law fit.

Sample 75-091812 is an example of a 75% degraded surrogate waste material sample made using Albuquerque goethite and compacted at 5.0 MPa that shows a behavior that is well described by the UF model Figure 34a. The lower line has a gradual slope until 1.82 Pa when mass erosion sets in. The good fitting upper line ($R^2 = 0.79$) also attests to the ability of the UF model to describe the data. This model predicts $\tau_m = 1.93$ Pa. Due to the sharp elbow in the dogleg of the data, the UCSB model results are in close proximity to the UF results. The UCSB linear interpolation method predicts a critical shear stress of $\tau_{cr} = 1.83$ Pa, while the power law model gives $\tau_{cr} = 1.86$ Pa.

The last 75% degraded surrogate waste material sample made using Albuquerque goethite and compacted at 5.0 MPa is Sample 75-092012. The test was conducted over two days. Analyses of this sample are shown in Figure 35. The data can be fit fairly well using the bilinear model. However, in so doing, the lower line exhibits increasing scatter with increasing shear stress Figure 35a. Nonetheless, a well-fitting upper line ($R^2 = 0.83$) yields an estimate of $\tau_m = 2.80$ Pa for the bilinear model. Also because of the scatter of erosion rates at lower shear stresses, the critical erosion rate threshold defined by UCSB is crossed at a lower stress than that predicted by the UF model. Shear stresses between 1.5 and 2.0 Pa are used in the SEDflume analyses. These give $\tau_{cr} = 1.63$ Pa for the linear interpolation model and $\tau_{cr} = 1.86$ Pa for the power law fit.

A compilation of the critical shear stress at which bulk erosion initiates according to the three methods of analysis for all the 75% degraded surrogate waste samples compacted at 5.0 MPa is given in Table 10. Also given is the average from each method. The two most commonly accepted methods of analysis for flume data are the UF bilinear fit and the UCSB power law fit, and the averages from these two are quit close. The UCSB linear interpolation method, which is believed to been used previously only by Herrick et al. (2007b), is the one having the greatest difference. It is also the method without any physical reasoning behind it.

Table 10. Compilation of critical shear stresses for the 75% degraded surrogate waste samples compacted at 5.0 MPa.

Sample No.	Critical Shear Stress (Pa)		
	UF bilinear τ_m	UCSB, linear interpolation τ_{cr}	UCSB, power law τ_{cr}
75-080212	2.22	1.61	1.90
75-082312	2.57	2.37	2.65
75-082812	1.60	1.85	2.16
75-083012	2.64	2.08	2.01
75-091212	1.46	1.31	1.34
75-091812	1.93	1.83	1.86
75-092012	2.80	1.63	1.86
Average	2.17	1.81	1.97

Based on visual inspection of the data as plotted in Figure 29 through Figure 35 it appears that the method that is most appropriate for the 75% degraded surrogate waste material compacted at 5.0 MPa is the method suggested by the UF bilinear fit proposed by Parchure and Mehta (1985). In every sample, there is a sharp increase in the erosion rate of the material with increasing stress after a certain stress level substantiating the idea that another mode of erosion is in action. When looking at all the 75% degraded samples regardless of the compaction pressure, the samples made with Socorro goethite tend to have no or little erosion before they undergo bulk erosion while those made with Albuquerque goethite sometimes produce a gradual slope in the surface erosion line.

The gradual slope of the surface erosion line in the samples made with Albuquerque goethite makes using the analyses using the UCSB methods difficult. As pointed out in Section 6.3.1, concerning the discussion of the behavior of the 75% degraded surrogate waste material samples compacted at 2.3 MPa, the critical erosion rate used to define the critical shear stress may work well for well sediments having a consistent grain size, but does not for these surrogate materials. In this section, as in the last section, the critical erosion rate was at times exceeded, but erosion of the bulk material away from the surface layer had not initiated. This conclusion is based on the clearly bimodal behavior of erosion rate with increasing shear stress. Crossing the critical erosion rate threshold forced some of the UCSB analyses to consider shear stresses not within the range of stresses where bulk erosion is taking place, i.e. Sample 75-083012 (Figure 32) and Sample 75-092012 (Figure 35).

6.3.3 Comparison of Results Using Socorro and Albuquerque Goethites

Two different goethites were used for the tests using 75% degraded surrogate materials as discussed in Section 6.3. One goethite was mined around Socorro, NM (“Socorro”) and the other from on Kirkland Air Force Base (“Albuquerque”). For purposes of comparison, the UF analysis

method results are used. The UF results for each surrogate waste type and compaction pressure from Table 9 and Table 10 are rewritten below in Table 11. Also given are the means and 95% confidence levels as calculated by Excel.

Table 11. Critical shear stress results from UF analyses on the 75% degraded surrogate waste materials by goethite type.

Goethite	Sample	2.3 MPa		5.0 MPa	
Socorro	75-080112	1.60			
	75-082212	1.22			
	75-082712	1.79			
Albuquerque	75-082912		2.00		
	75-091012		1.06		
	75-091312		1.84		
	75-091912		1.19		
Socorro	75-080212			2.22	
	75-082312			2.57	
	75-082812			1.60	
Albuquerque	75-083012				2.64
	75-091212				1.46
	75-091812				1.93
	75-092012				2.80
Mean		1.54	1.52	2.13	2.21
95% Confidence Level		0.72	0.74	1.22	1.00

The mean of the critical shear stresses for the Socorro goethite specimens is larger than the Albuquerque goethite specimens for specimens compacted at 2.3 MPa, while it is smaller for specimens compacted at 5.0 MPa. In addition, for both compaction pressures, the 95% confidence interval (= sample mean +/- the 95% confidence level) for specimens made with either goethite overlaps the mean of specimens made with the other goethite type. This indicates that the differences between mean critical shear stress results concerning specimens made using these two types of goethite are insignificant at a confidence level of 95%.

6.4 50% Degraded Surrogate Waste Material Tests

The 50% surrogate waste material samples were tested at the same time the 100% surrogate waste material samples were tested. The surrogate material descriptions are given previously in Section 3. Like the 100% surrogate waste material samples, these samples have the same materials and were made in a similar fashion to the samples tested by Hansen et al (1997, 2003)

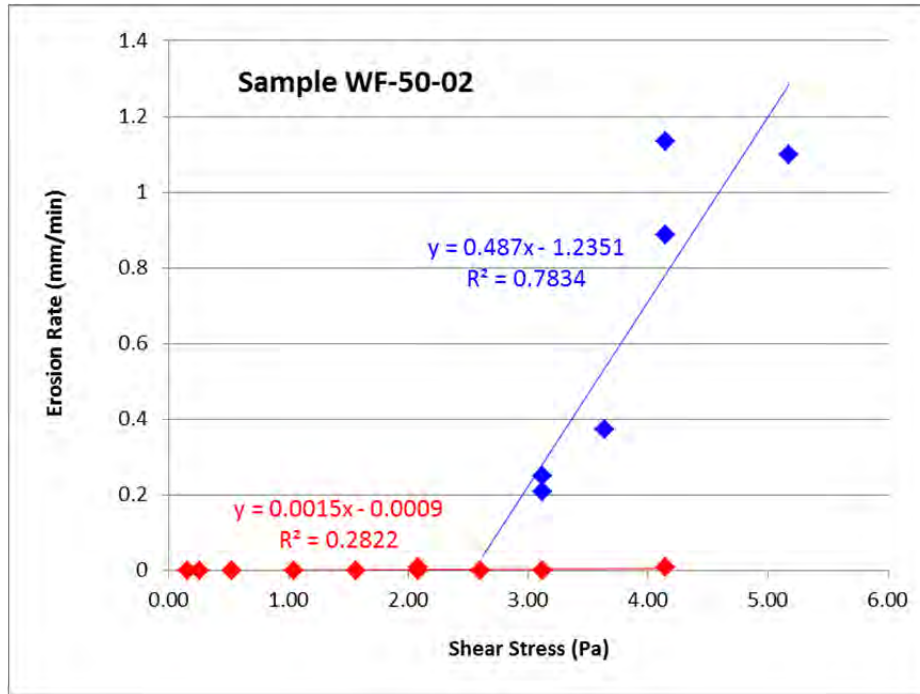
for the Spallings model parameter development and to the samples tested by Jepsen et al (1998) in SEDflume in a horizontal configuration.

A significant difference between these samples and the samples tested by Jepsen et al (1998) is that these samples were made in the sample holders, the ends were clamped, and the samples were hand carried to Carlsbad from the Geomechanics Laboratory at Sandia National Laboratories – Albuquerque. According to Mellegard (1998), the samples tested by Jepsen et al. (1998) were made by RESPEC at their facility in Rapid City, South Dakota. They were completely removed from the form used during compaction of the specimen, thereby becoming unstressed. The RESPEC samples were weighed and packaged. Packaging consisted of wrapping the specimens in Saran Wrap, aluminum foil, and dunking them in wax. The samples were shipped across country by a commercial carrier. Upon arrival at UCSB the samples were unpackaged. In addition, the samples had to be machined down from 6”×6”×4” size to 6”×4”×2.8” to fit into the SEDflume sample holder. Testing usually occurred within one to two months after fabrication (Jepsen and Roberts, 1998). It is likely, that the structure and internal cohesion of the samples was affected by removal of confinement of the form and pressure of the loading system, being wrapped in packaging, being shipped across country by a commercial carrier, being unwrapped, and machined down to fit in the SEDflume sample holders. By making the samples in the sample holders, making the samples at a Sandia National Laboratories facility, and hand carrying them to the testing facility, it is believed that many of these possibly damaging processes were mitigated or removed.

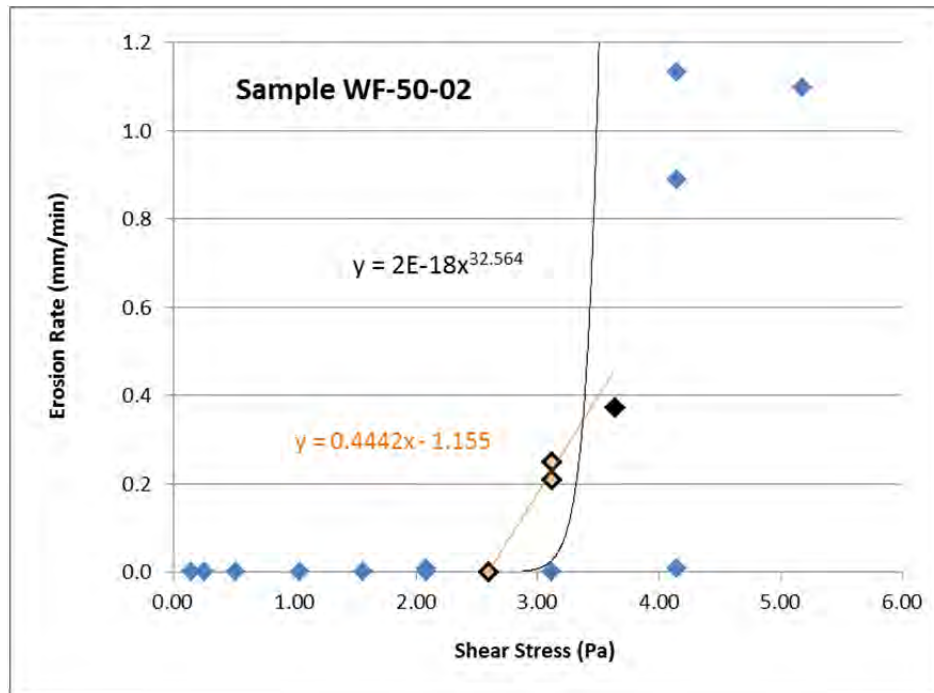
All of the samples were made in the Lexan sample holders. As mentioned in Section 6.2, the Lexan sample holders created problems in testing the 100% surrogate waste material samples. The 50% surrogate waste material samples experienced the same problems. However, being a stronger material, it is not felt that the stick-slip motion, sample deformations, and possible misalignment of the testing system affected the flume testing results for these materials to a significant degree. This is based only on visual inspection of the specimens as they moved. They did not lose any material off sample faces as they were pushed into position.

6.4.1 50% Degraded Surrogate Waste Material Tests, Die Compacted to 2.3 MPa

The results for the five 50% degraded surrogate waste material tests die compacted to 2.3 MPa are given graphically in Figure 36 through Figure 40, on the next five pages.

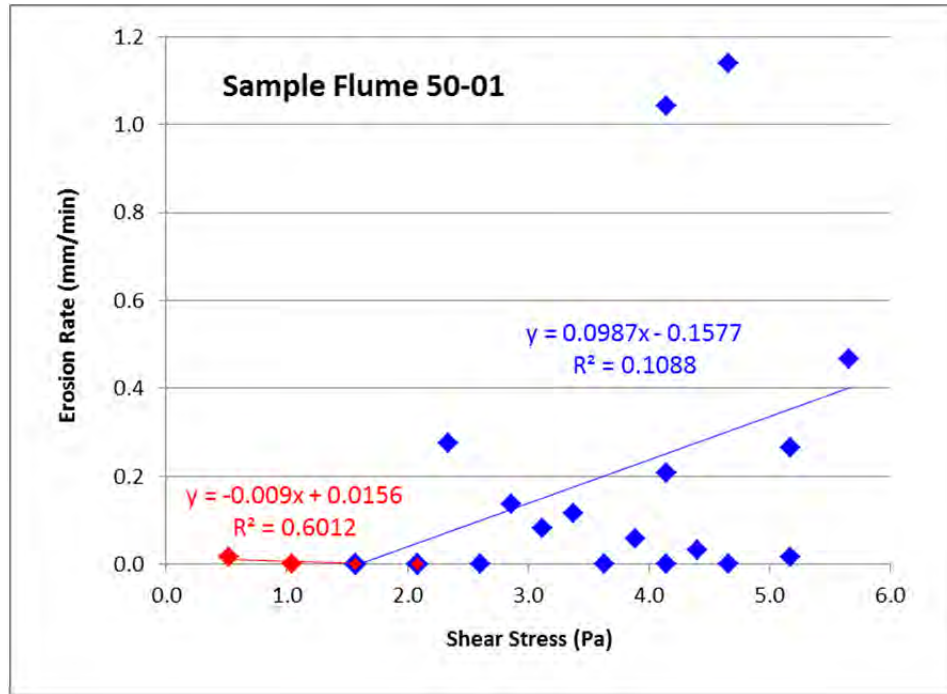


(a)

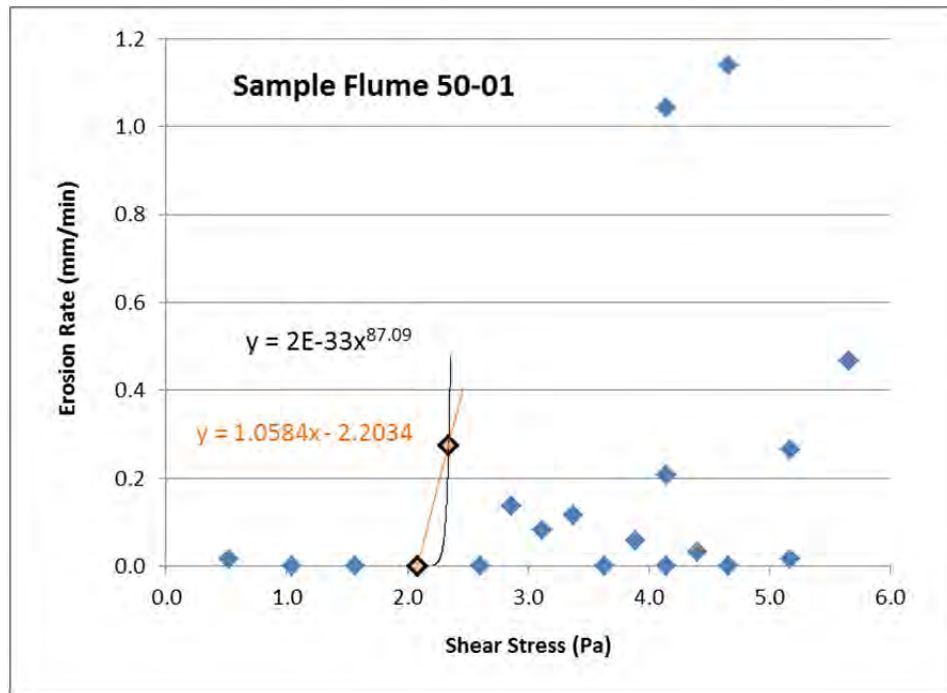


(b)

Figure 36. Analyses of the test results for Sample WF-50-02. (a) UF bilinear fit yielding $\tau_m = 2.54$ Pa and (b) the UCSB fits around a critical shear stress of 10^{-4} cm/sec giving for the linear interpolation $\tau_{cr} = 2.74$ Pa (three orange filled points) and for the power law fit $\tau_{cr} = 3.21$ Pa (four black points).

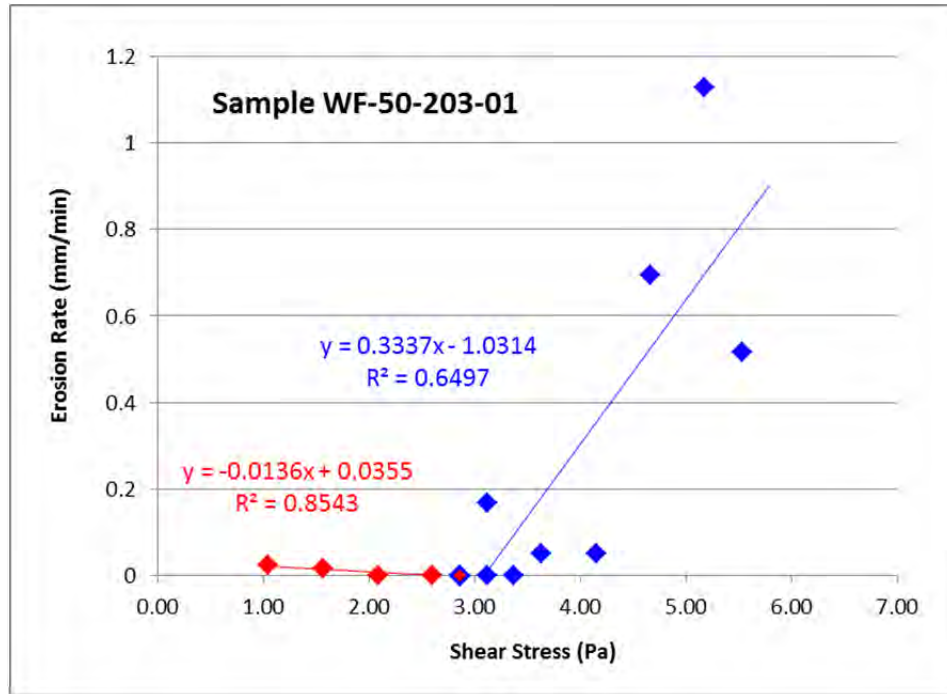


(a)

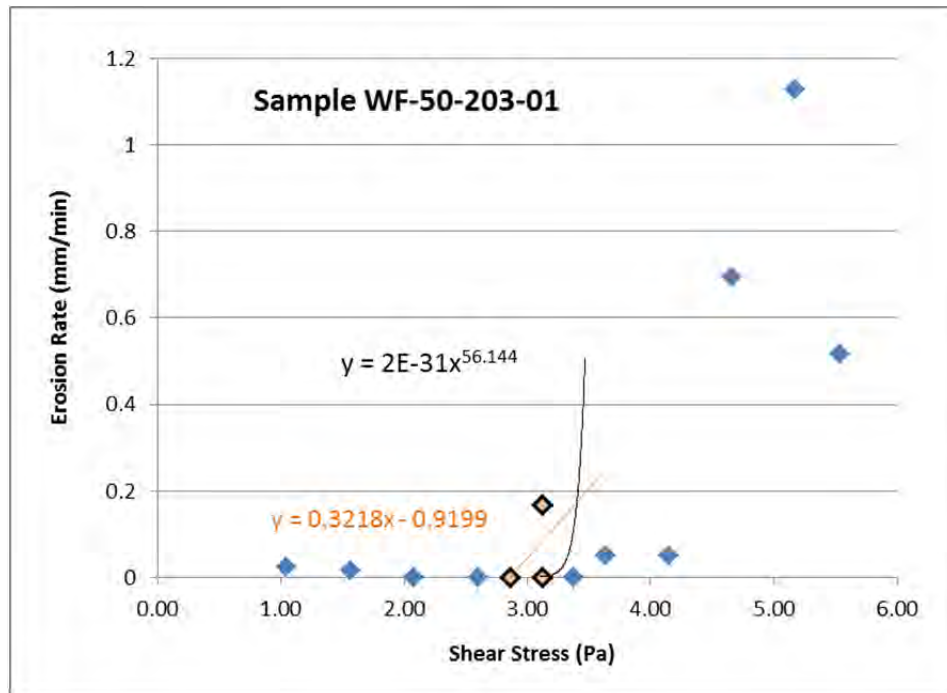


(b)

Figure 37. Analyses of the test results for Sample Flume 50-01. (a) UF bilinear fit yielding $\tau_m = 1.60$ Pa and (b) the UCSB fits around a critical shear stress of 10^{-4} cm/sec giving for the linear interpolation $\tau_{cr} = 2.14$ Pa and for the power law fit $\tau_{cr} = 2.30$ Pa (two orange filled points).

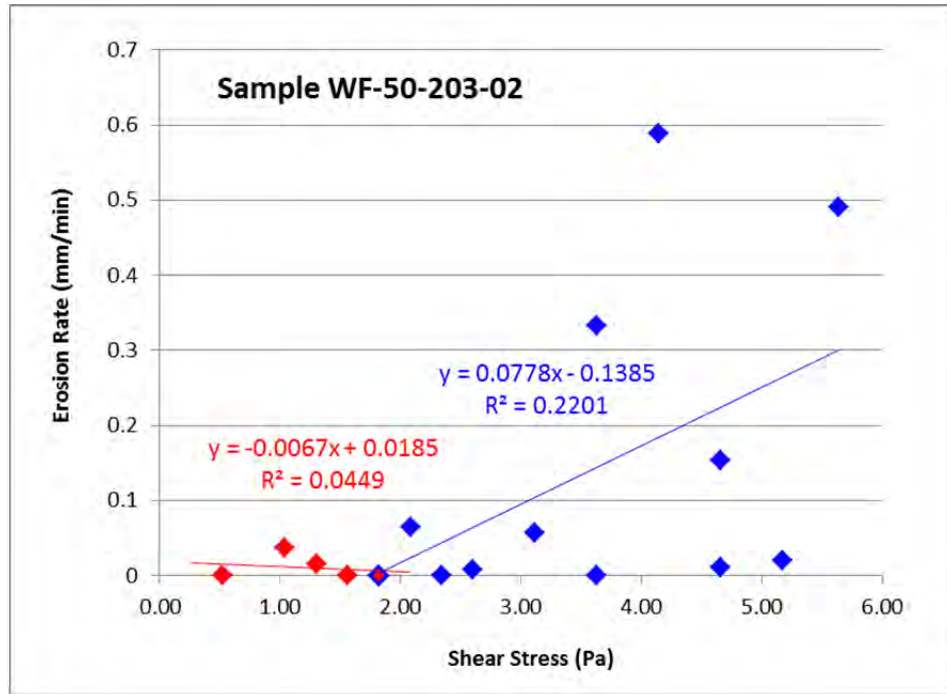


(a)

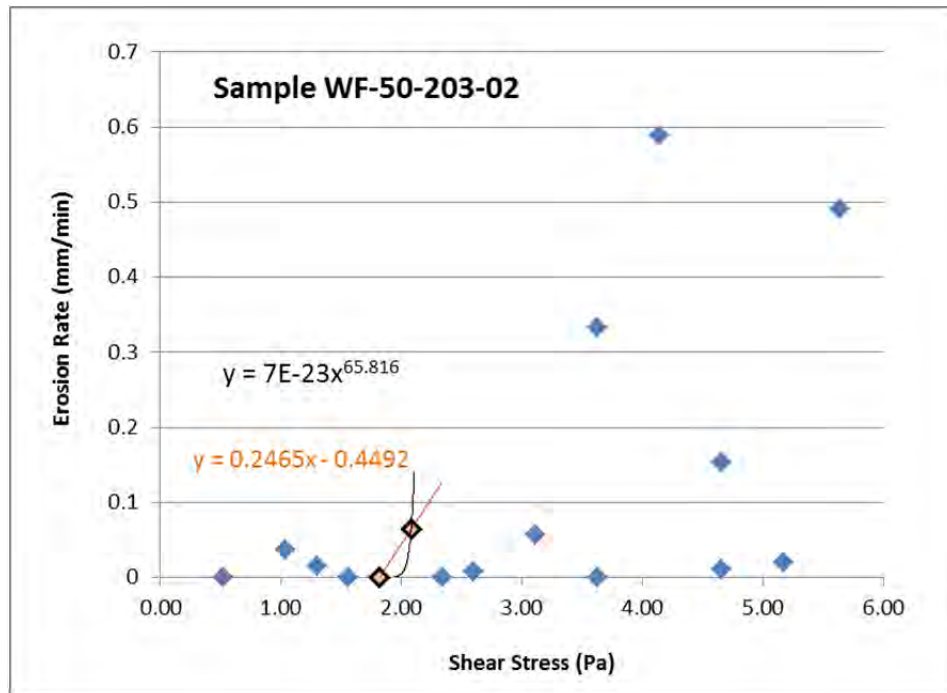


(b)

Figure 38. Analyses of the test results for Sample WF 50-203-01. (a) UF bilinear fit yielding $\tau_m = 3.09$ Pa and (b) the UCSB fits around a critical shear stress of 10^{-4} cm/sec giving for the linear interpolation $\tau_{cr} = 3.05$ Pa and for the power law fit $\tau_{cr} = 3.35$ Pa (three orange filled points).

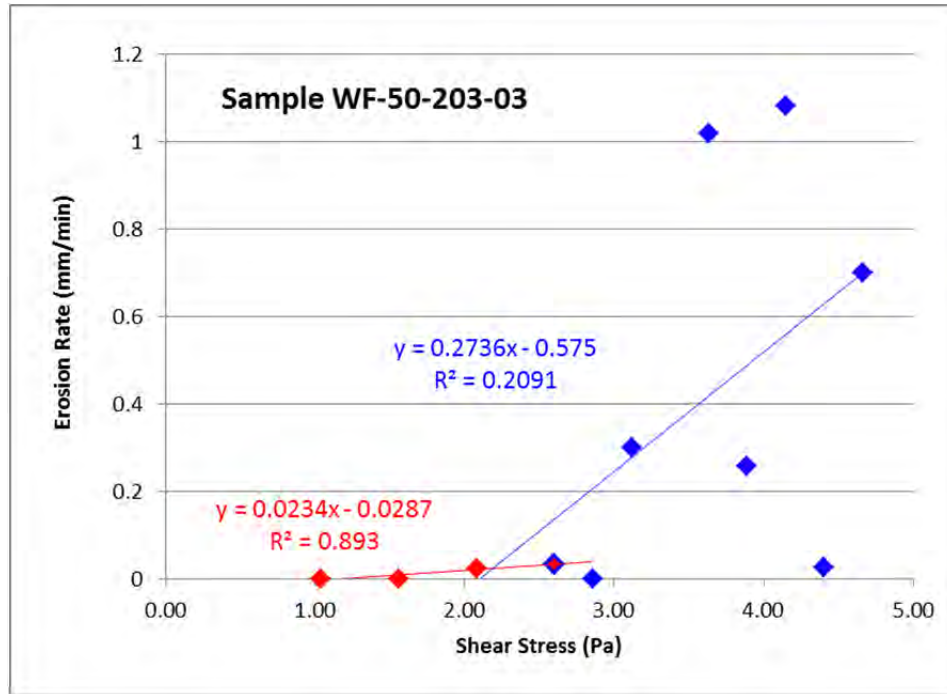


(a)

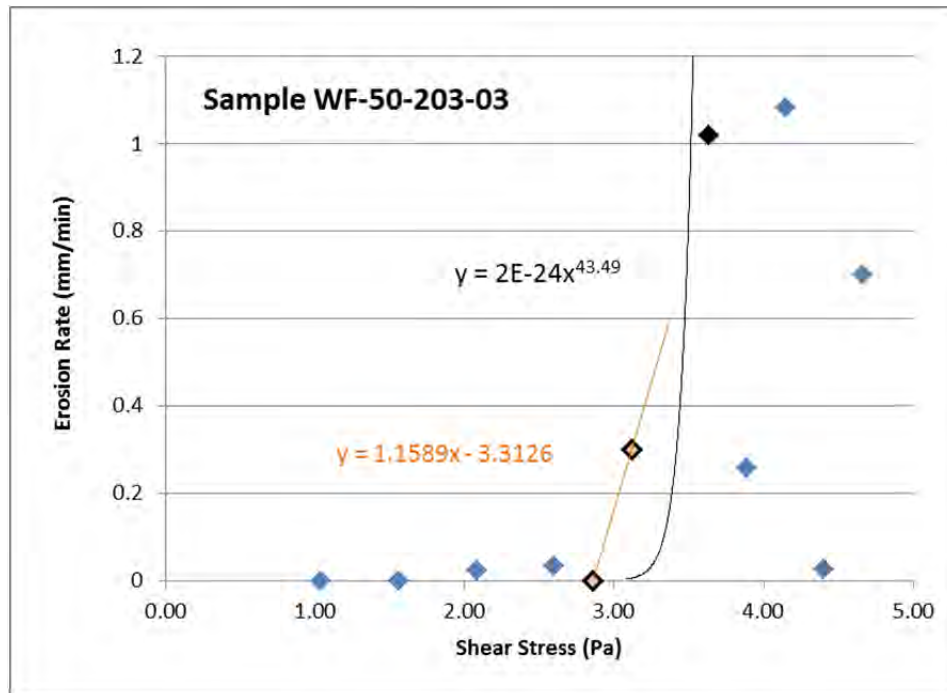


(b)

Figure 39. Analyses of the test results for Sample WF-50-203-02. (a) UF bilinear fit yielding $\tau_m = 1.78$ Pa and (b) the UCSB fits around a critical shear stress of 10^{-4} cm/sec giving for the linear interpolation $\tau_{cr} = 2.07$ Pa and for the power law fit $\tau_{cr} = 2.08$ Pa (two orange filled points).



(a)



(b)

Figure 40. Analyses of the test results for Sample WF-50-203-03. (a) UF bilinear fit yielding $\tau_m = 2.10$ Pa and (b) the UCSB fits around a critical shear stress of 10^{-4} cm/sec giving for the linear interpolation $\tau_{cr} = 2.91$ Pa (two orange filled points) and for the power law fit $\tau_{cr} = 3.29$ Pa (three black points).

6.4.1.1 Discussion of results for 50% Degraded Surrogate Waste Material Tests, Die Compacted to 2.3 MPa

Sample WF-50-02 was the only sample that was not compacted overnight. Instead, it was compacted for only 1 hr. No reason was given by personnel at the Geomechanics Laboratory who made the specimen. The reduced time under load did not appear to affect the results. The sample was tested over two days. The shear stresses on this sample were increased up to 5.17 MPa before erosion of the sample began (Figure 36). The data points in which erosion took place were obtained after erosion began at 5.17 MPa and the shear stresses were reduced. The data with erosion fall along a line fairly well ($R^2 = 0.78$), as the UF model would suggest. Only the data in which erosion was taking place were used for the UF analysis. This model yields a $\tau_m = 2.54$ Pa.

Choosing the data to use for the UCSB/SEDflume models was difficult since surface seems to be harder to erode than the interior of the specimen. If the data were used in which erosion first began are used, the UCSB method would yield give $\tau_{cr} = 4.20$ Pa for the linear interpolation model and $\tau_{cr} = 4.55$ Pa for the power law fit. The decision of what data to use was based on the trend of the data in which erosion was occurring after the initial surface was eroded away. Unfortunately, a shear stress was not tested at in which the erosion rate stopped or dropped below the critical threshold. Therefore, the data point (2.60, 0) was included. Using this point, the UCSB method predicts $\tau_{cr} = 2.74$ Pa for the linear interpolation model and $\tau_{cr} = 3.21$ Pa for the power law fit. The critical shear stresses are much more in line with the trend of the erosion data in Figure 36.

Sample Flume 50-01 was tested over three days. After erosion began at approximately 2.3 Pa, the erosion rate tended to be sporadic with increasing shear stress (Figure 37). For seven out of sixteen shear stress levels, the erosion rate dropped to or below the critical threshold. On the other hand, there are a couple of points in which the erosion rate is above 1 mm/min, which is high for this sample. The spread of the data after erosion beginning at 2.3 produces a poorly fit line to the bulk erosion part of the UF model. The upper line has a low $R^2 = 0.11$. Also, the data does not have a sharp dogleg shape to it. The UF model suggests that the critical shear stress is a $\tau_m = 1.60$ Pa. The UCSB were applied to the results at 2.08 and 2.34 Pa only. These models predict critical shear stresses for the linear interpolation analysis $\tau_{cr} = 2.14$ Pa and for the power law fit $\tau_{cr} = 2.30$ Pa.

The results of Sample WF-50-203-01 are shown in Figure 38. Testing occurred over two days. The data produce an appearance that can be described well by the UF bilinear model. The data assumed to belong to the surface, those less than 3.12 Pa, layer have a slightly negative slope. At 3.12 Pa and beyond, the erosion rate data show a consistent increase with shear stress. The fit of the upper data is fair, having an $R^2 = 0.65$. According to the UF bilinear model, the critical shear stress is $\tau_m = 3.09$ Pa. The SEDflume methods of analysis were applied to the data where the critical erosion rate was first exceeded. The results from these methods were consistent with the UF model; the linear interpolation analysis gives $\tau_{cr} = 3.05$ Pa and for the power law fit gives $\tau_{cr} = 3.35$ Pa.

The test data for Sample WF-50-203-02 is quite spread out (Figure 39). The best fit to the UF model is shown in Figure 39a. This gives a lower line that has a slightly negative slope and upper line that has a poor fit ($R^2 = 0.22$). Even though the overall fit of the UF model is poor, it is consistent with the SEDflume models in that the data used to fit the bulk erosion line begin with the points used to calculate the critical shear stresses in the UCSB models (Figure 39b). The UF model predicts $\tau_m = 1.78$ Pa; the SEDflume methods give $\tau_{cr} = 2.07$ Pa for the linear interpolation analysis and $\tau_{cr} = 2.08$ Pa for the power law fit. The spread of the data pertaining to the bulk erosion line for the UF model makes the slope small. The small slope causes the x-axis intercept to be less than the range of stress values used to obtain the line and used for the SEDflume models. The SEDflume methods are more appropriate for predicting the stress at the beginning of erosion for this sample.

The last 50% degraded surrogate waste sample compacted at 2.3 MPa was Sample WF-50-203-03. The erosion rate data for this sample becomes quite spread out once erosion begins to take place at 3.12 Pa. The best fit to the UF model is shown in Figure 40a. The fit to the bulk erosion data is poor, $R^2 = 0.21$, producing a critical shear stress of $\tau_m = 2.10$ Pa. Like the previous sample, the spread of the data lower the slope of the fit line, pushing the x-axis intercept outside the range of stresses used to define the line. Therefore, the SEDflume models appear to be more appropriate for determining the critical shear stress in this sample. They give for the linear interpolation analysis $\tau_{cr} = 2.91$ Pa and for the power law fit $\tau_{cr} = 3.29$ Pa.

A summary of the 50% degraded surrogate waste samples compacted at 2.3 MPa is given in Table 12. The UF bilinear model predicts the smallest critical shear stress prediction for the majority of the samples. The reason can be attributed to the spread of the data once erosion finally initiates which decreases the slope of the fit line, causing the x-axis intercept to become less the range of values used to define the line. The data points used to determine the UCSB predicted critical shear strengths are the same as those used at the beginning of the upper line in the UF model. Therefore, the SEDflume predicted critical strengths are greater than the UF values.

Table 12. Compilation of critical shear stresses for the 50% degraded surrogate waste samples compacted at 2.3 MPa.

Sample No.	Critical Shear Stress (Pa)		
	UF bilinear τ_m	UCSB, linear interpolation τ_{cr}	UCSB, power law τ_{cr}
WF-50-02	2.54	2.74	3.21
Flume 50-01	1.60	2.14	2.30
WF-50-203-01	3.09	3.05	3.35
WF-50-203-02	1.78	2.07	2.08
WF-50-203-02	2.10	2.91	3.29
Average	2.22	2.58	2.85

In general for the 50% degraded surrogate waste samples compacted at 2.3 MPa there is very little sample end effect. This is evidenced by the no or typically negative slope for the surface erosion line in the UF models. The average depth of the surface layer from the five samples is about 1.5 mm (0.05 in) and the largest is about 2 mm (0.08 in).

6.4.2 50% Degraded Surrogate Waste Material Tests, Die Compacted to 5.0 MPa

The results for the five 50% degraded surrogate waste material tests die compacted to 5.0 MPa are given graphically in Figure 41 through Figure 45, on the next four pages. Discussion of the results follows the presentation of the test results.

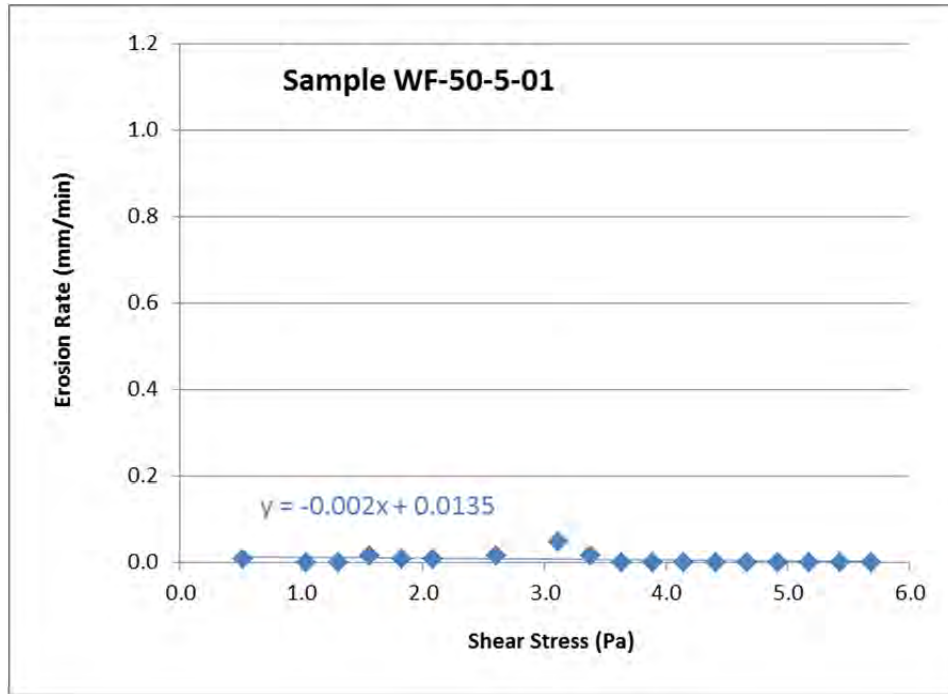


Figure 41. Flume results for Sample WF-50-5-01 plotted on a scale typically used for 50% degraded surrogate waste samples. The bulk erosion of the sample was not considered to have been started. In addition, the UCSB critical erosion rate was never reached. Beyond a shear stress of 3.5 Pa, erosion stopped. After 17½ hrs of testing, less than 7.5 mm (¼ inch) of material was removed.

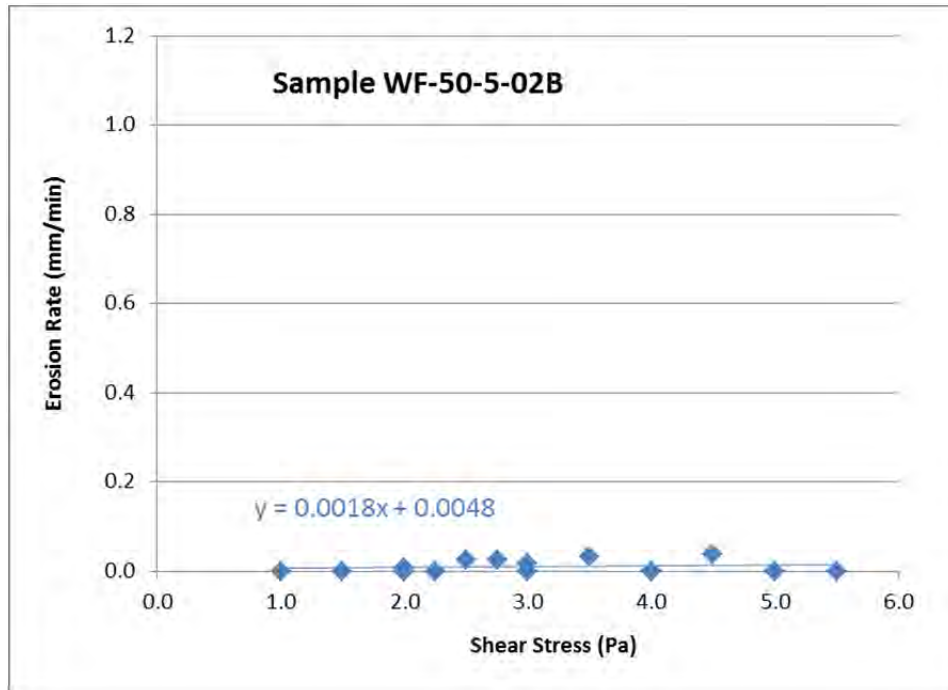
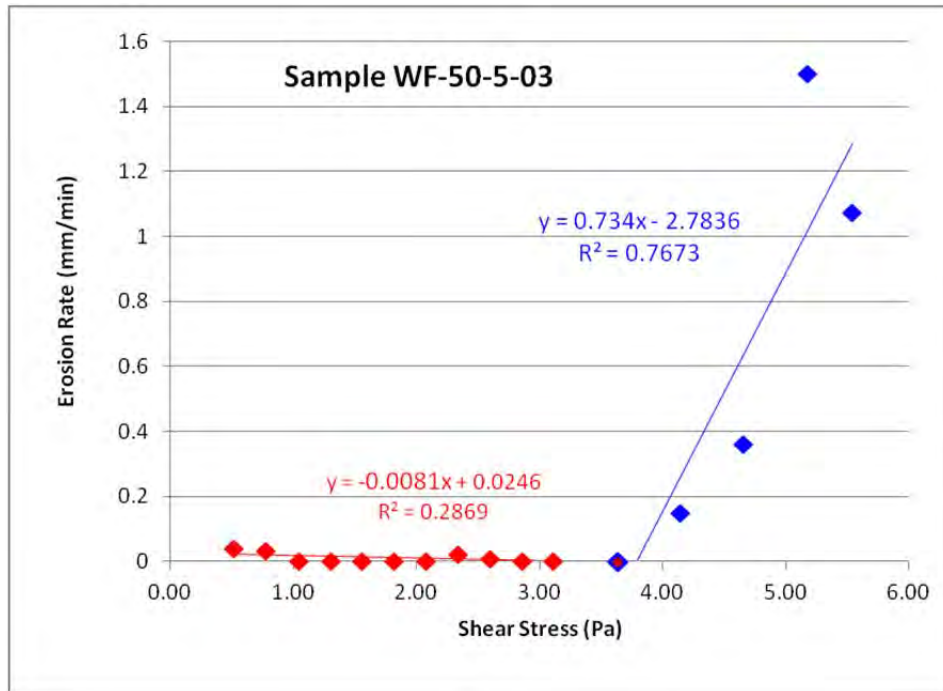
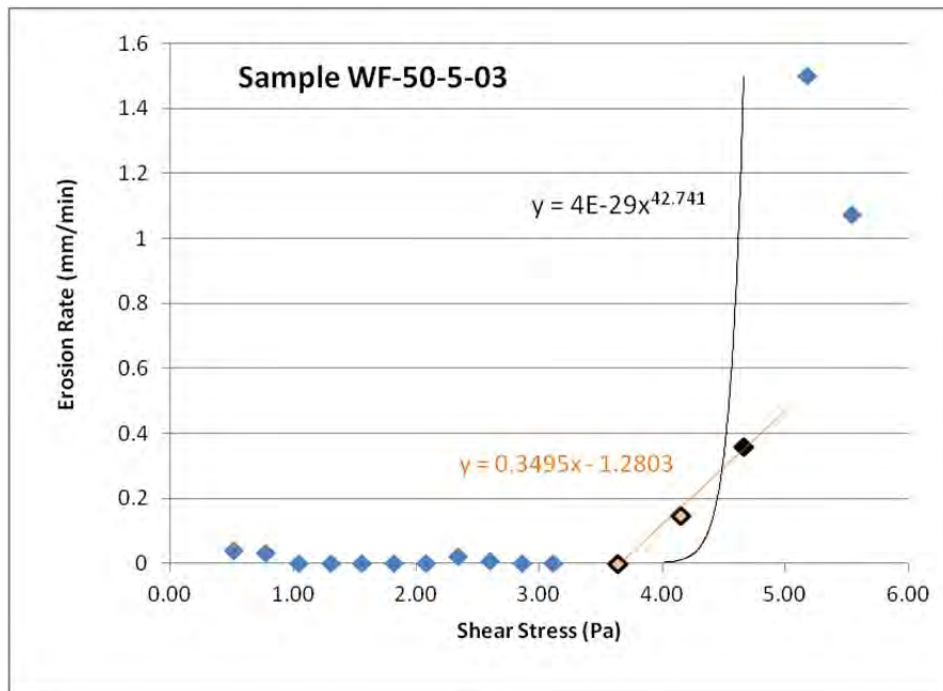


Figure 42. Flume results for Sample WF-50-5-02B plotted on a scale typically used for 50% degraded surrogate waste samples. The bulk erosion of the sample was not considered to have been started. In addition, the UCSB critical erosion rate was never reached. Beyond a shear stress of 4.5 Pa, erosion stopped. After 12½ hrs of testing, less than 9 mm (⅓ inch) of material was removed.

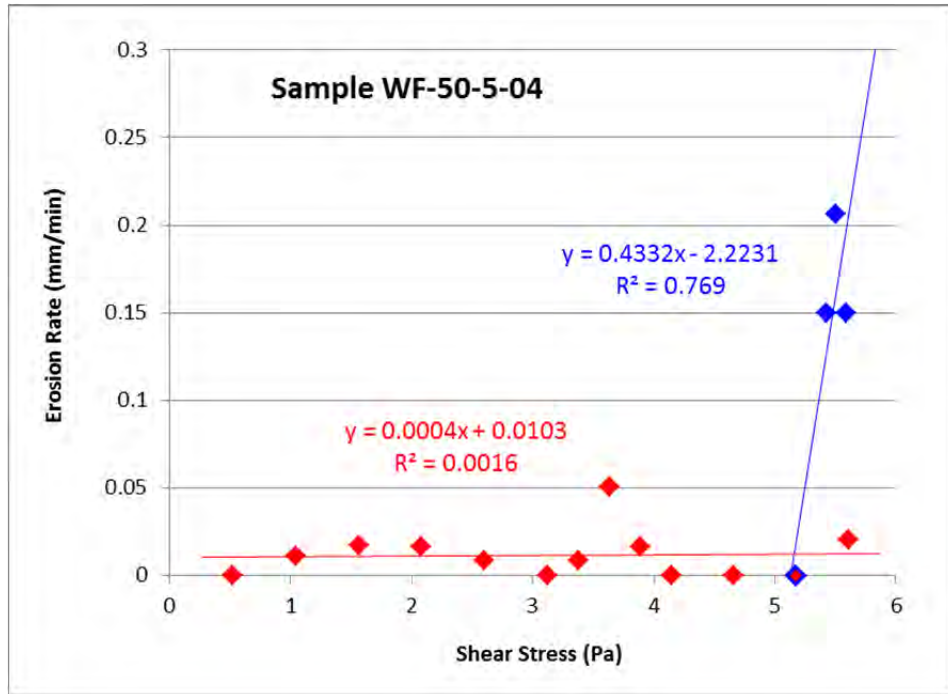


(a)

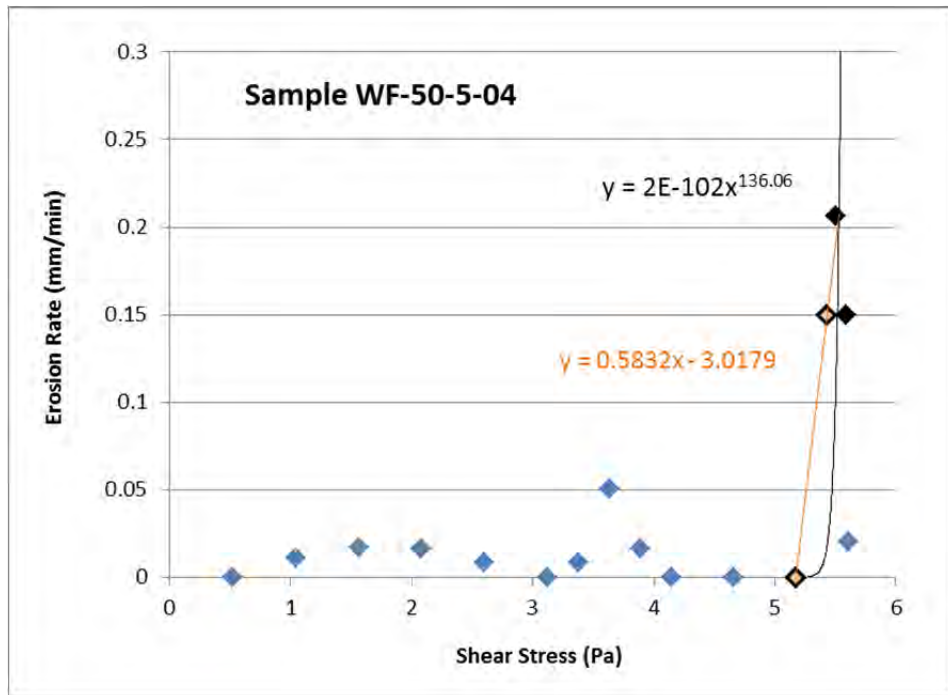


(b)

Figure 43. Analyses of the test results for Sample WF-50-5-03. (a) UF bilinear fit yielding $\tau_m = 3.79$ Pa and (b) the UCSB fits around a critical shear stress of 10^{-4} cm/sec giving for the linear interpolation $\tau_{cr} = 3.84$ Pa (two orange filled points) and for the power law fit $\tau_{cr} = 4.32$ Pa (three black points).

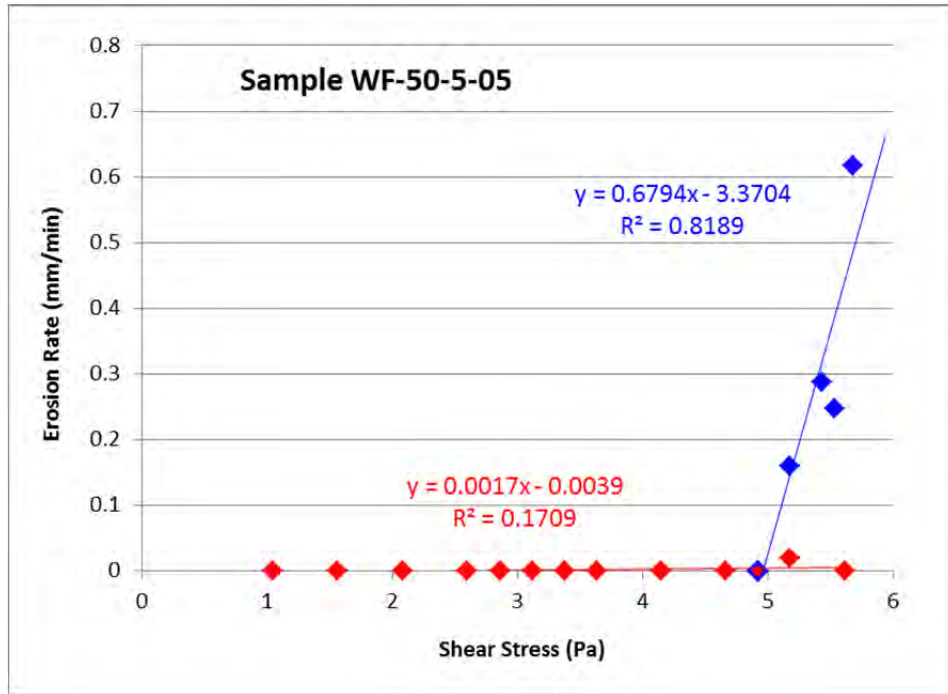


(a)

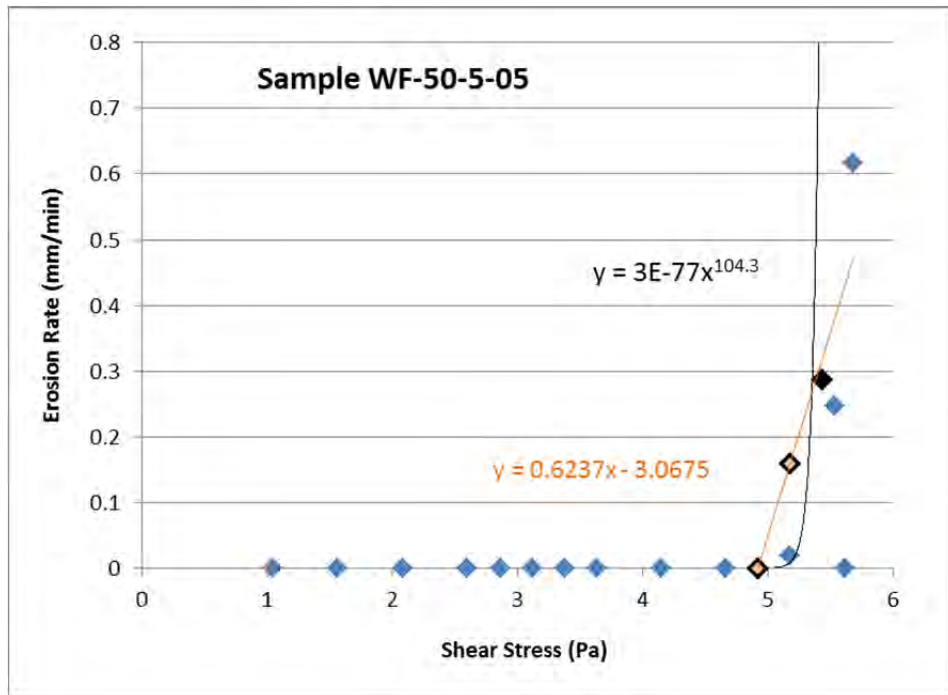


(b)

Figure 44. Analyses of the test results for Sample WF-50-5-04. (a) UF bilinear fit yielding $\tau_m = 5.13$ Pa and (b) the UCSB fits around a critical shear stress of 10^{-4} cm/sec giving for the linear interpolation $\tau_{cr} = 5.28$ Pa (two orange filled points) and for the power law fit $\tau_{cr} = 5.48$ Pa (four black points).



(a)



(b)

Figure 45. Analyses of the test results for Sample WF-50-5-05. (a) UF bilinear fit yielding $\tau_m = 4.96$ Pa and (b) the UCSB fits around a critical shear stress of 10^{-4} cm/sec giving for the linear interpolation $\tau_{cr} = 5.01$ Pa (two orange filled points) and for the power law fit $\tau_{cr} = 5.27$ Pa (three black points).

6.4.2.1 Discussion of results for 50% Degraded Surrogate Waste Material Tests, Die Compacted to 5.0 MPa

Mass erosion is not considered to have initiated in either Sample WF-50-5-01 (Figure 41) or Sample WF-50-5-02B (Figure 42). For the former sample it is more obvious that bulk erosion never started because the trend of the erosion rate with increasing shear stress is negative (Figure 41). Any semblance of erosion came to a stop regardless of the shear stress after a total of less than 7.5 mm ($\frac{1}{3}$ inch) of material loss over 17.5 hours of testing. In addition, the critical erosion rate defined by UCSB was never exceeded. For Sample WF-50-5-02B the trend of the erosion rate with increasing shear stress is positive (Figure 42). Like Sample WF-50-5-01, erosion stopped for this sample at the highest shear stresses the system could produce. The sample was even protruded into the channel to try to induce erosion to no avail. The specimen lost a total of about 9 mm ($\frac{1}{3}$ inch) of material loss over 12.5 hours of testing. In addition, the critical erosion rate defined by UCSB was never exceeded. It has been concluded that any erosion seen in these two samples is only a surface phenomenon. To help visualize this, both sets of results were plotted on a scale typical for 50% degraded surrogate waste material samples.

The erosion results of Sample WF-50-5-03 are shown in Figure 43. When the UF model is used to describe the behavior of the specimen, the lower line is seen to have a negative slope. At about 3.6 Pa, bulk erosion of the sample begins as evidenced by a sharp dogleg. The upper line shows good fit, $R^2 = 0.77$. This model yields $\tau_m = 3.79$ Pa. The SEDflume methods produce estimates of the critical shear stress that are consistent with the UF model. The linear interpolation method gives $\tau_{cr} = 3.84$ Pa, whereas the power law fit gives $\tau_{cr} = 4.32$ Pa.

Perhaps Sample WF-50-5-04 should be considered as a sample that did not undergo erosion when subjected to the highest flow the flume can generate. Testing was conducted over two days. The flow was originally increased to the maximum of 5.61 Pa without bulk erosion beginning. At 5.17 Pa the sample was rotated and at 5.61 Pa pushed out into the current about 12 mm ($\frac{1}{2}$ inch). After shearing off the face, erosion began. Erosion continued at a shear stress of 5.25, but stopped at 5.0. Upon looking at the data as being described by the UF model, the lower line has very slight slope (Figure 44a). The upper line is conservatively fit to erosion data beyond a shear stress greater than 5.0 Pa for those data obtained after the face was sheared off. The critical shear stress according to the UF model is $\tau_m = 5.13$ Pa. The UCSB models were also fit to the erosion data at shear stresses greater than 5.0 Pa after the shearing off of the face. The linear interpolation method gives $\tau_{cr} = 5.28$ Pa, whereas the power law fit gives $\tau_{cr} = 5.48$ Pa (Figure 44b).

Sample WF-50-5-05 also needed help getting erosion to begin. Testing on this specimen took two days. The shear stresses were increased to the maximum flow rate the flume can generate, applying 5.62 Pa. No bulk erosion of the specimen was observed. Surface erosion up to this time was 3 mm ($\frac{1}{9}$ inch). The specimen was then pushed into the channel about 10 mm (0.4 inch) and sheared off to create a new face. All erosion of any consequence occurred after this new surface was created. The results of fitting the various models to the erosion results are shown in Figure 45. The UF model gives $\tau_m = 4.96$ Pa, while the UCSB models gives $\tau_{cr} = 5.01$ Pa using the linear interpolation method and $\tau_{cr} = 5.27$ Pa using the power law method.

A summary of the testing results on the 50% degraded surrogate waste material samples compacted to 5.0 MPa is given in Table 13. The UF method yields a lower estimate for the critical shear stress of these samples than the UCSB methods. In general, for those data points considered pertaining to bulk erosion of the samples, the data was fit well by a straight line. This caused the estimates of the critical shear stresses to approximately lie within the range of shear stresses used to describe the bulk erosion lines increasing the confidence of the estimate. The UCSB methods also used this range of shear stresses. Therefore, all methods of analysis yielded fairly consistent estimates of the critical shear stress.

Table 13. Compilation of critical shear stresses for the 50% degraded surrogate waste samples compacted at 5.0 MPa.

Sample No.	Critical Shear Stress (Pa)		
	UF bilinear τ_m	UCSB, linear interpolation τ_{cr}	UCSB, power law τ_{cr}
WF-50-5-01	5.69	5.69	5.69
WF-50-5-02B	5.68	5.68	5.68
WF-50-5-03	3.79	3.84	4.32
WF-50-5-04	5.13	5.28	5.48
WF-50-5-05	4.96	5.01	5.27
Average	5.05	5.10	5.29

Two of the samples, WF-50-5-01 and WF-50-5-02B, never reached a stress level sufficient to cause bulk erosion of the material. Therefore the critical shear stress values reported in Table 13 are the highest shear stresses applied to the specimens. Also, two other samples, WF-50-5-04 and WF-50-5-05, had to have their faces shear off to create a new surface and expose material further into the interior of the sample before mass erosion would take place. The critical shear stress values for these samples in Table 13 consist of those data points obtained after the sample was sheared off. It is felt, therefore, that the values listed in Table 13 are conservative estimates of the critical shear stress values for the 50% degraded surrogate waste material samples compacted to 5.0 MPa.

7 TESTING SUMMARY AND RECOMMENDATION FOR THE LOWER LIMIT OF TAUFAIL

Vertical flume testing of surrogate waste samples was successfully accomplished. Three surrogate waste materials representing degrees of degradation of WIPP waste were used. All three materials correspond to possible end states of the waste after 10,000 years in the underground consistent with future repository conditions. Papenguth and Myers (Appendix A, Hansen et al., 1997) developed the rationale used to define and build the materials. The model materials created by Hansen et al. (1997) were developed from the estimated inventory of standard waste drums, the anticipated future state of the waste, expected underground conditions including their evolution with time, and relevant experimental results. Hansen et al. (1997) considered degradation of each constituent of the waste. Subsurface processes leading to extreme degradation are based on a number of contributing conditions including ample brine availability, extensive microbial activity, corrosion, and the absence of cementation, and salt encapsulation effects. Hansen et al. (1997) argued that the degraded waste material properties represented the lowest plausible realm of the future waste state because no strengthening processes were included such as cementation, mineral precipitation, more durable packaging, compaction of the waste, and inhibited corrosion. The surrogate waste materials are comprised of a mixture of raw materials including iron, glass, cellulose, rubber, plastic, degradation byproducts, solidified cements, soil, and WIPP salt. It is believed that the surrogate materials used during the testing reported herein represent an unobtainable degraded state of the waste, are thus far weaker than any possible future state, and will cover any changes that may occur in the waste inventory (Hansen et al 2003, Hansen 2005).

Two of the surrogate waste materials had been used before (Hansen et al., 1997, Broome et al., in preparation). They are the 100% and 50% degraded surrogate materials. A third, intermediate material was developed based on the methodology prescribed by Papenguth and Myers (Appendix A, Hansen et al., 1997). It represents 75% degradation of WIPP waste. The materials were compacted to two compaction pressures. The first compaction pressure was 5.0 MPa. It was shown by Hansen et al. (1997, 2003) to represent a conservative amount of compaction the waste in the underground is expected to withstand. The second compaction pressure was based on numerical modeling results given in Herrick et al. (2007a). They showed that the minimum possible compaction pressure at the waste would undergo is 2.3 MPa based on underground conditions assumed in CRA-2004. Of particular importance is that the 50% degraded surrogate waste materials compacted at 5.0 MPa were accepted by the Spallings Conceptual Model Peer Review Panel (Yew et al. 2003) to develop parameters for the Spallings model and incorporated into the CRA-2004 PABC (EPA, 2006) as part of the regulatory baseline.

Results from vertical flume testing on the six surrogate materials have been given previously for each material representing one of three degrees of degradation of the waste constituents and the two compaction pressures the wastes are conservatively considered to have undergone. Below in Table 14 is a comparison of the average shear strength, that is, average critical shear stress, of the surrogate materials based on the method used to analyze the results. The results from the 100% degraded tests are not included since they are considered unreliable due to a number of testing issues that had to be overcome. These issues are discussed in Section 6.2 and include deformation of the sample holders, possible misalignment of the testing system, and excessive

friction between the surrogate material and sample holder wall. The 50% degraded surrogate waste samples were tested at the same time as the 100% degraded surrogate waste samples and were therefore subjected to the same testing issues. However, being stronger than the 100% degraded surrogate waste samples, it was felt that the results for the 50% degraded surrogate waste samples experiments were not affected to a significant degree based on visual inspection of the sample as it moved. If they were affected, the results reported herein would be conservative because the testing issues would have weakened the material and the reported experimental results would be less than the actual values. By the time the 75% degraded surrogate waste samples were tested, the known testing issues had been remedied.

Table 14. Average shear strengths, or critical shear stress, for each type of surrogate waste material and compaction pressure as determined by the three analysis methods.

Sample Type	Average Shear Strength [Pa]		
	UF Bilinear	UCSB Linear Interpolation	UCSB Power Law Fit
100% degraded waste, 2.3 MPa compaction pressure	---- *	---- *	---- *
100% degraded waste, 5.0 MPa compaction pressure	---- *	---- *	---- *
75% degraded waste, 2.3 MPa compaction pressure	1.53	1.38	1.49
75% degraded waste, 5.0 MPa compaction pressure	2.17	1.81	1.97
50% degraded waste, 2.3 MPa compaction pressure	2.22	2.58	2.85
50% degraded waste, 5.0 MPa compaction pressure	5.05	5.10	5.29

* as discussed in Section 6.2, the test results for 100% degraded surrogate waste samples were considered unreliable due to deformation of the sample holders and an inability to advance the samples smoothly.

It is apparent from Table 14 that the less the surrogate material represents degradation of the waste, the stronger the material. In other words, the 50% degraded surrogate waste samples are stronger than the 75% degraded surrogate waste samples which are stronger than the 100% degraded surrogate waste samples. It is also apparent from Table 14 that the more compaction the materials undergo, the better able they are to resist erosion. Therefore, the materials compacted at 5.0 MPa are stronger than the materials compacted at 2.3 MPa.

Of the methods of analysis, it appears that the University of Florida (UF) model is more applicable to the surrogate materials reported herein than are the University of California – Santa Barbara (UCSB) methods. The latter are also known as SEDflume methods. Part of the discrepancy arises from the reason SEDflume was developed and why it is considered the state-of-the-art flume for field testing system. Before SEDflume, practitioners would overestimate the amount of erosion expected to take place because typical results from flume tests reported the value of incipient motion of the material. This value is based on the first movement of a particle

of a material. The problem is that it is typically obtained from the surface layer of the sample, whether it was built or rebuilt in the laboratory or obtained from the field. The surface layer was usually unconsolidated and therefore much weaker than the material within the interior of the sample. SEDflume was developed to obtain shear strengths from within the interior of the core samples, what is referred to herein as the bulk of the material or the mass of the material. Sediment cores can be several feet long. When operating SEDflume, the overlying layers of sediment are sheared off. Hence it was given the name SEDflume, which is short for "Sediment Erosion at Depth Flume." This system enables the operator to conduct erosion testing on the sediment core at specified depths from the surface and surface layer. There is no surface layer to contend with and the investigator is able to begin testing immediately on the bulk of the material. Any erosion is assumed to represent the interior material only. However, since sediment cores are obtained from the field where gravity has acted upon them, consolidation of the sample is a function of depth. Therefore the investigator has only a short distance with which to obtain their strength estimate of the material before he/she may be into a material with different properties. It is for these reasons the SEDflume methods of analysis have the investigator consider only two or three shear stress levels above and below the shear stress required to produce a critical erosion rate.

The UF method was developed from laboratory experimental results acknowledges the existence of a surface layer (Parchure and Mehta, 1985). It has also been used successfully on field sediments. It also shows that the surface layer will behave in a manner differently than the bulk of the material. The results obtained herein were obtained from samples built and tested in the laboratory; therefore, a method of analysis developed for those conditions is expected to work better. Also, as mentioned a few times in the sections discussing the individual experimental results, there were a number of cases in which the critical erosion rate as defined by UCSB was exceeded while the erosion data and UF model showed these times to be prior to when bulk erosion had initiated. The suitability of the critical erosion rate criterion was questioned for surrogate materials without considering whether or not bulk erosion is taking place.

The 50% degraded surrogate waste material compacted to 5.0 MPa was accepted for use in obtaining the experimental parameters for another WIPP Performance Assessment model (Yew et al 2003). Hansen et al. (1997, 2003) showed that for the vast majority of their performance assessment calculations, half or more of the initial iron and CPR inventory remains. They also showed that the 5.0 MPa compaction load is a conservative estimate of the compaction the waste will undergo. Since their approach was deemed to be adequate by a previous conceptual model peer review panel (Yew et al. 2003) and the EPA for the development of parameters for the Spallings model (EPA 2006), we recommend following this approach to establish consistency between models. Therefore, it is recommended that the experimental results for the 50% degraded samples compacted at 5.0 MPa be accepted as the lower limit of BOREHOLE : TAUFAL. The average shear strength of the recommended surrogate material based on the UF bilinear model is 5.05 Pa (see Table 14).

In addition, we recommend changing the distribution from log-uniform to uniform since the new distribution spans less than two orders of magnitude, i.e.

$$\log_{10}\left(\frac{77}{5.05}\right) = 1.18 \tag{7}$$

The use of a uniform distribution is appropriate when all that is known about a parameter is its range, as is the case here for TAUFAIL. The uniform distribution is the maximum entropy distribution under these circumstances. Log-uniform distributions are appropriate for parameters that span many orders of magnitudes (Tierney 1996).

Therefore parameter statistics for BOREHOLE : TAUFAIL to be entered into the parameter database are given in Table 15.

Table 15. Statistics for BOREHOLE : TAUFAIL to be entered into the parameter database.

Minimum	5.05 Pa
Maximum	77.00 Pa
Distribution	Uniform
Mean	41.025 Pa
Median	41.025 Pa
Standard Deviation	20.770 Pa

8 REFERENCES

- Berglund, J.W. (1992). *Mechanisms Governing the Direct Removal of Wastes from the Waste Isolation Pilot Plant Repository Caused by Exploratory Drilling*. SAND92-7295. Sandia National Laboratories, Albuquerque, NM.
- Berglund, J.W. (1996). "Parameters required for the CUTTINGS_S code for use in WIPP Performance Assessment." ERMS 236766. WIPP Records Center, Sandia National Laboratories, Carlsbad, NM.
- Brush, L.H. (1995). *Systems Priority Method – Iteration 2 Baseline Position Paper: Gas Generation in the Waste Isolation Pilot Plant*. Sandia National Laboratories. Albuquerque, NM
- Butcher, B.M., T.W. Thompson, R.G. VanBuskirk, and N.C. Patti. (1991). *Mechanical Compaction of Waste Isolation Pilot Plan Simulated Waste*. SAND90-1206. Sandia National Laboratories, Albuquerque, NM.
- Butcher, B.M. (1994). "A Model for Cuttings Release Waste Properties." A memorandum to distribution. January 6, 1994, ERMS 309846. WIPP Records Center, Sandia National Laboratories, Carlsbad, NM.
- Butcher, B.M., S.W. Webb, J.W. Berglund, and P.R. Johnson. (1995). *Systems Prioritization Method – Iteration 2. Baseline Position Paper: Disposal Room and Cuttings Models, Vol. 1*. ERMS 228729. WIPP Records Center, Sandia National Laboratories, Carlsbad, NM.
- Coons, W.E., J.F. Gibbons A.S. Burgess. (2007). "Interim Report for the Revised DRZ and Cuttings & Cavings Sub-models Peer Review." Conducted for the Carlsbad Field Office Technical Assistance Contractor in support of the U.S. Department of Energy, Carlsbad Field Office, Carlsbad, NM.
- CTAC (Carlsbad Area Office Technical Assistance Contractor). (1997). *Expert Elicitation on WIPP Waste Particle Diameter Size Distribution(s) during the 10,000-year Regulatory Post-closure Period: Final Report*. ERMS 541365. WIPP Records Center, Sandia National Laboratories, Carlsbad, NM.
- DOE (U.S. Department of Energy). (1996a). *Title 40 CFR Part 191 Compliance Certification Application for the Waste Isolation Pilot Plant*. DOE/CAO-1996-2184.
- DOE (U.S. Department of Energy). (1996b). *Waste Isolation Pilot Plant Transuranic Waste Baseline Inventory Report (Revision 3)*. DOE/CAO-95-1121. Carlsbad, NM: U.S. Department of Energy, Carlsbad Area Office.
- EPA (U.S. Environmental Protection Agency). (1998). "Technical Support Document for Section 194.23: Parameter Justification Report," Docket A-93-02, V-B-14. Office of Air and Radiation, U.S. Environmental Protection Agency, Washington, DC.

EPA (U.S. Environmental Protection Agency). (2006). *40 CFR Part 194: Criteria for the Certification and Re-Certification of the Waste Isolation Pilot Plant's Compliance with the Disposal Regulations: Recertification Decision. Final Notice*. Federal Register, Vol. 71 (April 10, 2006), pp. 18010-18021.

Hansen, F.D., M. K. Knowles, T. W. Thompson, M. Gross, J. D. McLennan, and J. F. Schatz. (1997). *Description and Evaluation of a Mechanistically Based Conceptual Model for Spall*. SAND97-1369. Sandia National Laboratories, Albuquerque, NM.

Hansen, F.D., T.W. Pfeifle, and D.L. Lord. (2003.) *Parameter Justification Report for DRSPALL*. SAND2003-2930. Sandia National Laboratories, Albuquerque, NM.

Hansen, F.D. (2005). "A Revisit of Waste Shear Strength.," ERMS 541354. WIPP Records Center, Sandia National Laboratories, Carlsbad, NM.

Herrick, C.G., M. Riggins, and B.Y. Park. (2007a). "Recommendation for the Lower Limit of the Waste Shear Strength (Parameter BOREHOLE : TAUFAIL), Rev. 0." ERMS 546033. WIPP Records Center, Sandia National Laboratories, Carlsbad, NM.

Herrick, C.G., M. Riggins, B.Y. Park, and E.D. Vugrin. (2007b). "Recommendation for the Lower Limit of the Waste Shear Strength (Parameter BOREHOLE : TAUFAIL), Rev. 1." ERMS 546343. WIPP Records Center, Sandia National Laboratories, Carlsbad, NM.

Jepsen, R., J. Roberts, and W. Lick. (1997). "Effects of bulk density on sediment erosion rates." *Water, Air, and Soil Pollution*, Vol. 99, pp. 21-31.

Jepsen, R., J. Roberts, and W. Lick. (1998). "Development and Testing of Waste Surrogate Materials for Critical Shear Stress." ERMS 533809. WIPP Records Center, Sandia National Laboratories, Carlsbad, NM.

Jepsen, R. and J. Roberts. 1998. Scientific Notebook: Development & Testing of Waste Surrogate Materials for Critical Shear Stress. Work performed under Sandia Contract AX-9022 with UCSB. ERMS 252862. WIPP Records Center, Sandia National Laboratories, Carlsbad, NM.

Lick, W. (2009). *Sediment and Contaminant Transport in Surface Waters*. CRC Press, Boca Raton, FL.

Mellegard, K.D. (1998). "Fabrication of surrogate waste bricks for erosion studies." Laboratory Notebook (Volume I of I). Maintained for Sandia National Laboratories, Contract No. AG-4911, RSI Job 325 Task 20.1. ERMS 251625. WIPP Records Center, Sandia National Laboratories, Carlsbad, NM.

McNeil, J., C. Taylor, and W. Lick. (1996). "Measurements of erosion of undisturbed bottom sediments with depth." *Journal of Hydraulic Engineering, ASCE*, Vol. 122, No. 6, pp. 316-324.

Parchure, T.M. and A.J. Mehta. (1985). "Erosion of soft sediment deposits," *Journal of Hydraulic Engineering*, Vol. 111, No. 10, pp. 1308-1326.

Partheniades, E. and R.E. Paaswell. (1970). "Erodibility of Channels with Cohesive Boundary." *Journal of the Hydraulics Division, Proceedings of the American Society of Civil Engineers*, Vol. 96, No. HY3, pp. 755-771.

Roberts, J., R. Jepsen, and W. Lick. (1998). "Effects of particle size and bulk density on erosion of quartz particles." *Journal of Hydraulic Engineering, ASCE*, Vol. 124, No 12, pp 1261-1267.

Roberts, J.D. and C.G. Herrick. (2009). "Waste Erodibility with Vertical and Horizontal Erosion Flumes." Test Plan TP 09-01. Sandia National Laboratories, Carlsbad, NM.

Roselle, G.T. (2012). "Determination of Corrosion Rates from Iron/Lead Corrosion Experiments to be used for Gas Generation Calculations." ERMS 558210. Sandia National Laboratories, Carlsbad, NM.

Schlichting, H. (1979). *Boundary-Layer Theory, seventh ed.* McGraw-Hill.

Schuhen, M. (2011). "Data Report for Analysis Plan for Demonstration Test Process: Soil Flume Sixnet Data Acquisition System." ERMS 555892. Sandia National Laboratories, Carlsbad, NM.

Taylor, C., and W. Lick. (1996). "Erosion properties of Great Lakes sediments." Report, Department of Mechanical and Environmental Engineering, University of California, Santa Barbara, California.

Teeter, A.M. (1987). "Alcatraz Disposal Site Investigation, Report 3: San Francisco Bay-Alcatraz Disposal Site Erodibility," Miscellaneous Paper HL-86-1, AD Number A181837. Department of the Army, Waterways Experimental Station, Corps of Engineers, Vicksburg, MS.

Tierney, M.S. (1996). "Distributions," ERMS 235268. WIPP Records Center, Sandia National Laboratories, Carlsbad, NM.

Trovato, E.R. (1997a). Letter to G. Dials (DOE) dated April 17, 1997. Docket A-93-02, II-I-25. Office of Air and Radiation, U.S. Environmental Protection Agency, Washington, DC.

Trovato, E.R. (1997b). Letter to G. Dials (DOE) dated April 25, 1997. Docket A-93-02, II-I-27. Office of Air and Radiation, U.S. Environmental Protection Agency, Washington, DC.

Wang, Y. (1997). "Estimate WIPP waste particle sizes based on expert elicitation results: revision 1," memorandum to M.S.Y. Chu and M.G. Marietta, Aug 5, 1997, ERMS 246936, WIPP Records Center, Sandia National Laboratories, Carlsbad, NM.

Wang, Y. and K.W. Larson. (1997). "Estimate waste critical shear stress for WIPP PA caving model" Memorandum to M.S.Y. Chu and M.G. Marietta, dated June 27, 1997. ERMS 246696. WIPP Records Center, Sandia National Laboratories, Carlsbad, NM.

Wawersik, W.R. (2001). *One-Quarter-Scale Laboratory Crush Tests on Unconfined Waste Cans and a Confined Waste Package in Support of the Waste Isolation Pilot Plant (WIPP)*. SAND98-2574. Albuquerque, NM: Sandia National Laboratories.

Yew, C., J. Hanson, and L. Teufel. (2003). "Waste Isolation Pilot Plant Spallings Conceptual Model Peer Review Report." ERMS 532520. WIPP Records Center, Sandia National Laboratories, Carlsbad, NM.